

# **LOW-TEMPERATURE CATALYTIC OXIDATION OF VOLATILE ORGANIC COMPOUNDS USING NOVEL CATALYSTS**

by

PRAVEEN KOLAR

(Under the Direction of James R. Kastner)

## **ABSTRACT**

Exhaust gases from poultry rendering facilities contain volatile organic compounds (VOCs) that are a nuisance, odorous, and smog and particulate matter precursors. Present treatment options, such as wet scrubbers, do not eliminate a significant fraction of the VOCs emitted including, 2-methylbutanal (2-MB), 3-methylbutanal (3-MB), and hexanal. Other available treatment options, such as thermal and catalytic incineration require temperature intensive inputs and form additional greenhouse gases. Hence, an inexpensive alternative technology is needed to eliminate these air pollutants. This research investigated the low-temperature (25-160 °C) catalytic oxidation of aldehyde vapors using novel catalysts derived from renewable carbon sources. In the first phase, 8-150 ppmv of 2-MB, 3-MB, and hexanal were oxidized using wood fly ash as a catalyst and molecular oxygen as an oxidant. The oxidation rates of 2-MB, 3-MB, and hexanal were between  $3.0$  and  $3.5 \times 10^{-9}$  mol/g-s at 25 °C. The activity of wood fly ash in oxidizing aldehydes was comparable to other commercially available metal and metal-oxide catalysts. It is theorized that wood fly ash catalyzed a free radical reaction in which

acetone and 2-butanone were formed as end products of 3-MB and 2-MB oxidation respectively, while pentanal and butanal were formed as end products of hexanal oxidation. When tested as a binary mixture at 25 °C, the presence of 2-MB increased the oxidation rate of hexanal. However, under identical conditions, hexanal inhibited the oxidation of 2-MB. Additionally, when 1500 ppmv ozone was tested as an oxidant at 160 °C, 100 % removal was achieved for all aldehydes within a 4-second reaction time. In the second part of this research, nickel and cobalt oxide catalysts were dispersed on activated carbon using electrochemical deposition. When tested for oxidation of 50-250 ppmv propanal vapors using 1500 ppmv ozone, the electrochemically deposited catalysts exhibited significantly higher (25-50 %) activities ( $-r=100-450 \times 10^{-9}$  mol/g-s) than activated carbon. The results from this research may be used to design catalytic oxidation processes for VOC removal at poultry rendering facilities and potentially replace energy and intensive air pollution treatment technologies currently in use.

INDEX WORDS: Low-temperature, catalytic oxidation, wood fly ash, electrochemical deposition, activated carbon, ozone

**LOW-TEMPERATURE CATALYTIC OXIDATION OF VOLATILE ORGANIC  
COMPOUNDS USING NOVEL CATALYSTS**

by

PRAVEEN KOLAR

B.S., Sri Venkateswara University, India, 1991

M.S., Indian Institute of Technology, India, 1995

M.S., Louisiana State University, 2004

A Dissertation Submitted to the Graduate Faculty of the University of Georgia in  
Partial Fulfillment of the Requirements for the Degree

DOCTOR OF PHILOSOPHY

ATHENS, GEORGIA

2008

© 2008

Praveen Kolar

All Rights Reserved

**LOW-TEMPERATURE CATALYTIC OXIDATION OF VOLATILE ORGANIC  
COMPOUNDS USING NOVEL CATALYSTS**

by

PRAVEEN KOLAR

Major Professor: James R. Kastner

Committee: James L. Anderson

Keshav C. Das

Mark A. Eiteman

Electronic Version Approved:

Maureen Grasso  
Dean of the Graduate School  
The University of Georgia  
May 2008

## **DEDICATION**

To my beloved wife Chandrika Patwari

## **ACKNOWLEDGEMENTS**

I express my sincere gratitude to my advisor and mentor, Dr. James Kastner for serving as my major professor and guiding me throughout my graduate program. I also thank my committee members Drs. James Anderson, Keshav Das, and Mark Eiteman for their feedback and advice from time to time. Ms. Joby Miller deserves special thanks for her excellent advice on chromatographic techniques that were extensively used in this project. Special acknowledgments are due to our graduate coordinator, Dr. William Kisaalita and our head of the department Dr. Dale Threadgill for their valuable advice.

I take this opportunity to acknowledge my fellow graduate students especially Rajan Gangadharan and Venki Anandan for their help with catalyst synthesis and Dr. Guigen Zhang for providing laboratory facilities. I also extend my thanks to Ms. Sherry Wrona, Ms. Patsy Adams, and Ms. Ellen King.

Finally, I thank the University of Georgia's College of Agricultural and Environmental Sciences and Biological and Agricultural Engineering for providing the facilities and research assistantship, and United States Egg and Poultry Association and Georgia FOODPAC for funding this project.

## TABLE OF CONTENTS

	Page
ACKNOWLEDGEMENTS.....	v
CHAPTER	
1 Foreword.....	1
2 Introduction.....	4
3 Catalytic oxidation of volatile organic compounds: mechanism, applications, and literature review .....	8
3.1 Introduction.....	9
3.2 General steps and mechanism of a catalytic reaction.....	9
3.3 Catalytic oxidation using molecular oxygen .....	10
3.4 Catalytic oxidation using molecular ozone .....	17
3.5 Electrochemical deposition .....	29
4 Research objectives and hypotheses .....	37
5 Low temperature catalytic oxidation of aldehydes using wood fly ash and molecular oxygen.....	40
5.1 Introduction.....	41
5.2 Experimental methods .....	43
5.3 Results and Discussion.....	51
5.4 Conclusion .....	61

6	Low temperature catalytic oxidation of aldehyde mixtures using wood fly ash: kinetics, mechanism, and effect of ozone .....	78
6.1	Introduction .....	79
6.2	Materials and methods.....	81
6.3	Results and discussion .....	90
6.4	Conclusion .....	103
7	Room-temperature ozonation of aldehydes using catalysts synthesized by electrochemical deposition.....	131
7.1	Introduction .....	131
7.2	Experimental methods .....	134
7.3	Results and discussion .....	139
7.4	Conclusion .....	142
8	Scaleup, design, and economics of catalytic oxidation applied to the poultry rendering industry .....	156
8.1	Introduction .....	156
8.2	Scale up calculations .....	157
9	Summary, conclusion, and future directions .....	162

## CHAPTER 1

### FOREWORD

The goal of this research was to develop a low-temperature (25-160° C) catalytic oxidation process using novel catalysts. Wood fly ash (WFA) and activated carbon were used as novel catalysts for treating volatile organic compounds (VOCs). Specific objectives within the scope of this dissertation were to: 1) evaluate wood fly ash as a catalyst for oxidation of aldehydes at room temperature, (2) determine the oxidation kinetics of a binary aldehyde mixture, and (3) synthesize advanced catalysts using activated carbon via electrochemical deposition techniques.

This research was funded in part by the Georgia FOODPAC Association, Traditional Industries Program, the United States Poultry and Egg Association (USPEA), and the United States Department of Energy (USDOE). Portions of this research (chapters three and six) have been prepared for publication in peer reviewed journals while chapter five has already been published in *Applied Catalysis B: Environmental* (76: 203-217). Additionally this research was presented in various scientific conferences (Table 1).

This dissertation is organized into nine chapters. The second chapter briefly describes the poultry rendering process and highlights the problems faced by animal rendering operations. The third chapter provides the reader with the fundamental principles, mechanisms, and current state-of-the-art in catalytic oxidation technology. The goals and objectives are listed in fourth chapter. In the fifth chapter, WFA is

evaluated as a potential catalyst to treat 3-methylbutanal vapors. Results from this part of the research indicated that wood fly ash exhibited catalytic properties. Chapter six dealt with oxidation kinetics of a 2-methylbutanal and hexanal mixture using oxygen and ozone as oxidants and WFA as a catalyst. The seventh chapter covered the synthesis, characterization, and testing of novel catalysts developed using electrochemical deposition techniques. The data obtained in the chapters five and six were used to propose design, scale-up, and estimated costs of catalytic oxidation for application in the poultry rendering industry, which is outlined in chapter eight. The summary, conclusion, and recommendations are covered in chapter nine.

**Table 1.1.** List of technical presentations resulted from this research.

---

Authors	Title of the presentation	Conference, location, and date
Kolar, P and J. R. Kastner	Enhanced air pollution control by coupling catalytic ozonation and biofiltration.	IBE annual conference, Tucson, AZ, March 9-12, 2005
Kolar, P and J. R. Kastner	Advanced environmental catalysts from biomass	IBE annual conference, Tucson, AZ, March 9-12, 2005
Kolar, P and J. R. Kastner	Catalytic ozonation of propanal using metal nano-particle impregnated carbon	ASABE annual conference, Portland, OR, July 9-12, 2006
Kolar, P and J. R. Kastner	Catalytic oxidation of volatile organic compounds using metal oxides and wood fly ash	GAWP annual conference, Atlanta, GA, March 14-15, 2007
Kolar, P, J. Miller, and J. R. Kastner	Catalytic oxidation of volatile organic compounds using solid wastes	IBE annual conference, St. Louis, MO, March 30, 2007

---

Legend:

IBE: Institute of Biological Engineering ([www.ibe.org](http://www.ibe.org))

ASABE: American Society of Agricultural and Biological Engineers ([www.asabe.org](http://www.asabe.org))

GAWP: Georgia Association of Water Professionals ([www.gawp.com](http://www.gawp.com))

## **CHAPTER 2**

### **INTRODUCTION**

In poultry rendering operations, poultry waste products such as feathers, offal, and meat byproducts are converted into value added products such as fertilizers, protein extracts, and oil. Typically, the raw material is hydrolyzed in batch systems or continuous systems under high temperature and pressure (140-150 °C and 276-345 kPa) (Kastner and Das, 2002). As proteins and fats break down under these extreme conditions, volatile organic compounds (VOCs) are generated as intermediate by products (Table 2.1). The cooked protein is thereafter processed into fertilizers and other products of commercial value.

Volatile organic compounds (VOCs) are a class of air pollutants that are considered hazardous (Xi et al., 2005). These compounds encompass a variety of chemicals containing carbon and hydrogen in their structure and are usually liquids at room temperature with a high vapor pressure (toxics.usgs.gov). Besides being noxious, a nuisance, and irritable (epa.gov), the VOCs can react with NO<sub>x</sub> in presence of ultra violet radiation to form atmospheric ozone (Manuel et al., 1997).

The rendering industry presently employs wet scrubbing technology to treat these compounds. The principle of wet scrubbing involves a liquid phase-counter current reaction between the contaminant (s) and an oxidizer such as ozone and ClO<sub>2</sub>. The process typically occurs in large cylindrical vessels (2.5 m x 1.0m dia), where contaminant (s) and oxidizer are brought into contact from opposite directions

**Table 2.1.** List of VOCs that were identified from poultry rendering emissions (Kastner et al., 2002).

VOC	Concentration (ppmv)
2 methyl butanal	0-50
3 methyl butanal	0-50
Dimethyldisulfide	0-25
Hexanal	0-50
Methanethiol	0-20

(2- 4 ft/s) while water is continuously sprayed from the top. As the contaminant (s) and the oxidizer are dissolved in water,  $\text{ClO}_2$  oxidizes the volatile organic carbon into carbon dioxide as a result of complete oxidation of contaminants.

However, recent analyses of data obtained from wet scrubbing operations indicated limited removal of the certain contaminants. For instance, while volatile sulfur compounds (VOSC) such as methanethiol were completely removed from the system, the removal of aldehydes such as 2-methylbutanal (2-MB), 3-methylbutanal (3-MB), and hexanal was limited to 20-80 % (Kastner and Das, 2002), due to low reactivity. Additionally, wet scrubbers require expensive chemicals such as  $\text{ClO}_2$  and the process itself is water intensive (Kastner et al., 2005).

Other treatment technologies such as adsorption, condensation, incineration, and biological filtration are possible although each has limitations (Tsou et al., 2003). Adsorption only transfers and concentrates the VOCs from a gas phase onto a solid phase and needs further treatment for complete abatement of the concentrated organics (Everaert and Baeyens, 2004). Incineration processes, which involve

combustion of the VOCs at high temperatures (1000-1200°C) using fuel gases (Gervasini and Ragaini, 2000) are not only cost intensive, but also contribute to production of green house gases (Tsou et al., 2003) by generating large amounts of CO<sub>2</sub>. Biological filtration systems often need longer residence times resulting in large reactors and large amounts of filter media. Additionally biological filtration systems and cannot handle fluctuations. Hence an alternative and efficient technology is needed to treat the VOC emissions from rendering facilities.

Catalytic oxidation has emerged as a promising alternate technology to treat the VOCs emitted from various industries (Gervasini et al., 1996). The process involves reaction between VOCs and an oxidant, aided by presence of a catalyst. The use of the catalyst lowers the temperatures required to facilitate complete oxidation of the organics by providing alternate pathways having lower activation energies compared to non-catalytic reactions (Smith, 1981). Lowering the reaction temperatures not only result in lowering the treatment costs, but also reduce production of green house gases and micro pollutants (such as dioxins, phosgene, etc). Hence, it is proposed to use catalytic oxidation technology to treat the odorous pollutants emitted from poultry rendering operations.

## References

1. Everaert, K and J. Baeyens. 2004. Catalytic combustion of volatile organic compounds. *Journal of Hazardous Materials*. B109: 113-139.
2. Gervasini, A., G. C. Vezzoli, and V. Ragaini. 1996. VOC removal by synergic effect of combustion catalyst and ozone. *Catalysis Today*. 29: 449-455.

3. Gervasini, A and V. Ragaini. 2000. Catalytic technology assisted with ionization/ozonization phase for the abatement of volatile organic compounds. *Catalysis Today*. 60: 129-138.
4. Kastner, J. R. and C. Das. 2002. Wet scrubber analysis of volatile organic compounds removal in rendering industry. *Journal of the Air & Waste Management Association*. 52 (4): 459-469.
5. Kastner, J. R., Q. Buquoi, R. Gangavaram, and K. C. Das. 2005. Catalytic oxidation of gaseous reduced sulfur compounds using wood fly ash. *Environmental Science and Technology*. 39 (6), 1835 -1842.
6. Manuel, L., A. Guenther, and R. Monson. .Plant production and emission of volatile organic compounds. *Bioscience*. 47 (6): 373-383.
7. Smith, J.M., Chemical Engineering Kinetics. McGraw-Hill, New York, 1981.
8. Tsou, J., L. Pinard, P. Magnoux, J. L. Figueiredo, and M. Guisnet. 2003. Catalytic oxidation of volatile organic compounds (VOCs): oxidation of 0-xylene over Pt/HBEA catalysts. *Applied Catalysis B: Environmental*. 46: 371-379.
9. Xi, Y., C. Reed, Y.K. Lee, and S. T. Oyama. 2005. Acetone oxidation using ozone on manganese oxide catalysts. *J. Phys. Chem. B*. 109: 17587-17596.

**CHAPTER 3**  
**CATALYTIC OXIDATION OF VOLATILE ORGANIC COMPOUNDS:**  
**MECHANISM, APPLICATIONS, AND LITERATURE REVIEW<sup>1</sup>**

**Praveen Kolar and James Kastner\***

Air Pollution Engineering Laboratory

Biological and Agricultural Engineering, Driftmier Engineering Center,

The University of Georgia, Athens, Georgia

**\*Corresponding author contact: [jkastner@engr.uga.edu](mailto:jkastner@engr.uga.edu), 706-583-0155**

---

<sup>1</sup> Kolar, P. and J. R. Kastner. To be submitted to the *Journal of Hazardous Materials*

### **3.1 Introduction**

Catalytic oxidation is emerging as a promising alternative technology to treat volatile organic compounds (VOCs) emitted from various industrial operations (Zhang, 2005; Fonseca et al., 2005). The process involves a reaction between VOCs and an oxidant, on a catalyst surface (Gangwal et al., 1988). The reaction is believed to occur on the catalyst surface either between adsorbed reactants, between the adsorbed VOC and gas-phase oxidant or by a surface redox cycle (Gaur et al., 2005). A catalyst provides alternate routes to end products whose activation energies are less than that of non-catalytic reactions (Smith, 1981). Hence use of the catalyst lowers the temperatures (300-500 °C) required for oxidation of VOCs when compared to thermal incineration (1000-1200 °C) (Tsou et al., 2003). This chapter provides the reader with the general principles of catalytic processes, the mechanisms and mathematical models applied to catalytic reactions, and the future outlook of oxidation catalysts.

### **3.2 General steps and mechanism of a catalytic reaction**

In a heterogeneous catalytic reaction, the interactions between reactants follow a sequence of steps (Fogler, 1991). In the first step, the reactants diffuse from the bulk fluid surrounding the catalyst to the surface. If the catalyst is porous, then the reactants diffuse into the pores and reach the catalyst surface. On the catalyst surface, the reaction occurs and products are formed. The products then diffuse from the pores to the catalytic surface. Finally, the products desorb from the catalytic surface to the bulk fluid. Any of the above mentioned steps can be rate limiting depending on catalyst structure and flow properties. In catalytic oxidation reactions

of volatile organics, the oxidant reacts with volatile organics to form stable end products. Although several oxidants such as ozone, oxygen, hydrogen peroxide, and UV are used in catalytic oxidation, the goal of this chapter is to present a brief overview of catalytic oxidation using oxygen and ozone.

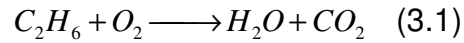
### **3.3 Catalytic oxidation using molecular oxygen**

Catalytic oxidation using oxygen involves reaction between oxygen and its associated products and VOCs on a catalyst surface. As an oxidant, oxygen is very effective. The oxygen molecule is electronically imbalanced as it has two unpaired electrons in separate orbitals in its outer shell. This makes the oxygen molecule susceptible to form various reactive oxygen species, which are very reactive.

It is theorized that oxygen participates in a catalytic oxidation reaction either by abstraction of hydrogen in an adsorbed state from the VOC molecule resulting in a VOC radical or by forming reactive oxygen species ( $O_2^-$  or  $O_2^{2-}$ ) and attacking the VOC molecule or by forming a lattice oxygen molecule ( $O^{2-}$ ) after acquiring four electrons (Che and Tench, 1983). However it is possible to have more than one of the above mentioned processes occurring simultaneously in any given oxidation reaction.

Several kinetic models have been proposed to describe catalytic oxidation using oxygen. Spivey (1987) described catalytic oxidation using two approaches: a simple empirical power law and a more complex mechanistic approach that provides insight into the reaction mechanism. A power law describes the oxidation rate as a function of a rate constant and the concentration of the reactants. For example, in

complete combustion reaction of  $C_2H_6$  into  $CO_2$  and  $H_2O$  (Fogler, 1999) the rate of combustion can be expressed using a power law model as



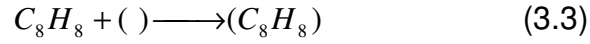
$$r = kC_{C_2H_6}^n C_{O_2}^m \quad (3.2)$$

where  $r$  is the rate of combustion of  $C_2H_6$ ,  $C_{C_2H_6}$  and  $C_{O_2}$  are concentrations of ethane and oxygen,  $n$  and  $m$  are orders of reaction, and  $k$  is the reaction rate constant.

It may however be noted that in many oxidation reactions, the concentration of oxygen is in excess. Hence in the above equation, oxygen concentration essentially remains unchanged and the oxidation rate is independent of oxygen concentration and depends only on the concentration of the reactants ( $C_2H_6$  in the above example). This idea was extensively utilized by Kastner et al (2005, 2006, and 2007) to oxidize odorous VOCs (5-100 ppmv) using oxygen or ozone at room temperature (25 °C). They assumed the oxygen concentration (208,000 ppmv) was in excess and fit simple empirical power law model to describe the catalytic oxidation of propanal (ozone as oxidant), hydrogen sulfide, and 3-methylbutanal.

A power law model, although mathematically simple and useful in industrial reactor designs, does not allow for a potential understanding of the reaction mechanism. Hence, more complex models based on the fundamental steps of the reaction, have been proposed to obtain an understanding of catalytic oxidation processes. For example, oxidation of styrene using manganese-iron oxides was studied by Tseng and Chu (2001). They proposed that molecular oxygen and styrene adsorbed on catalytic surface at 200 °C and reacted to form products (also

known as Langmuir-Hinshelwood mechanism) water and CO<sub>2</sub> which desorbed immediately.



where ( ) is a catalytically active site and (O<sub>2</sub>) represents adsorbed oxygen on active site.

Based on the above proposed mechanism, the oxidation rate of styrene was expressed as:

$$r = k \frac{K_S C_S K_O C_O}{(1 + K_S C_S + K_O C_O)^2} \quad (3.6)$$

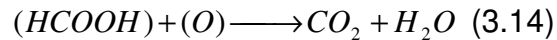
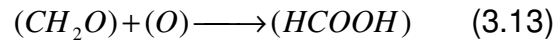
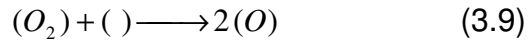
where  $r$  is the oxidation rate of styrene,  $C_S$  and  $C_O$  are the concentrations and  $K_S$  and  $K_O$  are the adsorption equilibrium constants of styrene and oxygen and  $k$  is the overall oxidation rate constant .

In a similar scheme proposed by Chang and Weng (1993), oxygen also reacted with VOCs via disassociative interaction. They tested complete oxidation of toluene using perovskite catalysts and proposed that oxygen after adsorption on the catalyst surface disassociated into oxygen atoms. The atomic oxygen then reacted with the VOC adsorbed to form products. Based on the disassociative mechanism a mathematical model was proposed as,

$$r = k \frac{K_T C_T (K_{O_2} C_{O_2})^{\frac{1}{2}}}{\left(1 + K_T C_T + (K_{O_2} C_{O_2})^{\frac{1}{2}}\right)^2} \quad (3.7)$$

where  $r$  is the oxidation rate of toluene,  $C_T$  and  $C_{O_2}$  are the concentrations of toluene and oxygen,  $K_T$  and  $K_{O_2}$  are the adsorption coefficients of toluene and oxygen.

Golodets (1983) proposed a slightly different mechanism based on the Eley-Rideal mechanism for oxidation of volatile organics. In a study on oxidation of methane, Golodets proposed that molecular oxygen adsorbed on the catalyst and reacted directly with methane from the gas phase, which was expressed by Spivey (1987) as,

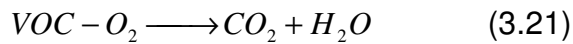
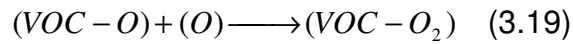


The overall reaction can be expressed as equation 3.15

$$r = \frac{k_{O_2} k_M P_{O_2} P_M}{k_{O_2} P_{O_2} + k_M P_M} \quad (3.15)$$

where  $r$  is the oxidation rate of methane,  $P_{O_2}$  and  $P_M$  are the partial pressures of oxygen and methane, and  $k_{O_2}$  and  $k_M$  are the rate constants of oxygen reduction and methane oxidation reactions.

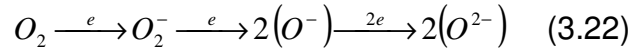
Additionally, Gangwal (1988) notes that many reactions involving oxidation of VOCs using oxygen proceed via an alternate reduction and oxidation of VOCs on catalyst surfaces, as proposed by Mars van Krevelen, and represented below as,



where ( ) is the catalytically active site on the metal oxide surface,

(VOC - O) represents VOC and oxygen adsorbed on the active site

All steps in the above mechanism are considered irreversible. Steps 3.17-3.20 involve reduction in which electrons are transferred from VOC, (VOC-O), and (VOC-O<sub>2</sub>) to the catalyst surface. Subsequently, the catalyst transfers these electrons to gaseous oxygen to form oxygen free radicals and in the process reoxidizing the catalyst.



Based on the above mechanism the following rate expression was proposed for oxidation of benzene using oxygen on a nickel-aluminum catalyst (Gangwal et al., 1988)

$$r = \frac{k_{O_2} k_{VOC} P_{O_2} P_{VOC}}{k_{O_2} P_{O_2} + k_{VOC} P_{VOC}} \quad (3.23)$$

It is interesting to note that the rate expressions based on the Mars van Krevelen redox based oxidation and the Eley-Rideal surface-gas interface reactions are very similar in form. The participation of the atomic anions of adsorbed oxygen is an essential feature in catalytic oxidation reactions based on Mars van Krevelen's model. These anions are formed on the catalyst surface by gaining electrons from the catalyst.

It may be noted that the type of catalyst can also determine the nature of the oxygen anion radical species. In oxidation reactions, two types of catalysts are used: metal oxides and noble metals (Spivey, 1987). For example, when metal oxides are used as catalysts, the formation of  $O_2^-$  and  $(O^{-1})$  are not rate-limited due to availability of free electrons in the catalyst. It follows that  $(O^{2-})$  and  $(O^{-1})$  species are predominant in reactions catalyzed by metal oxides (Bielanski and Haber, 1979). Studies on metal oxides using electron paramagnetic resonance spectroscopy have corroborated this theory. However in catalysts that do not have excess electrons (metals), formation of  $(O^{2-})$  species is limited and the catalyst surface is dominated by  $(O^{-1})$  radicals.

So, based on their ability to adsorb and form oxygen radicals, metal oxides have been divided into three groups (Bielanski and Haber, 1979): (1) Oxides (Ni, Mn, Co, etc) having affinity towards electron rich oxygen species  $(O^{-1})$ , (2) oxides (Zn, Ti, etc) on which less electron rich oxygen is adsorbed  $(O_2^-)$ , and (3) oxides (Mo, W, etc) with no affinity for oxygen. Depending of the type of oxide used (or the concentration on electron donor sites) as a catalyst, either  $O^{-1}$  or  $O_2^-$  radicals are

formed on the surface as a result of oxygen adsorption and oxidation of the VOC is thought to be carried out by these radicals.

Similarly, based on their electrical conductivities, metal oxides are classified into n-type semiconductors, p-type semiconductors, and insulators (Spivey, 1987). N-type semiconductors (e.g. ZnO) are rich in electrons and cannot accept more electrons from VOCs. These oxides are usually not active catalysts for oxidation. P-type semiconductors (e.g. NiO) on the other hand are deficient in electrons and can accept electrons from VOCs. These are generally considered as good oxidation catalysts. The insulators do not conduct electrons and are not catalysts, but are often used as supports for catalysts.

Catalytic oxidation using oxygen has been successfully applied to treat organic and inorganic gases. Spivey (1987) provided an excellent summary on oxidation of VOCs on different types of catalysts and the reader is encouraged to refer to Spivey's work. For example, oxidation of hexane and benzene was studied at 140-360°C by Gangwal et al (1988) using platinum catalysts dispersed on nickel and aluminum supports. 100 % removal of benzene was obtained around 240°C while hexane was completely oxidized at 350° and Mars van Krevelen's redox model was found to adequately describe the oxidation process. Additionally, when studied as mixtures (hexane and benzene), the conversion was lower than obtained as individual compounds. Similarly, other VOCs were treated using platinum, and include alcohols, ketones, aldehydes, xylenes, polychlorinated alkanes, and toluene (Hermia and Vigneron 1993; Tsou et al., 2003; Everaert and Baeyens, 2004; Zhang et al., 2005).

For instance, in study a conducted by Tsou et al (2003), 1700 ppmv o-xylene was oxidized in a fixed bed plug flow reactor at 180-240 °C that contained 140 mg of platinum dispersed on zeolite supports. They observed two parallel reactions depending on the platinum loading; complete oxidation (higher platinum loading) yielding CO<sub>2</sub> and H<sub>2</sub>O formation and partial oxidation (lower loading) resulting in coke formation. In a similar study by Zhang et al (2005), formaldehyde was completely oxidized by oxygen at room temperature (25 °C) into CO<sub>2</sub> and H<sub>2</sub>O when treated with a 1% w/w platinum catalyst impregnated on titanium dioxide packed in a fixed bed reactor.

Tidahy (2007) demonstrated 100 % removal of toluene around 200 °C. They tested 1000 ppmv of toluene in a fixed bed micro reactor that contained 0.5 % w/w of copper dispersed on zirconia and 0.5 % w/w palladium on zeolite. They concluded that palladium exhibited higher catalytic activity than copper although copper and palladium completely oxidized toluene into CO<sub>2</sub> and H<sub>2</sub>O.

Despite several applications, catalytic oxidation using oxygen requires high temperatures (200-700 °C) to activate oxygen to form reactive oxygen species. One alternate approach is use of ozone as an oxidant to catalytically treat VOCs.

### **3.4 Catalytic oxidation using molecular ozone**

Ozone is a three oxygen allotropic molecule (Xi et al., 2005) with a high oxidation potential (2.07 eV) (Gervasini et al., 1996). It is thermally unstable (Oyama, 2000), an oxidant (Gunten, 2003) and highly reactive. Its reactivity with many organic compounds makes it an attractive candidate in water and air treatment applications. Usually ozone is generated at the site via a corona discharge process.

Ozone has been traditionally used to remove colors and organic compounds in water (Ma and Graham, 1998; Imamura et al., 1991). Ozone can react with the organics in two ways (Langlais et al., 1991): (i) direct reaction with organics and (ii) indirect reaction via formation of radical species from ozone decomposition.

In direct reactions with organic compounds, an ozone molecule acts as a dipole, electrophile and a nucleophile (Horden et al., 2003). As a dipole molecule, ozone can only react with compounds with unsaturated bonds (e.g., cyclo-addition with alkenes). Similarly the reactions associated with its electrophilic nature are limited to molecules of high electron density (aromatics, such as phenols). Finally, ozone can react with electron deficient molecules (aliphatics such as butanol). It follows that the reactions of ozone are selective and are limited to unsaturated, aromatic, and aliphatic compounds (Langlais and Reckhow. 1991).

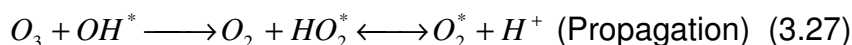
However, when ozone is decomposed in water under high pH (10-12), it disassociates itself into oxygen and free radicals (Gunten, 2003) and the rate of decomposition is usually expressed as a pseudo-first order reaction equation (Langlais and Reckhow. 1991) depending on the pH of the solution (Horden et al., 2003).

$$\left[ \frac{d(O_3)}{dt} \right]_{pH} = -k'(O_3) \quad (3.24)$$

where  $k'$  is the pseudo-first order rate constant for any given pH.

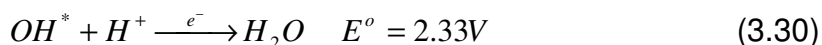
As ozone decomposes in water, it follows a multi-step-initiation-propagation-chain reaction





In the above chain reaction, while the  $OH^-$  acts an initiator to produce a superoxide radical ion ( $O_2^-$ ), ozone acts as a promoter and reacts with hydroxyl radical ( $OH^*$ ) to regenerate superoxide radical ions ( $O_2^-$ ). Organics and other impurities (e.g., carbonate and bicarbonates) can consume the hydroxyl radical ( $OH^*$ ) without producing superoxide radical ions ( $O_2^-$ ) and are appropriately termed as inhibitors or scavengers.

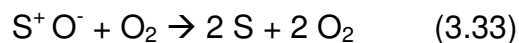
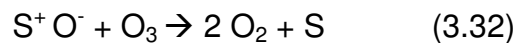
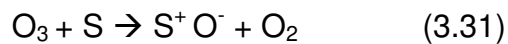
Among the free radicals formed during the ozone decomposition, the hydroxyl radical ( $OH^*$ ) is one of the most reactive (Hoigne, 1997) ( $10^6 - 10^9 \text{ M}^{-1}\text{s}^{-1}$ ) and strongest oxidants.



Unlike ozone,  $OH^*$  radicals are not selective and can react with all types of organics and inorganics (Horden et al., 2003).

There are various methods to increase the concentration of  $OH^*$  radicals in an ozonation reaction including combination of ozone/UV, mixtures of ozone/hydrogen peroxide, and catalysts for ozone decomposition, all of which are termed advanced oxidation processes (AOPs). When a catalyst is used in combination with ozone, the process is termed *catalytic ozonation*.

Catalytic ozonation is slowly gaining prominence and is increasingly being used to treat volatile organic compounds in the aqueous and gas phase. The process involves a reaction between ozone and VOCs on a heterogeneous catalyst surface. In aqueous phase ozonation reactions, the oxidation occurs either by direct reaction with ozone or by reaction with extremely active hydroxyl radicals that are formed due to catalytic decomposition of ozone. Mechanisms of aqueous phase catalytic ozonation have been discussed earlier (Gunten, 2003; Langlais and Reckhow, 1991; Horden et al., 2003). However, in a gas phase ozonation process (without water), the reaction is considered to occur in several steps and has been described using several mechanisms most of which are available only in patent literature (Naydenov et al., 1995). In general the mechanisms include: 1) decomposition of ozone into oxygen radicals, 2) reaction between oxygen radicals and VOCs. One proposed mechanism of ozone decomposition can be described as below (Stoyanova et al., 2006)



where S is the active site of the catalyst. Similar mechanisms are proposed by Reed et al., (2005) and Einaga and Futamura (2005) although the actual mechanism is specific to the type of the catalyst used. In any case, from the above reactions, it follows that catalysts capable of changing their oxidation states, could exhibit higher ozone decomposition properties and hence can allow for greater oxidation of VOCs.

In a study on catalytic decomposition of ozone, Mehandjiev et al (2001) proposed a reaction mechanism based on changes in the oxidation states of metals.



where  $M^{n+}$  is the metal ion and R represents the VOC.

Per the above equations, as a first step, ozone decomposes on the active site to form an intermediate catalytically active complex ( $M^{n+1} O^-$ ) (Konova et al., 2006) and generation of radical oxygen species ( $O^-$ ) (Dimitrova, 2004). In the second step, the catalytically active complex allows for the reaction between oxygen radicals and VOCs resulting in regeneration of the catalyst surface (Stoyanova et al., 2006) for subsequent reactions.

Catalytic oxidation using ozone has been successfully applied to treat various gaseous pollutants. In a study by Imamura et al (1991), 10 % carbon monoxide was oxidized by 10,000 ppmv ozone at 50 °C using oxides of manganese, tin, zinc, nickel, silver, cerium, iron, copper, and lead. However, silver showed highest activity by decomposing 100 % ozone and 59 % carbon monoxide, while ozone alone contributed to only 6 % removal of carbon monoxide. Similar studies by Naydenov et al (1995) on CO removal using 99 % cerium oxide and 14,000 ppmv of ozone revealed reactive oxygen radicals on cerium oxide surface when analyzed by a thermogravimetric analyzer. Ozone has also been found effective for oxidation of VOCs. For example, 1000 ppmv of ozone was used along with 5 % manganese

dioxide supported on aluminum oxide at 25 °C in a continuous reactor. The analysis of spent catalyst extracted in methanol indicated partially oxidized products such as ketones, alcohols, and carboxylic acids. In separate studies by Reed et al (2005) and Xi et al (2005), acetone was completely oxidized by manganese oxide catalysts. In the work of Reed et al, 10 % manganese oxide impregnated on silica was used to oxidize 1000-4000 ppmv of acetone using 10,000 ppmv of ozone between 40-50 °C, while within the reactor *in situ* measurements were recorded via Raman spectroscopy to reveal peroxide formation on catalyst surface. These results were found to be in agreement with studies performed by Xi et al (2005). They tested manganese oxide catalysts impregnated on silica and alumina to oxidize 1000 ppmv of acetone using 1000-8000 ppmv of ozone between 25-300 °C. Their results indicated that alumina supported manganese oxide was found to have high oxidation activity and formed peroxide on catalyst surface as observed by Reed et al (2005). Recently iso-propanal has been used as a model VOC in catalytic ozonation. Konova et al (2006) for example used 10,300 ppmv ozone and 5 % cobalt oxide impregnated on aluminum oxide support in an isothermal plug flow reactor (25-250 °C) to completely treat 1000 ppmv iso-propanal. Similar reactor configuration was used by Stoyanova et al (2006) in completely treating 1000 ppmv iso-propanal using alumina supported nickel oxide catalysts and 5600-6500 ppmv ozone at 25-250 °C. However, the efficiency of contaminant removal and, catalyst activity depends on (temperature, concentration, flow rate) and catalyst type or structure (e.g., dispersion, crystal structure, surface area, oxidation state, thermal stability, etc). One of the problems associated with catalytic oxidation using ozone is the need

for post treatment and monitoring of ozone. Although most of the published literature demonstrated successful removal of VOCs ozone concentrations between 1,000-1,000,000 ppmv were used in the experiments to achieve high removal efficiencies. Generating high concentrations of ozone continuously may not be economically feasible. Also unreacted ozone needs to be treated after the termination of the experiments before disposal.

Based on the literature analysis on catalytic oxidation of VOCs, further research is warranted in the following areas:

**Catalytic oxidation of mixtures:** Very few authors have reported systematic studies on VOC mixtures. Most of the literature on VOC oxidation deals with extensive analysis of single compounds. Extensive studies on single compounds were conducted by studying the effect of concentrations, pressures, temperatures, etc. However, most studies on mixtures were based on overall performances rather than studying the effects of reaction conditions. The overall performance of the mixtures does not provide information on the fundamental processes involved. Hence research on studying oxidation of mixtures is justified, as it is not possible to predict the behavior of the mixture based on information available from oxidation of single compounds.

**Use of solid wastes and renewable resources as catalysts:** All the available reports on catalytic oxidation studies involved either pure metal or metal oxides. The catalysts were either commercially procured or synthesized in the laboratory based on transfer of technology from related applications. Little research has been done to use alternative sources. Several types of solid wastes are produced every year,

some of which are catalytically active. Examples include ash from burning coal and wood. Similarly high surface area active carbon could be produced from agricultural wastes; a few reports of applications of such active carbons are available.

**Low-temperature oxidation of VOCs (with oxygen):** Catalytic oxidation using oxygen has been successfully applied to treat organic and inorganic gases that are frequently encountered in industrial emissions. However, the applications were a direct transfer of technology from other established technologies and high temperatures (300-500 °C) were required. For example, catalytic oxidation of hydrocarbons from automobile exhausts has been directly applied to treat volatile organics from industrial waste gas streams. Additionally, Spivey (1987) notes that the catalytic oxidation applied to an industrial setting is different from a pollution abatement perspective. For example, in an industrial scenario, chemicals are oxidized using oxygen and a variety of catalysts. Because of high concentrations of the reactants (usually neat compounds), and oxidation being exothermic, the process is usually economically feasible. For pollution abatement applications, catalysis which will be henceforth called environmental catalysis (Centi et al., 2002), involve VOCs at low concentrations (< 10,000 ppmv) and excess oxygen. The oxidation rates in such cases are low and hence for complete removal the gases are required to be heated to a higher temperature to enhance higher oxidation rates, thereby making the system a net consumer of heat and expensive. Hence, it is important to develop catalysts that are active at lower temperatures. Efforts have recently been made focusing on the development of highly active catalysts using oxygen as an oxidant. Researchers such as Gomez et al (1999) synthesized high

surface area catalysts by dispersing metal on high-surface area supports, thereby increasing the effective surface area and catalytic activity. However, with advances in nanotechnology and textural characterization techniques efforts are focused towards development of nano-catalysts.

Recent developments in nanotechnology have allowed for the synthesis of nanoparticles of a defined size. The physical, chemical and electronic properties of materials change as the sizes approach a nano-level (Daniel and Astruc, 2004; Li et al., 2006). These properties are being utilized in many medical (Xu and Zhu, 2006), electronic (Matsui, 2005), and catalytic applications (Narayan and Sayed, 2005). Nano structured properties that could be useful in heterogeneous catalysis are based on surface and size.

Nano-scale particles have a high surface to volume ratio compared to bulk metal, allowing for exposing most of the catalytically active area for the reaction to occur. Additionally, due to their nanoscale dimensions, the surface atoms of nanoparticles are higher in number and chemically more active than their bulk counterparts. Moreover, due to the size imperfections, they can also act as electron-hole centers (Zhang and Erkey, 2006). Similarly, when compared to an average bacterial size (1 micron), nano particles are smaller (1-100 nm) (Zhang, 2003). These sizes allow easy transportation and deposition of particles within the entire structure of the catalyst support. Considering that a support matrix has a surface area in several hundreds of  $\text{m}^2/\text{g}$  of the support mass and the reaction is mainly surface based, the catalytic utilization of the material is increased many folds (Tauster et al., 1981). This is important, especially if precious metals are used as precursors. It may also

be noted that the size (particle diameter) of the dispersion may be controlled by manipulating key variables during the catalyst preparation.

As explained above, such nano-sized catalysts if dispersed on a high surface area support could increase the activity and when applied to VOC treatment might allow for higher removal and reaction rates at lower temperature ( $< 200^{\circ}\text{C}$ ). Among the supports widely used are silica and, alumina, although activated carbon supports are also becoming popular. Alumina or silica supports suffer from deactivation especially in humid conditions (Gaur, et al., 2005). Additionally, metal based supports are not stable at higher temperatures and pH conditions ( $\text{pH} > 7$ ) (Auer et al., 1998). Activated carbon on the other hand, provides much higher surface areas than their metal counterparts and can still remain stable at higher temperatures ( $> 200^{\circ}\text{C}$ ) (Juntgen, 1986), acidic or basic pH conditions (Auer et al., 1998) and also allows for recovery and recycling of the impregnated metal especially, if precious metals are used. Furthermore, as activated carbon is hydrophobic, it can minimize water adsorption on the surface that would otherwise interfere with and inhibit the reaction.

Activated carbon as a support for catalytic oxidation of VOCs is not new. Earlier studies have also documented the advantages of using activated carbon supports to disperse metals and metal oxides. For example, Ferraz et al (1999) demonstrated that activated carbon prepared from almond shells impregnated with cobalt and chromium successfully oxidized cyclohexane and benzene. Similar studies on catalytic oxidation of toluene and m-xylene using activated carbon fibers impregnated with transition metals have shown that up to 90 % conversion

efficiencies were achieved (Gaur et al., 2005). Several other reports on catalytic oxidation of VOCs using activated carbons deposited with metal oxides are also available. Some of the available techniques for depositing nano-catalysts on supports are by impregnation, precipitation, and chemical vapor deposition.

Impregnation is a technique by which a solution of a metal precursor is deposited (dispersed) on a support. The method involves bringing the precursor and the support together and provides the necessary conditions (temperature, pH, drying time, etc) to facilitate the deposition of the precursor either by chemical reaction or simply by adsorption. Metal precursors can be impregnated on either metal supports (alumina) or non-metal supports (silica) or even inert matrices (activated carbon). Although, the general principles of impregnation are same for all types of supports, the surface chemistry and chemical interaction between support and precursor can influence the effectiveness of impregnation to a large extent.

In any impregnation process the typical sequence of steps include transport of solute (precursor) into the pore structure of the support, diffusion of the solute within the support pore structure, and uptake (chemical or physical) of the solute by support walls (Anderson and Garcia, 2005). Two types of impregnation techniques are usually used: dry impregnation in which just enough liquid is used to fill the pore volume of the support (also termed incipient wetness), and wet impregnation in which the support is immersed into an excess solution of precursor. As mentioned above, the quality of dispersion of the metal precursor depends on the operating conditions and interaction between support surface and the metal precursor. For

example as explained subsequently, the pH of the process can affect the dispersion to a large extent.

The precursors are attached to the support surface is either via a chemical reaction or physical adsorption. In case of a chemical reaction between support surface and the metal precursor, the surface properties of the support, especially the surface oxygen groups are important. The concentration of these surface oxygen groups can determine the extent of the chemical reaction. On the other hand, for adsorption-based dispersion, the surface charge of the support determines the nature of the dispersion. For example, if the pH of the surface is higher than its isoelectric point (IEP) (pH at which there is no net charge), the surface of the support would be negatively charged. This would allow dispersion of cations effectively. However, if anions were to be dispersed, a pH below IEP would be ideal.

On the other hand, precipitation is a two-process method (Haber et al., 1995): The first process called nucleation in which an in-equilibrium is created on the support by supersaturating the support with any given metal precursor solution. In the subsequent growth step, the precursor moves towards an equilibrium by crystallizing either separately or on the support surface. Precipitation is routinely used to synthesize metals and metal-oxides catalysts by adding the precursor solution to a precipitating solution.

Chemical vapor deposition (CVD) is based on a chemical reaction in which gas molecules are deposited on a support as thin films or powders. This is predominantly used in semiconductor industry and has not been widely used in

catalytic treatment of air pollutants. Hence discussion on CVD will be limited in this chapter.

The above mentioned deposition methods have been successfully used to synthesize catalysts on supports which were used in oxidation of VOCs (Ferrez, et al., 1999; Gaur et al., 2005). However, the control over the physical (size and shape) and chemical (activity) characteristics of the deposited particles was highly limited until recently. However, the development of new techniques in nano science and engineering has led to synthesis of particles whose physical and chemical properties could be controlled (Rao and Trivedi, 2005). One such technique is based on electrochemistry in which the substrate could be deposited with a thin film of catalyst (Natter and Hempelmann, 2003).

### **3.5 Electrochemical deposition**

Electrochemical deposition is increasingly being used to synthesize nano structures. The technique involves transfer of cations from a metal salt solution onto the cathode. A metallic salt is disassociated into anions and cations when dissolved in water. Sufficient electric current through this solution (electrolyte) moves the cations towards the cathode. The cathode provides the electrons to the cations and deposits them on cathode as metals. Electro chemical deposition allows for synthesis of extremely thin films of the metals on the surface area of the supports, which are not possible using a traditional impregnation method.

Noble and transition metals such as gold, silver, platinum, cobalt have successfully deposited using electrochemical processes in form of nano rods in porous alumina. Similarly noble metals have been deposited on activated carbon

rods and fibers. However, literature on electrochemical deposition of metals on granular activated carbon is scarce probably due to practical consideration of preparing granular activated carbon electrodes.

Hence, in addition to the focusing on using wood fly ash to oxidize VOC mixture at low temperature, research is also needed for development of highly active nano-metal catalysts from solid wastes (active carbon and char) by using the principles of nanotechnology and electrochemistry.

## References

1. Anderson, J. A and M. F. Garcia. 2005. Supported Metals In Catalysis. Imperial College Press.
2. Auer, E., A. Freund, J. Pietsch, and T. Tacke. 1998. Carbons as supports for industrial precious metal catalysts. *Applied Catalysis A: General*. 173: 259-271.
3. Bielanski, A and J. Haber. 1979. Oxygen in catalysis on transition metal oxides. *Catal. Rev.-Sci. Eng.* 19 (1): 1-41.
4. Centi, G., P. Ciambelli, S. Perathoner, and P. Russo. 2002. Environmental catalysis: trends and outlook. *Catalysis Today*. 75: 3-15.
5. Chang, C. C and H. S. Weng. 1993. Deep oxidation of toluene on perovskite catalyst. *Ind. Eng. Chem. Res.* (32): 2930-2933.
6. Che, M and A. J. Tench. 1983. Characterization and reactivity of molecular oxygen species on oxide surfaces. *Advances in Catalysis*. (32):1-148.

7. Daniel, M. C. and D. Astruc. 2004. Gold nanoparticles: assembly, supramolecular chemistry, quantum-size-related properties, and applications toward biology, catalysis, and nanotechnology. *Chem. Rev.* 104:293-346.
8. Dimitrova, S., G. Ivanov, and D. Mehandjiev. 2004. Metallurgical slag as a support of catalysts for complete oxidation in presence of ozone. *Applied Catalysis A: General.* 266: 81-87.
9. Einaga, H and S. Futamura. 2005. Oxidation behavior of cyclohexane on alumina-supported manganese oxides with ozone. *Applied Catalysis B: Environmental.* 60: 49-55.
10. Everaert, K and J. Baeyens. 2004. Catalytic combustion of volatile organic compounds. *Journal of Hazardous Materials.* B109: 113-139.
11. Ferraz, M. C. M. A, S. Moser, and M. Tonhaeuser. 1999. Control of atmospheric emissions of volatile organic compounds using impregnated active carbons. *Fuel.* 78 (13): 1567-1573.
12. Fogler, H. S. 1999. Elements of chemical reaction engineering. 4 th Ed. Prentice Hall International Series.
13. Fonseca, R. L., J. I. G. Ortiz, J. R. G. Velasco. 2005. Noble metal loaded zeolotes for the catalytic oxidation of chlorinated hydrocarbons. *React. Kinet. Catal. Lett.* 86 (1): 127-133.
14. Gangwal, S. K., M. E. Mullins, J. J. Spivey, and P. R. Caffrey. 1988. Kinetics and selectivity of deep catalytic oxidation of n-hexane and benzene. *Applied Catalysis.* 36: 231-247.

15. Gaur, V, A. Sharma, and N. Verma. 2005. Catalytic oxidation of toluene and *m*-xylene by activated carbon fiber impregnated with transition metals. *Carbon*. 43 (15): 3041-3053.
16. Gervasini, A, G. C. Vezzoli, V. Ragaini. 1996. VOC removal by synergic effect of combustion catalyst and ozone. *Catalysis Today*. (29): 449-455.
17. Golodets, G. I. 1983. Heterogeneous catalytic reactions involving molecular oxygen. Elsevier Publications.
18. Gomez, M. J. I, E. Raymundo-Piñero, A. García-García, A. Linares-Solano, and C. Salinas-Martínez de Lecea. 1999. Catalytic NO<sub>x</sub> reduction by carbon supporting metals. *Applied Catalysis B: Environmental*. 20 (4): 267-275.
19. Gunten, U. V. 2003. Ozonation of drinking water: part I. Oxidation kinetics and product formation. *Water Research*. 37: 1443-1467.
20. Haber, J, J. H. Block, and B. Delmon. 1995. Manual of Methods and Procedures for Catalyst Characterization. *Pure and Applied Chemistry*. 67 (8-9): 1257-1306.
21. Hermia, J and S. Vigneron. 1993. Catalytic incineration for odor abatement and VOC destruction. *Catalysis Today*. (17): 349-358.
22. Hoigne, J. 1997. Inter-calibration of OH radical sources and water quality parameters. *Wat. Sci. Tech*. 35 (4): 1-8.
23. Horden, B. K., M. Ziolk, and J. Nawrocki. 2003. Catalytic ozonation and methods of enhancing molecular ozone reactions in water treatment. *Applied Catalysis B: Environmental*. 46: 639-669.

24. Imamura, S., M. Ikebata, T. Ito, and T. Ogita. 1991. Decomposition of ozone on a silver catalyst. *Ind. Eng. Chem. Res.* 30: 217-221.
25. Juntgen, H. Activated carbon as a catalyst support. 1986. *Fuel.* 65:1436-1446.
26. Kastner, J. R., Q. Buquoi, R. gangavaram, and K. C. Das. 2005. Catalytic oxidation of gaseous reduced sulfur compounds using wood fly ash. *Environmental Science and Technology.*
27. Konova, P., M. Stoyanova, A. Naydenov, St. Christoskova, and D. Mehendjiev. 2006. Catalytic oxidation of VOCs and CO by ozone over alumina supported cobalt oxide. *Applied Catalysis A: General.* 298: 109-114.
28. Langlias, B., D. A. Reckhow, and D. R. Brink. 1991. Ozone in water treatment: application and engineering: cooperative research report. Lewis Publishers, New York, 1991.
29. Langlais, B and D. A. Reckhow. 1991. Ozone in water treatment: application and engineering: cooperative research report/American water works association research foundation.
30. Li, L., M. Fan, R. C. Brown, J. V. Leeuwen, J. Wang, W. Wang, Y. Song, and P. Zhang. 2006. Synthesis, properties, and environmental applications of nanoscale iron-based materials: A review. *Critical Reviews in Environmental Science and Technology.* 36: 405-431.
31. Ma, J and N. J. D. Graham. 1999. Degradation of atrazine by manganese-catalysed ozonation: Influence of humic substances. *Water Research.* 33 (3): 785-793.

32. Matsui, I. 2005. Nanoparticles for electronic device applications: a brief review. *Journal of Chemical Engineering of Japan*. 38(8): 535-546.
33. Mehandjiev, D., A. Naydenov, and G. Ivanov. 2001. Ozone decomposition benzene and CO oxidation over  $\text{NMnO}_3$ -ilmenite and  $\text{NiMn}_2\text{O}_4$ -spinel catalysts. *Applied Catalysis A: General*. 206: 13-18.
34. Narayan, R and M. A. E. Sayed. 2005. Carbon-supported spherical palladium nanoparticles as potential recyclable catalysts for the Suzuki reaction. *Journal of Catalysis*. 234 (348-355).
35. Natter, H and R. Hempelmann. 2003. Tailor-made nanomaterials designed by electrochemical methods. *Electrochimia Acta*. 49: 51-61.
36. Naydenov, A., R. Stoyanova, and D. Mehandjiev. 1995. Ozone decomposition and CO oxidation on  $\text{CeO}_2$ . *Journal of Molecular Catalysis A: Chemical*. 98: 9-14.
37. Oyama, S. T. 2000. Chemical and catalytic properties of ozone. *Catal. Rev. - Sci. Eng.* 42 (3): 279-322.
38. Rao, R. K. C and D. C. Trivedi. 2005. Chemical and electrochemical depositions of platinum group metals and their applications. *Coordination Chemistry Reviews*. 249: 613-631.
39. Reed, C, Y. K. Lee, and S. T. Oyama. 2006. Structure and Oxidation State of Silica-Supported Manganese Oxide Catalysts and Reactivity for Acetone Oxidation with Ozone. *J. Phys. Chem. B*, 110 (9): 4207-4216.
40. Smith, J.M., *Chemical Engineering Kinetics*. McGraw-Hill, New York, 1981.

41. Spivey, J. J. 1987. Complete catalytic oxidation of volatile organics. *Ind. Eng. Che. Res.* 26: 2165-2180.
42. Stoyanova, M., P. Konova, P. Nikolov, A. Naydenov, St. Christoskova, and D. Mehandjiev. 2006. Alumina-supported nickel oxide for ozone decomposition and catalytic ozonation of CO and VOCs. *Chemical Engineering Journal.* 122: 41-46.
43. Tauster, S. J., S. C Fung, R. T. K. Baker, and J. A. Horsley. 1981. Strong interactions in supported-metal catalysts. *Science.* 211(4487):1121-1125.
44. Tidahy, H. L, S. Siffert, F. Wyrwals, J. F. Lamonier, and A. Aboukais. 2006. Catalytic activity of copper and palladium based catalysts for toluene total oxidation. *Catalysis Today.* (119): 317-320.
45. Tseng, T. K and H. Chu. 2001. The kinetics of catalytic incineration of styrene over a MnO/Fe<sub>2</sub>O<sub>3</sub> catalyst. *The science of total Environment.* (275): 83-93.
46. Tsou, J., L. Pinard, P. Magnoux, J. L. Figueiredo, and M. Guisnet. 2003. Catalytic oxidation of volatile organic compounds (VOCs): oxidation of o-xylene over Pt/HBEA catalysts. *Applied Catalysis B: Environmental.* 46: 371-379.
47. Xi, Y., C. Reed, Y.K. Lee, and S. T. Oyama. 2005. Acetone oxidation using ozone on manganese oxide catalysts. *J. Phys. Chem. B.* 109: 17587-17596.
48. Xu, Q., Y. Zhao, J. Z. Xu, and J. J. Zhu. 2006. Preparation of functionalized copper nanoparticles and fabrication of glucose sensor. *Sensors and Actuators B.* 114 (379-386).

49. Zhang, W. 2003. Nanoscale iron particles for environmental remediation: overview. *Journal of Nanoparticle Research*. 5: 323-332.
50. Zhang, Y, and C. Erkey. 2006. Preparation of supported metallic nanoparticles using supercritical fluids: A review. *J. of supercritical Fluids*. 38 (252-267).
51. Zhang, C., H. He, K. Tanaka. 2005. Perfect catalytic oxidation of formaldehyde over a Pt/TiO<sub>2</sub> catalyst at room temperature *Catalysis Communications*. 6: 211-214.

## CHAPTER 4

### RESEARCH OBJECTIVES AND HYPOTHESES

Based on the literature review on catalytic oxidation of VOCs and previous experience on catalytic oxidation of a limited number VOCs, this research will focus on:

- 1) Studying the kinetics of low-temperature (25-150 °C) catalytic oxidation of aldehydes using wood fly ash.
  - Determination of kinetic parameters for 2-methylbutanal (2-MB), 3-methylbutanal (3-MB), and hexanal,
  - Develop empirical (Power Law) and redox-based mechanistic models describing aldehyde oxidation,
  - Study the oxidation rates of a binary aldehyde mixture,
  - Determination of inhibitory effects due to a mixture, and
  - Study the effect of ozone as an oxidant in the catalytic process.
- 2) Synthesis of novel metal-oxide catalysts by electrochemical deposition process.
  - Synthesize nickel and cobalt oxide nano particles on activated carbon by an electrochemical process,
  - Characterize the catalysts in terms of their structural and textural properties, deposition patterns, and

- Compare the catalytic activity of the electrochemically generated nano-catalysts for propanal removal to activated carbon without metal deposition (i.e., a control).

## **Hypotheses**

1. Kinetic studies on catalytic oxidation of VOC mixtures (aldehydes) at low temperatures (25-160 °C) using wood fly ash: As will be shown later in this report, wood fly ash contains metals (iron, cobalt, etc), metal oxides, and active carbon in its structure. These components are known to exhibit catalytic properties particularly in oxidizing VOCs. Additionally active carbon, due to its structure might promote sorption (physical or chemical) followed by chemical catalysis of the target VOCs by the metallic fraction. The target VOCs on the other hand are known to undergo auto oxidation processes by forming highly reactive free radicals (by hydrogen abstraction from the VOC and converting VOC into a radical) when they react with oxygen in the presence of a catalyst. This free radical chain reaction is theorized to oxidize the VOCs.

2. Develop nano-metal catalysts by depositing transition metals on activated carbon using an electrochemical processes: The physical, chemical and electronic properties of materials change as their sizes approach the nano-level. Some of these properties can be used for applications in heterogeneous catalysis. Electrochemical deposition allows for synthesis of extremely small particles with high surface areas (for instance nanotubes and rods) which are not possible using a traditional impregnation method. Additionally in traditional impregnation techniques, non uniform metal clusters are formed on the surface

underutilizing a large fraction of available support surface area. Electrochemical process on the other hand is expected to cover entire surface area with a nano-layer of the metal precursor thereby increasing the catalytic active surface area.

The chapters that follow address the above mentioned objectives. The first objective was studied in chapters five and six. In chapter five, wood fly ash was tested as a catalyst for oxidizing 3-MB. Based on the experimental data obtained, the kinetic and activation parameters were determined. Additionally, a reaction mechanism was proposed that described the oxidation of 3-MB. In chapter six, we extended our hypothesis on wood fly ash to treat 2-MB and hexanal. The aldehydes, 2-MB and hexanal, were tested individually to obtain kinetic and activation parameters, and as a mixture to study the effect of the presence of each aldehyde. A carbon balance was also performed on each of the aldehydes tested. Additionally, ozone was tested as an oxidant to determine if 100 % removal of the aldehydes could be obtained.

In chapter seven, nickel and cobalt catalysts were synthesized on granular activated carbon (GAC) pellets using electrochemical deposition. These catalysts were tested for oxidation of propanal using ozone as an oxidant and compared with GAC which acted as a control.

## CHAPTER 5

### LOW TEMPERATURE CATALYTIC OXIDATION OF ALDEHYDES USING WOOD FLY ASH AND MOLECULAR OXYGEN<sup>1</sup>

**Praveen Kolar, James R. Kastner\*, Joby Miller**

Dept. of Biological and Agricultural Engineering

Driftmier Engineering Center

The University of Georgia, Athens GA 30602, USA

\*Corresponding author: [jkastner@engr.uga.edu](mailto:jkastner@engr.uga.edu); Phone: 706-583-0155

---

<sup>1</sup> Kolar, P., J. R. Kastner., and J. Miller. 2007. *Applied Catalysis B: Environmental*, 76: 203-217.  
Reprinted here with the permission of publisher.

## 5. 1. Introduction

Poultry rendering operations convert organic wastes (feathers, offal, dead birds, blood, and hatchery by-products) to products such as feed additives and fertilizer, typically hydrolyzing these components in batch mode at 140-150°C (276-345 kPa) for 20-45 minutes to breakdown the keratin, and the meat by-products or offal are typically treated at 121-135°C (172-517 psig) with varying residence times depending on the mode of operation, batch or continuous [1]. During these thermal degradation and drying steps, volatile organic compounds (VOCs) are generated, some of which are odorous. Overhead vapors from the feather hydrolyzer and driers are passed through condensers to remove some VOCs and volatile organic sulfur compounds (VOSCs). The non-condensables are typically passed through chemical wet scrubber units, using for example hypochlorite (HOCl), chlorine dioxide (ClO<sub>2</sub>) or ozone (O<sub>3</sub>), to remove the VOC fraction not removed in the condensers.

Poultry rendering operations in the U.S. have recently come under regulatory scrutiny for odor and volatile organic compound (VOC) air quality issues [2]. Although the industry has a good track record of minimizing odors, urbanization and odor complaints have resulted in the need for low cost, effective treatment options. Rendering facilities in non-attainment areas are also facing EPA regulations, that limit VOC emissions and potentially requires new air pollution control technology for the industry. Most rendering operations use wet scrubbers for off gas treatment and typically obtain efficiencies of 85-90%, based on odor dilution to thresholds units, but use chemicals for oxidation (e.g., ClO<sub>2</sub> and/or O<sub>3</sub>). However, previous analysis of wet scrubber systems for VOC removal indicated very poor performance towards VOCs - only 40-65% removal of VOCs using ClO<sub>2</sub> [2]. Detailed kinetic analysis has

indicated that chlorine dioxide ( $\text{ClO}_2$ ), one of the primary oxidizing chemicals used in the rendering industry, does not react with hexanal, 2-methylbutanal, and 3-methylbutanal (compounds identified in rendering emissions) under any conditions (e.g., high pH or temperatures  $> 25^\circ\text{C}$ ), all of which constitute a major fraction of VOC emissions [3]. However, hexanal, 2-methylbutanal, and 3-methylbutanal are VOCs and have been associated with negative odor properties such as grassy, rancid, painty, and chemical smells [4, 5]. Hexanal has been identified as the primary odor causing compound in the overuse of frying oil and the branched aldehydes associated with wastewater odors [4, 5]. In addition ozone ( $\text{O}_3$ ), another oxidizing agent sometimes used in wet scrubbers does not react with aldehydes at a high reaction rate [6] and GC/MS analysis of an industrial scale chemical wet scrubber using  $\text{ClO}_2$  and  $\text{O}_3$  (without catalysts) indicated no enhancement in the removal of the aldehyde fraction relative to  $\text{ClO}_2$  alone [7]. One possibility which has not been explored extensively is to utilize a catalyst, either suspended in the scrubbing liquid (in fine powder form), coated on the surface of the packing material, or in a packed-bed treating the dissolved components in liquid recycle, to promote a reaction between the dissolved VOC (i.e., aldehydes in this case) and the oxidizing agent (e.g.,  $\text{ClO}_2$ ). This concept has been explored in Advanced Oxidation Processes (AOP) such as catalytic ozonation ( $\text{O}_3$  plus a heterogeneous catalyst [8]) and in the use of a nickel based catalyst coupled with sodium hypochlorite ( $\text{NaClO}$ ) for  $\text{H}_2\text{S}$  and volatile organic sulfur (e.g., methylmercaptan) oxidation [9]. However, there has been limited research on catalytic oxidation using  $\text{ClO}_2$ , especially for VOC oxidation, and the development of inexpensive catalysts.

Many solid waste sources contain metals or metal oxides of high surface area such that they could potentially be recycled and used as environmental catalysts [10]. Wood fly ash is produced in large and growing volumes in the USA (5.5 million tons/yr) with a majority landfilled [11]. Recent research has demonstrated that wood fly ash can catalytically oxidize H<sub>2</sub>S using molecular oxygen (O<sub>2</sub>), and volatile organic sulfur compounds (e.g., methylmercaptan) and propanal, in the presence of ozone [12-14]. It was theorized that wood fly ash given its reasonably high surface area (~45 m<sup>2</sup>/g), the presence of carbon (potential adsorbent and/or catalyst), and crystalline metal oxides phases (magnetite and hematite), acted as a catalyst to promote the oxidation of these compounds. Since many rendering facilities use ClO<sub>2</sub> as an environmentally friendly oxidizing agent (relative to NaOCl which can produce chlorinated hydrocarbons), it was of interest to determine if wood fly ash would act as a catalyst to promote the low temperature (20-25°C) oxidation of critical aldehydes detected in rendering emissions. Our primary objectives were to determine if wood fly ash could act as a low-cost catalyst to oxidize 3-MB, identify any partial oxidation products, measure oxidation rates, and determine phases in the ash responsible for activity.

## **5.2. Experimental Methods**

### **5.2.1 Catalyst and Characterization**

Wood fly ash from a pulp mill was used in this study. The physical and chemical characteristics of the fly ash, including pH, surface area, bulk density, and the elemental composition were previously determined [13, 14] and are reported in Table 1. The measured pH of wood fly ash in solution was 12.

### 5.2.2 XRD Methods

X-ray diffraction (XRD) analyses were performed with a Scintag XDS 2000 diffractometer equipped with a cobalt X-ray tube. Powdered samples were mounted on quartz plates and stepped scanned over the angular range 15-50° 2 $\theta$  [13].

### 5.2.3 Batch Studies

Oxidation studies were performed in batch reactor systems consisting of 120 ml amber or dark, serum bottles (Fischer Scientific) capped with Mininert™ valves (Valco Instruments Co. Inc, Houston TX). Batch reactors received a defined mass of catalyst (typically 1 g) plus 30 ml of water (deionized) contacted with a known, initial amount of aldehyde (e.g., gas phase of 60-300 ppmv) at time zero. Time zero and multiple samples thereafter were taken via gas-tight syringes (500  $\mu$ l; VICI Precision Sampling, Inc. Baton Rouge, LA) from the gas phase and quantified using gas chromatography to define the rate of compound loss from the headspace. To potentially identify reaction by-products in the liquid phase, liquid samples (a slurry containing liquid and catalyst particles) were collected at the end of the reactions and analyzed by GC/MS analysis (details later in section). All batch reactions were performed in triplicate.

Typically, 1 gram of ash in 30 ml of water was contacted with 3-methylbutanal (97% Sigma-Aldrich) ranging in gas phase concentrations at time zero from 60-300 ppmv. All chemicals were stored at 4°C in the dark. After addition of the neat aldehyde, reactors were agitated for approximately 1 minute at 250 rpm and 30°C on an Innova 4000 Incubator shaker table before sampling the reactors in the shaker (New Brunswick Scientific, Edison NJ). In these reactor systems, the headspace was sampled infrequently, approximately every 24 hours, and the batch

reactors were used to determine if a catalytic reaction occurred. In order to better evaluate the overall rate of oxidation within the batch reactors, another set of experiments was performed in which the headspace was sampled more frequently, at approximately 15-30 second intervals; in these systems the reactors were hand agitated and sampled at room temperature (23-25°C).

## **5.2.4 Continuous Flow Studies**

### **5.2.4.1 Isothermal Conditions**

The extent of 3-methylbutanal (3-MB) conversion was also measured in a continuous flow, packed bed reactor as outlined in Kastner et al., 2003, except that 3-MB (97% Sigma-Aldrich) was added via a syringe pump (Cole-Parmer, Model 74900-30) downstream from the humidifier and up-stream from the static bed mixer [13]. Typically, liquid 3-MB was injected 8-9 hours before sampling the reactor and then fractional conversion was measured over the course of 3 hours for different inlet conditions. Periodically, for a defined inlet condition, the reactor was operated overnight (12-24 hours) and then sampled to measure fractional conversion. Fractional conversion was measured in two ways. Tedlar bags were used to collect outlet gases and injected on the GC/FID, followed by tedlar bag sampling of the inlet, and finally tedlar bag sampling of the outlet for confirmation. Alternatively, inlet and outlets were simultaneously sampled through ports with septum using gas-tight syringes (VICI Precision Sampling, Inc. Baton Rouge, LA Model Pressure-Lok, 1-2 ml) and directly analyzed via GC/FID. The two methods resulted in similar concentrations and the results for the latter method are reported. For the experimental results reported here the inlet 3-MB concentration ranged between 8 and 67 ppmv (at 24°C and 1 atm). The syringe used in this process was a Becton

Dickinson syringe (plastipak 10 cc, 14.48 mm i.d.) and 3-MB was injected via a tee (stainless steel, Swage-Lock) into the main airflow upstream from the bubble column into the static mixer.

Wood fly ash (10 g ash, 40% H<sub>2</sub>O (g/g), wet basis) was distributed in glass wool (8 μm, Corning Glass NY) and packed over a defined height in the reactor (27 cm). Glass wool was also distributed above and below the distributed ash to promote plug flow (over the entire reactor height). The residence time based on the gas flow rate and packing height of the catalyst was fixed at 2.0 seconds and inlet reactant concentrations ranged from 8 to 67 ppmv (0.0008 – 0.0067 % (v/v)). The reactor was covered in black felt to prevent artifacts due to photochemical oxidation. All kinetic studies were carried out at 23-25°C and atmospheric pressure and demonstrated to be isothermal and constant pressure [102.4 kPa or 1.01 atm, 13].

Control experiments were also performed in which 3-MB vapor in humidified air was fed to the reactor with only glass wool present and the fractional conversion measured. At inlet 3-MB concentrations of 15 and 41 ppmv fractional conversions ( $X = \frac{C_{g,in} - C_{g,out}}{C_{g,in}}$ ) of 0.083 and 0.076 were measured respectively, compared to 0.27, 0.25, and 0.20 for 8, 17, and 67 ppmv inlet concentrations of 3-MB in the presence of glass wool and wood fly ash. The low level of measured 3-MB removal without the presence of wood fly ash may have been due to a gas phase reaction and/or a surface reaction.

#### **5.2.4.2 Temperature Effect**

Additional kinetic studies were performed isothermally at three higher temperatures (80, 120, and 160 °C) and a constant pressure (1.01 atm). The entire reactor was wrapped in thermal heating tape and the temperature manually

controlled via a thermolyne stepless input controller (Model 45515, Barnstead International, Dubuque, IA).

#### **5.2.4.3 Analytical Methods**

The gas phase of the batch reactor headspace and inlet and outlet concentrations in the continuous flow experiments was analyzed using a Hewlett-Packard 5890 gas chromatograph, equipped with a SPB-1 (30 m, 0.32 $\mu$ m) sulfur capillary column, and operated with split injection and a flame ionization detector (FID). Separations were performed under both isothermal and temperature ramped conditions with the SPB-1 capillary column (Supelco, Bellefonte, PA). Ramped temperature conditions consisted of an initial oven temperature of 30°C for 1 minute, increasing to 80°C @ 5 degrees a minute, and held at 80°C for 1 minute. The inlet and detector temperatures were set at 250°C, the split flow ratio at 30:1 and the sample injection volume was 500  $\mu$ l. The isothermal temperature conditions consisted of an oven (column) temperature of 80°C, inlet and detector temperatures of 250°C, and a split ratio and sample size the same as above. Standard curves were prepared from gas and liquid standards in the range of 0-200 ppmv using 1L tedlar bags and calibrated gas syringes.

#### **5.2.4.4 Analyses of Partial Oxidation Products (Headspace GC/MS)**

At the end of the reactions between 3-MB and the wood fly ash, a sub-sample of the well mixed slurry (catalyst in suspension) was analyzed via headspace GC/MS analysis (HAPSITE Inficon, East Syracuse NY). A 10 ml aliquot of the slurry was rapidly transferred to a vial with a septum and heated at 80°C for 5 minutes. The headspace was then transferred by N<sub>2</sub> purging through a needle and

heated probe (50°C) to the GC/MS. The resultant gas sample was analyzed under isothermal conditions (70°C) using an SPB-1 SULFUR column (Supelco, Bellefonte PA) and MS detector (Inficon, m/z ratio from 45-150) as outlined in Kastner et al., 2002 [2].

#### **5.2.4.5 Henry's Law Constants**

Equilibrium partitioning in a closed system (EPICS) was used to estimate the partitioning coefficients of 3-MB with water; the partition coefficient for 2-MB and 3-MB were assumed to be similar [16, 17]. The partition coefficient, was calculated from measurements of the vapor concentration in the headspace over water and a defined concentration of 3-MB. Solutions were prepared using nanopure water, and all experiments were performed in 120 ml serum vials sealed with Mininert™ valves. Five to ten microliters of neat liquid 3-MB were added to sealed bottles of the same total volume (120 ml), but different liquid volumes ( $V_l$ , 30 or 60 ml) through the valve with a glass microliter syringe. The bottles were incubated for 24 h at 250 rpm and 20-23°C and each system (#1-30 ml  $V_l$ , 90 ml  $V_g$  and #2-60 ml  $V_l$ , 60 ml  $V_g$ ) was performed in triplicate.

The partition coefficient was found to be  $7.42 \times 10^{-3}$  (25.2-25.5°C) and the Henry's constant for 3-MB in water was calculated to be  $1.8 \times 10^{-4}$  atm m<sup>3</sup>/mole at 25°C, which is consistent with values reported by Staudinger and Roberts, 1996 [18]. This result was similar to the partition coefficients for straight chain aldehydes of 5 carbons. The partition coefficients of propanal, butanal, pentanal, and hexanal are reported as  $2.25 \times 10^{-3}$ ,  $2.98 \times 10^{-3}$ ,  $4.44 \times 10^{-3}$ , and  $5.78 \times 10^{-3}$ , respectively at 20°C and  $3.1 \times 10^{-3}$ ,  $4.2 \times 10^{-3}$ ,  $6.3 \times 10^{-3}$ , and  $8.2 \times 10^{-3}$  at 25°C [18]. Correlations

found in the literature were used to calculate Henry's Law constants at different temperatures [18].

#### 5.2.4.6 Batch Kinetics

The initial, overall rate of oxidation was estimated in two manners - 1) from the change in gas phase concentrations (equation 1), and 2) from the indirectly calculated liquid phase concentration using Henry's Law and the mass of catalyst used (equation 2). Liquid phase concentrations were calculated from the measured gas phase concentrations (initial slope – 3-4 points after quasi equilibrium was established) and Henry's law constant – equilibrium between the gas and liquid phase was assumed. A constant volume batch reactor was assumed in the calculations.

$$-r_j = -\frac{dC_g}{dt} = kC_g \quad (1)$$

$$-r'_j = -\frac{dC_L}{dt} \frac{V_L}{W} = \frac{-d\left(\frac{C_g}{m}\right)}{dt} \frac{V_L}{W} \quad (2)$$

where, j is the reacting species, for example 3-MB;  $-r'_j$  is the reaction rate in the liquid phase (moles/g of catalyst-s);  $V_L$  is the liquid phase volume (L);  $C_L$  is the concentration of 2-MB or 3-MB in the liquid phase (moles/L);  $C_g$  is the gas phase concentration (moles/L); W is the mass of catalyst (g); m is the dimensionless

partition coefficient ( $C_g/C_L$ ) for 3-MB and water at the reaction temperature, and MW is the molecular weight of the reactant (e.g., 3-MB in g/mole).

#### 5.2.4.7 Continuous Flow Reactor Kinetics and By-Products

The overall rate of oxidation was calculated from the measured fractional conversion, mass of the ash, volumetric gas flow rate, inlet mole fraction, pressure, and temperature using the following equation.

$$-r = Q \frac{P}{RT} y \frac{X}{W} MW \quad (3)$$

where,  $-r$  is the reaction rate (mg/g-min),  $Q$  is the flow rate (L/min),  $y$  is the mole fraction in the inlet,  $X$  is the fractional conversion,  $W$  is the mass of catalyst (g),  $P$  is pressure (atm),  $R$  is the ideal gas constant,  $T$  is the temperature (K), and  $MW$  is the molecular weight of the reactant (e.g., 3-MB). Fractional conversion ( $X$ ) was determined as the difference between the inlet and outlet concentration divided by the inlet concentration. Inlet and outlet concentrations at each time point were analyzed in triplicate and the mean used in calculations.

#### 5.2.4.8 Identification of By-Products

In an additional experimental phase, the inlet and outlet gas samples from the continuous reactor were analyzed using a gas chromatograph (Model 6890, Agilent) equipped with a mass selective detector (Model 5973). Ultra high pure (99.99 %) helium (3.5 ml/min) was used as a carrier gas and a SPB-1 sulfur capillary column (0.32  $\mu$ m, 30 m) (by Supelco Inc. Bellefonte, PA) was used for separation of gases. A sample size of 250 $\mu$ L (splitless) was used. All separations were performed isothermally at a column oven temperature of 80°C and detector temperatures of 250°C. Samples were analyzed for 8 minutes using a full scan

mode ( $m/z$ : 40-150) and one additional experiment (160°C, 525 ppmv 3-MB inlet) was performed using both full scan and selective ion monitoring ( $m/z$ 's: 43 for acetone, 58 for 3-MB and 60 for isovaleric acid) to lower the detection limit and quantify acetone. Acetone standard curves were prepared from neat liquid using 1-L tedlar bags and calibrated gas-tight syringes (using the SIM method). The sample analyses was carried out using ChemStation software (Agilent) and identification was carried out using National Institute of Standards and Technology (NIST) database (version 1.6) equipped with an automated mass spectral deconvolution and identification system (AMDIS).

Reaction byproducts were not identified in experiments carried out at low 3-MB inlet concentrations even at higher temperatures (80, 120, and 160°C – all in full scan mode). However, when the inlet concentration was increased to 525 ppmv (160°C), acetone was identified using full scan mode with a retention time of 1.23 minutes (SPB-1) and matching quality of 9 out of 10. To minimize the spectral noise and lower detection limits, subsequent runs were carried out using a selective ion monitoring [ $m/z$ : 43 (acetone), 58 (3-MB) and 60 (isovaleric acid)]. To confirm our findings, retention time matching using neat acetone and 3-methylbutanoic acid was performed; retention times of the reaction byproduct and the acetone standard matched (1.23 minutes), but 3-methylbutanoic acid was not detected in any of the experiments.

## **5.3 Results and Discussion**

### **5.3.1 Evidence for Catalytic Activity**

Analysis of the batch reactor headspace versus time indicated that the presence of wood fly ash appeared to catalyze the oxidation of 3-methylbutanal with

oxygen appeared to act as an oxidant in the catalytic reactions (Figure 5.1 for 3-MB, WFA, and O<sub>2</sub> only). Relative to a control without the catalysts, repeated spikes of 2-MB or 3-MB to the reactors resulted in a reduction of these compounds below detection limits of the GC/FID and ultimately unknown peaks formed in the gas phase of the reactors. For example, GC/FID analysis of the headspace during addition of 3-MB to a slurry of wood fly ash (with O<sub>2</sub> only) indicated the formation of new unknown peaks that had not been observed in the initial phase of the reaction and the peak area of the predominant unknown peak increased with time, indicative of a catalytic reaction (Figure 5.2). A more detailed analysis of the GC/FID chromatograms indicated the formation of unknown compounds as a function of time in the wood fly ash/O<sub>2</sub> systems (Figure 5.3).

Thus, there are multiple lines of evidence that wood fly ash (WFA) acted as catalysts to promote the oxidation of 3-methylbutanal using O<sub>2</sub> as the oxidant. Oxidation of 3-MB in the presence of O<sub>2</sub> alone was very slow (Figures 5.1 and 4 - controls) and previous research has demonstrated that aldehydes do not react with ClO<sub>2</sub> alone [3]. The initial rate of oxidation (based on a simple first order rate law for removal of 3-MB from the gas phase in the batch reactors) was found to be proportional to the mass of WFA, indicative that a surface catalyzed reaction was promoted by the insoluble fly ash (Figure 5.5). Finally, as will be noted later, 3-MB was continuously removed in a reactor packed with wood fly ash, but only in the presence of O<sub>2</sub> (Figure 5.6). Taken together these results suggest that 3-MB was catalytically oxidized using the WFA or AC and removal was not solely due to adsorption. Although we did not test all of the aldehydes measured in rendering emissions, these data suggest that a majority of the aldehydes (e.g., the branched

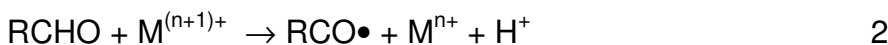
aldehydes are typically > 60% of the VOCs in poultry rendering emissions – based on a concentration basis; [2] Kastner et. al., 2002a) could be catalytically oxidized in the presence of wood fly ash using molecular oxygen, but this needs to be confirmed (e.g., test the catalytic oxidation of hexanal).

### 5.3.2 Potential Mechanism and End Products

#### 5.3.2.1 Oxygen as Oxidant.

Metal ions, such as  $\text{Co}^{2+}$ ,  $\text{Mn}^{2+}$  and  $\text{Fe}^{3+}$ , have been shown to catalytically initiate the oxidation of aldehydes using  $\text{O}_2$  in different solvents, leading to free radicals and a series of propagation and termination reactions [equations 1-6; 20,21,22]. It has also been suggested that oxygen can directly react with aldehydes on metal/metal oxide active sites initiating free radical formation (equation 1; 21). The primary product of the metal ion catalyzed oxidation is reportedly a carboxylic acid [equation 5; 20, 21].

Initiation:



Propagation:



Carboxylic Acid Production:



However, side reactions leading to the formation of  $\text{CO}$ ,  $\text{CO}_2$ , hydrocarbons, alcohols, and ketones have been reported for branched aldehydes [equations 8-12;

20, 22]. These side reactions appear to be promoted by metals; e.g., the branched aldehydes, 2-ethylhexanal and 2-methylpentanal were oxidized to products predominately other than carboxylic acids in the presence of Co, Mn, and Ni catalysts at 80°C [21].

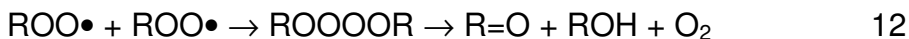
Termination and CO<sub>2</sub> Production:



Catalytic Propagation, CO, CO<sub>2</sub> and Hydrocarbon Production:



Ketone and Alcohol Formation:



Headspace analysis of the residual, liquid slurry phase using GC/MS analysis suggested the formation of ketones and hydrocarbons, but not carboxylic acids (batch reactors). Initially, acetone was identified to be the primary by-product in the reaction between 3-MB, O<sub>2</sub>, and wood fly ash (Figure 5.7). Additionally, the formation of acetone from 3-MB (based on continuous flow experiments discussed later) was conclusive based on potential oxidation pathway analysis (using equations 1-12), MS spectral analysis, and retention time matching with a pure standard (Figure 5.8).

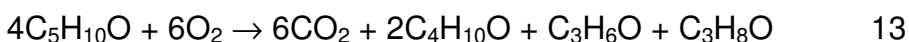
Although the match factor of the MS analysis of the “acetone” peak was high (>900), the probability value was low (60.6%, in the batch systems); for example, this compares to a match factor > 930 and a probability of 89.5% for identification of 2-butanone from the oxidation of 2-MB. This was probably due to the fact that our GC/MS analysis was performed in the total ion chromatogram (TIC) mode from a mass to charge ratio of 45 to 150 amu’s (batch system).

Subsequently, we performed continuous flow experiments at higher temperatures and 3-MB inlet concentrations coupled with MS analysis to determine the formation of end products. When we increased the inlet concentration of 3-MB to 525 ppmv (160°C), acetone was detected in the reactor outlet (determined via mass spectral matching and retention time matching with a standard - Figure 5.8). Based on the acetone concentration in the outlet and fractional conversion of 3-MB, the yield of the acetone (moles of acetone formed per mole of 3-MB reacted) during the oxidation reaction was determined to be 0.26 (160°C, 525 ppmv inlet, 10 g WFA).

The conclusive evidence for formation of acetone from 3-MB, the measured molar yield of acetone from 3-MB (0.26 mole/mole versus the theoretical value of 0.25 in equation 13), the lack of carboxylic acid formation, coupled with previous data indicating the formation of 2-butanone from 2-MB, does indicate a free radical reaction occurred between the aldehydes and O<sub>2</sub> that is catalyzed by the wood fly ash leading to the formation of CO<sub>2</sub>, ketones, and alcohols. Given the high concentration of oxygen relative to the aldehyde (~20% O<sub>2</sub> or 200,000 ppmv versus 45-525 ppmv for 3-MB), one would anticipate a rapid formation of free radicals on the surface of the catalyst (Eqs. 1 and 2), with a very low concentration of aldehyde available to react with the radicals to form a carboxylic acid (Eq. 5). We theorize that

under these conditions, reaction steps 6-12 would be promoted over step 5 (formation of carboxylic acid). In this scenario, 2-methylpropanal is proposed to be formed as an intermediate and 2-methylpropanol as a end product (step 6, 11, and 12, from 3-MB), in which the 2-methylpropanal undergoes further free radical oxidation to form acetone and 2-propanol (steps 6, 11 and 12) and due to the low level of aldehyde a hydrocarbon would not be formed (step 9).

Proposed Overall 3-MB Oxidation Reaction:



Such a proposed mechanism for free radical oxidation of 2-ethylhexanal and 2-methylpropanal has previously been validated [22, 23]. The primary difference between our work and these references was that our work was conducted with a gas phase substrate/reactant with O<sub>2</sub> in excess. Our results are similar to those reported for the observed the formation of acetone, methanol and *tert*-butylalcohol from isobutane when the oxidation was conducted in the gas phase at 155°C [24]. The one drawback to our proposed mechanism is the fact that we did not detect the formation of 2-methylpropanol or 2-propanol. It is possible that our GC column was not capable of resolving the alcohols or the concentrations produced in the outlet of the reactor were below our detection limits.

Finally, it was not possible to detect/quantify CO<sub>2</sub> in the experiments using the GC/MS system, since the column we used (SBP-1 Sulfur) was not capable of separating CO<sub>2</sub> from components in air (e.g., N<sub>2</sub>, O<sub>2</sub>) as well as other potential by-products, such as CO. The MS was operated in full scan above 45 to prevent a background signal from the carrier gas (in this case nitrogen, or contaminants in the carrier gas; Hapsite, Inificon) that would have overwhelmed any signals from other

compounds; e.g., low levels of H<sub>2</sub>O, O<sub>2</sub>, CO<sub>2</sub>, N<sub>2</sub>O or N<sub>2</sub>. Ultra high pure N<sub>2</sub> was used as the carrier gas and was required by the manufacturer due to the use of a different type of vacuum pump (Hapsite, Inficon). We did attempt to measure CO<sub>2</sub> on a separate GC, using a PLOT Q column (packed-bed column) and TCD detector; however, the TCD detection limit (200-300 ppmv) was higher than the anticipated CO<sub>2</sub> levels (or difference in CO<sub>2</sub> levels for the packed-bed experiments) that would be produced from oxidation of 3-MB in the 5-525 ppmv range (for the continuous flow experiments) or 60-300 ppmv in the batch reactors. Similarly, we were unable to accurately quantify the amount of CO<sub>2</sub> produced in the continuous flow apparatus when using the SBP-1 column and a GC/MS technique in full scan from 40-150 m/z due to interference from CO<sub>2</sub> in air.

It is clear that our GC/MS analysis did not detect the presence of carboxylic acids, since GC/MS analysis should have been conclusive (i.e., masses above 45 should have been present -Figure 5.8). Although we did not detect carboxylic acids, we can not rule out their formation, since it is possible that they were formed and subsequently reacted during the heating process of the GC/MS analysis (80°C versus 25°C in the batch reactors) or their levels were below the detection limit of our GC/MS method.

### **5.3.2.2 Kinetics in the Continuous Flow Reactor**

In order to support our batch results, the kinetics of 3-MB oxidation was studied under steady-state conditions in a continuous flow, packed-bed reactor. The mass of catalyst, flow rate, and oxygen concentration (21% v/v) were held constant, while inlet 3-MB levels were varied. Previous to GC/FID analysis of the inlet and outlet, and measurement of conversion, the reactor was allowed to equilibrate for 24

hours at the desired inlet 3-MB concentration. The branched aldehyde was apparently oxidized in the presence of O<sub>2</sub> and wood fly ash given the measured conversion between the inlet and outlet of the reactor (Fig. 5.9). Regardless of the inlet 3-MB concentration (8-67 ppmv, 24°C) we could not consistently detect the presence of any unknown compounds in the outlet using our GC/FID method. Thus, given our inability to detect unknowns, our inability to measure CO<sub>2</sub> and CO at the low levels required to perform a carbon balance, it is possible that partial oxidation products remained adsorbed to the wood fly ash or were below the detection limit of our GC/MS method under these conditions.

The overall rate of 3-MB removal increased with increasing concentration and the measured rates were slightly higher than those measured in the batch reactors, potentially due to mass transfer limitations in the batch reactors. Clearly the reaction rate of 3-MB increased in a linear fashion with increasing inlet concentrations, suggesting first order kinetics (Figure 5.9); linear regression analysis of the measured rate (-r, mol/g-s) versus 3-MB concentration (mol/L) resulted in a rate constant, k<sub>1</sub>, of 1.23 x 10<sup>-3</sup> L/g-catalyst-s (R<sup>2</sup>=0.99). Subsequently, the order of the reaction with respect to 3-MB concentration was determined. Utilizing a power law approach to describe the rate law (equation 14) and assuming the reaction rate was independent of O<sub>2</sub> concentration (m=0), the overall order of the reaction, n, and the pseudo rate constant was determined from a ln(-r<sub>3-MB</sub>) versus ln(C<sub>3-MB</sub>) plot, where the slope was equal to n and the intercept equal to ln k'.

$$-r_{3\text{-MB}} = k C_{\text{O}_2}^m C_{3\text{-MB}}^n \approx k' C_{3\text{-MB}}^n \quad \text{Equation 14}$$

From such a plot (R<sup>2</sup>=0.99), using data presented in Figure 5.9, the slope or overall order of the reaction was 0.9 and the rate constant, k', was 2.1 x 10<sup>-4</sup> mol<sup>0.14</sup>

$L^{0.86}/g\cdot s$  (Figure 5.9). These results indicate that a first order rate law reasonably fit the data (over the range of  $O_2$  and 3-MB concentrations tested). The assumption of excess oxygen and thus a constant  $O_2$  concentration across the catalytic bed was reasonable given the high  $O_2$  concentration relative to 3-MB levels (~20%  $O_2$  or 200,000 ppmv versus 67 ppmv for 3-MB). It should be noted that the range of 3-MB concentrations tested is industrially relevant, with aldehyde concentrations in emissions reported from 1-25 ppmv [1, 2].

It is very difficult to analyze these results (both batch and continuous studies) relative to previous work presented in the literature, since most research on the catalytic oxidation of  $C_5$  and  $C_6$  aldehydes has been conducted with the aldehydes in excess (e.g., liquid phase) and under oxygen rate limiting conditions (21, 22, 23). Recently, a CoOx loaded  $SiO_2$  xerogel (800-1050  $m^2/g$ ) was demonstrated to catalytically oxidize acetaldehyde at 25°C forming  $CO_2$ ,  $CH_4$ , and acetic acid (acetic acid was apparently adsorbed to the xerogel - 36). The kinetics of acetaldehyde oxidation were measured in an agitated batch reactor ( $-d[VC_A]/dt=r_A W$ , or  $-d[VC_A]/dt=k_1 C_A W$ ,  $V=305$  ml of reactor volume,  $W=100$  mg of catalyst) and found to be first order with a rate constant on the order of  $5.9 \times 10^{-3}$  L/g-catalyst-s, where  $r_A=k_1 C_A$  (this result was calculated from Martyanov et al., 2005 [36] using the initial change in acetaldehyde within the first five minutes). The higher first order rate constant for acetaldehyde oxidation compared to our measured value ( $1.23 \times 10^{-3}$  L/g-catalyst-s for  $n=1$ ) was probably due to higher active phase loading, activity, and surface area in the CoOx catalyst. Initiation of the autoxidation process and formation of the acetyl radical ( $CH_3\bullet CO$ ) was theorized to proceed via a superoxo complex ( $Co^{3+}-O-O\bullet$ ) or direct oxidation of  $CH_3CHO$  by  $Co^{3+}$  (36). Similarly, a mixed

oxide catalyst (MnOx-CeO<sub>2</sub>) catalytically oxidized formaldehyde at low temperatures (333-373K, 36). Utilizing data presented by these authors (Tang et al., 2006, 37) and equation 6 to estimate the reaction rate, an overall oxidation rate of  $5 \times 10^{-8}$  mol/g-s was calculated (data used: Q=100 ml/min, P=1 atm, T=333K or 60°C, y or inlet mole fraction of  $5.8 \times 10^{-4}$  or 580 ppmv, W=200 mg of catalyst, and a fractional conversion, X, of 0.28). If we extrapolate our results to an inlet concentration of 580 ppmv 3-MB ( $-r = 1.23 \times 10^{-3}$  L/g-s C<sub>3-MB</sub>), our estimated overall reaction rate of  $3 \times 10^{-8}$  mol/g-s is similar to the MnOx-CeO<sub>2</sub> catalyst. Again, this difference in measured oxidation rates is probably due to the higher loading of the active phase and larger surface area (124 m<sup>2</sup>/g) in the MnOx-CeO<sub>2</sub> catalyst, compared to the unknown active phase and surface area of 45 m<sup>2</sup>/g in our crude catalyst.

### 5.3.2.3 Temperature Effect

The effect of temperature on the rate of 3-MB oxidation and the rate constant was also determined. The measured reaction rate using the differential reactor increased with temperature, but appeared to plateau at 160°C (Figure 5.10). Assuming an overall first order reaction a reaction rate constant was determined at each temperature (except at 160°C) and an Arrhenius plot performed ( $k = A e^{-E/RT}$ , A=pre-exponential factor, E=activation energy), resulting in a pre-exponential factor of 0.045 L/g-s and an activation energy of 7811 J/mol (1.87 kcal/mol). Note, that we did not use the measured reaction rate and 1<sup>st</sup> order k at 160°C, since the Arrhenius plot indicated curvature at the higher temperature, indicative that kinetics was mass transfer limited at this temperature [38]. This low activation energy is indicative of an aldehyde free radical reaction and is similar to the activated energy reported for the liquid phase autoxidation of acetaldehyde using a Co-type resin (>18°C, E=2

kcal/mole; 39). Reaction byproducts were not identified at these temperatures with inlet 3-MB concentrations ranging from 45-68 ppmv. However, as noted earlier, when we increased the inlet concentration of 3-MB to 525 ppmv (160°C), acetone was detected in the reactor outlet. It is believed that we did not detect acetone at the other conditions due its concentration being below our detection limit of ~11 ppmv. Based on the acetone yield measurement at 160°C and 525 ppmv 3-MB inlet, the outlet acetone concentrations in our previous experiments could have been between 0.5- 3.5 ppmv, which were below our detection limits (11 ppmv).

#### **5. 4. Conclusion**

Our results clearly indicate that wood fly ash catalyzed the oxidation of 3-MB, in the presence of O<sub>2</sub> at low temperatures (23-25°C), potentially by a free radical mechanism indicated by the low activation energy, and formation of acetone from 3-MB. Oxidation of the aldehydes did not occur at measurable rates without the wood fly ash (WFA) and the reaction rate increased with the mass of added catalyst.

These results indicate that inexpensive materials (e.g., wood fly ash and air or O<sub>2</sub>) could potentially be used to breakdown aldehydes in rendering emissions (or other industrial emissions) to less odor offensive compounds, given adequate residence times and temperature. In order to evaluate these possibilities a more accurate measure of the reaction rates, end products formed, and a complete carbon balance on the reactions, must be performed. Oxidation rates and end product formation could be improved by changing the catalyst composition or structure, which requires a better understanding of which phases or functional groups within the wood fly ash or activated carbon are responsible for catalytic activity.

## Acknowledgements

This research was supported by the US Poultry and Egg Association and the State of Georgia through the Traditional Industries Program (FoodPac). We would also like to thank Ryan Adolphson (Director of the UGA Pilot Plant Facilities) and Joshua Pendergrass for their help in the chemical synthesis of chlorine dioxide.

## References

1. J.R. Kastner, K.C. Das. Comparison of Chemical Wet Scrubbers and Biofiltration for VOC Control Using GC/MS Techniques and Kinetic Analysis, *Journal of Chemical Technology and Biotechnology*. 80 (2005) 1170-1179.
2. J.R. Kastner, Das, K.C. Wet Scrubber Analysis of Volatile Organic Compound Removal in the Rendering Industry. *J. Air & Waste Manage. Assoc.* 52 (2002) 459-469.
3. J.R. Kastner C. Hu, K.C. Das, R. McClendon. Effect of pH and Temperature on the Kinetics of Odor Oxidation Using Chlorine Dioxide. *Journal of the Air and Waste Management Association*. 53 (2003) 1218-1224.
4. M.S. Brewer, J.D. Vega, E.G. Perkins, Volatile compounds and sensory characteristics of frying fats. *Journal of Food Lipids*. 6 (1999) 47-61.
5. S.E. Hrudey, A. Gac, S.A. Daignault, Potent odor-causing chemicals arising from drinking water disinfection. *Water Sci. Technol.* 20 (1988) 55-61.
6. J. Hoigne, H. Bader, Rate Constants of Reactions of Ozone with Organic and Inorganic Compounds in Water-I: Non-Dissociating Organic Compounds. *Wat. Res.* 17 (1983) 173-183.
7. J.R. Kastner, K.C. Das, C. Hue, R. McClendon, Q. Buquoi. Kinetics and Modeling of Odor Oxidation Using Chlorine Dioxide for Emission Control

- Utilizing Wet Scrubbers. Proceedings of the 3rd International Conference on Air Pollution From Agricultural Operations, Research Triangle Park, NC. October 12-15, 2003b, ASAE, p.215-241.
8. B. Kasprzyk-Hordern, M. Ziolek, J. Nawrocki. Catalytic ozonation and methods of enhancing molecular ozone reactions in water treatment. *Applied Catalysis, B: Environmental*, 46(2003) 639-669.
  9. G. Norval, T. Burton, C. Kanters. The removal of pulp mill odors by novel catalytic environmental technology. *Pulp & Paper Canada*. 102 (2001) 53-55.
  10. F. Klose, P. Scholz, G. Kreisel, B. Ondruschka, R. Kneise, U. Knopf. Catalysts from waste materials. *Applied Catalysis, B: Environmental*, 28(2000) 209-221.
  11. Demeyer, J.C. Voundi Nkana, M.G. Verloo, Characteristics of wood ash and influence on soil properties and nutrient uptake: an overview. *Bioresource Technol.* 77 (2001) 287-295.
  12. J.R. Kastner, K.C. Das, N.D. Melear. Catalytic oxidation of gaseous reduced sulfur compounds using coal fly ash. *J. Hazardous Materials*. 95 (2002) 81-90.
  13. J.R. Kastner, K.C. Das, J.Q. Buquoi, N.D. Melear. Low temperature catalytic oxidation of hydrogen sulfide and methanethiol using wood and coal fly ash. *Environmental Science and Technology*. 37 (2003) 2568-2574.
  14. J.R. Kastner, Q. Buquoi, R. Ganagavaram, K.C. Das. Catalytic Ozonation of Gaseous Reduced Sulfur Compounds Using Wood Fly Ash., *Environmental Science and Technology*, 39 (2005) 1835-1842.
  15. L.S. Clesceri, A.E. Greenberg, R.R. Trussel. 1989. *Standard Methods for the*

- Examination of Water and Wastewater*, 17th ed., American Public Health Association, Washington, D.C., 4–75 through 4–83.
16. J.M. Gosset, Measurement of Henry's Law constant for C<sub>1</sub> and C<sub>2</sub> chlorinated hydrocarbons. *Environ. Sci. Technol.* 21 (1987) 202-208.
  17. A.H. Lincoff, J.M. Gossett. The determination of Henry's Constant for volatile organics by equilibrium partitioning in closed systems. In: *Gas Transfer at Water Surfaces*. (Brutsaert, W. and Jirka, G.H., eds.). D. Reidel Publishing Company, Norwell, Massachusetts, 1984, 17-25.
  18. J. Staudinger, P.V. Roberts A Critical Review of Henry's Law Constants for Environmental Applications. *Critical Reviews in Environmental Science and Technology.* 26 (1996) 205-297.
  19. J.R. Kastner, R. Gangavarum, Q. Buquoi. N. Melear, A. Teja, C. Xu. Advanced Catalysts from Biomass. Tenth Annual Meeting of the Institute of Biological Engineering. March 4-6, 2005, The University of Georgia, Athens, Georgia.
  20. V. Haisman, P. Stampachova, J. Vcelak, V. Chvalovsky. The Oxidation of Aldehydes to Carboxylic Acids and Accompanying Side Reactions. *Oxidation Communications.* 4 (1983) 229-236.
  21. R.A. Sheldon, J.K. Kochi. *Metal-Catalyzed Oxidations of Organic Compounds*. Academic Press. New York. 1981.
  22. Lehtinen, G. Brunow. Factors Affecting the Selectivity of Air Oxidation of 2-Ethylhexanal, an  $\alpha$ -Branched Aliphatic Aldehyde. *Organic Process Research & Development.* 4 (2000) 544-549.
  23. Larkin. The Role of Catalysts in the Air Oxidation of Aliphatic Aldehydes. *J.*

- Org. Chem.* 55 (1990) 1563-1568.
24. F.R. Mayo, Free radical autoxidations of hydrocarbons. *Accts. Chem Resch.* 1(1968) 193.
25. J. Hoigne, H. Bader, Kinetics of reactions of chlorine dioxide (OCIO) in water - I. Rate constants for inorganic and organic compounds. *Water Research* 28(1) (1994) 45-55.
26. Rav-Acha, Transformation of aqueous pollutants by chlorine dioxide: reactions, mechanisms and products. Editor(s): Hrubec, Jiri. *Handbook of Environmental Chemistry* (1998), 5(Pt. C), 143-175. Springer, Berlin, Germany.
27. D.E. Jackson, R.A. Larson, V.L. Snoeyink. Reactions of chlorine and chlorine dioxide with resorcinol in aqueous solution and adsorbed on granular activated carbon. *Wat. Res.* 21(1987) 849-857.
28. A.S.C. Chen, R.A. Larson, V.L. Snoeyink. Importance of free radical in an aqueous chlorination reaction (Indan-ClO<sub>2</sub>) promoted by granular activated carbon. 1984. *Carbon.* 22 (1984) 63-77.
29. R.C. Bansal, J.B. Donnet, F. Stoeckli. In: *Active Carbon*. 1988. Marcel Dekker Inc., New York. Chapters 2, 4, and 6.
30. E.K. Rideal, M.W. Wright. *J. Chem. Soc.* 128 (1926) 1813.
31. R.D. Vidic, M.T. Suidan, R.C. Brenner. Oxidative coupling of phenols on activated carbon: impact on adsorption equilibrium. *Environ. Sci. Technol.* 27 (1993) 2079-2085.
32. C. Aguilar, R. Garcia, G. Soto-Garrido, R. Arraigada. Catalytic oxidation of aqueous methyl and dimethylamines by activated carbon. *Topics in Catalysis*.

- 33(2005): 201-206.
33. G.K. Vasilyeva, V.D. Kreslavski, P.J. Shea. Catalytic oxidation of TNT by activated carbon. *Chemosphere*. 47 (2002) 311-317.
34. J.M. Pickard, E.G. Jones. Catalysis of Jet-A Fuel Autoxidation by  $\text{Fe}_2\text{O}_3$ . *Energy and Fuels*. 11 (1997) 1232-1236.
- 35.32. Mukherjee, W.F. Graydon. Heterogeneous Catalytic Oxidation of Tetralin. *The Journal of Physical Chemistry*. 71(1967) 4232-4240.
36. I.N. Martyanov, S. Uma., S. Rodrigues., K.J. Klabundle. Decontamination of Gaseous Acetaldehyde over CoOx-Loaded  $\text{SiO}_2$  Xerogels under Ambient, Dark Conditions. *Langmuir*. 21(2005) 2273-2280.
37. X. Tang, Y. Li, X Huang., Y Xu., H Zhu., J Wang., W. Shen. MnOx-CeO<sub>2</sub> mixed oxide catalysts for complete oxidation of formaldehyde: Effect of preparation method and calcination temperature. *Applied Catalysis B: Environmental*. 62 (2006) 265-273.
38. Smith, J.M., Chemical Engineering Kinetics. McGraw-Hill, New York, 1981
39. Chou, T-C.; Lee, C-C. Heterogenizing Homogeneous Catalyst. 1. Oxidation of Acetaldehyde. 1985. *Ind. Eng. Chem. Fundam.* 24: 32-39.

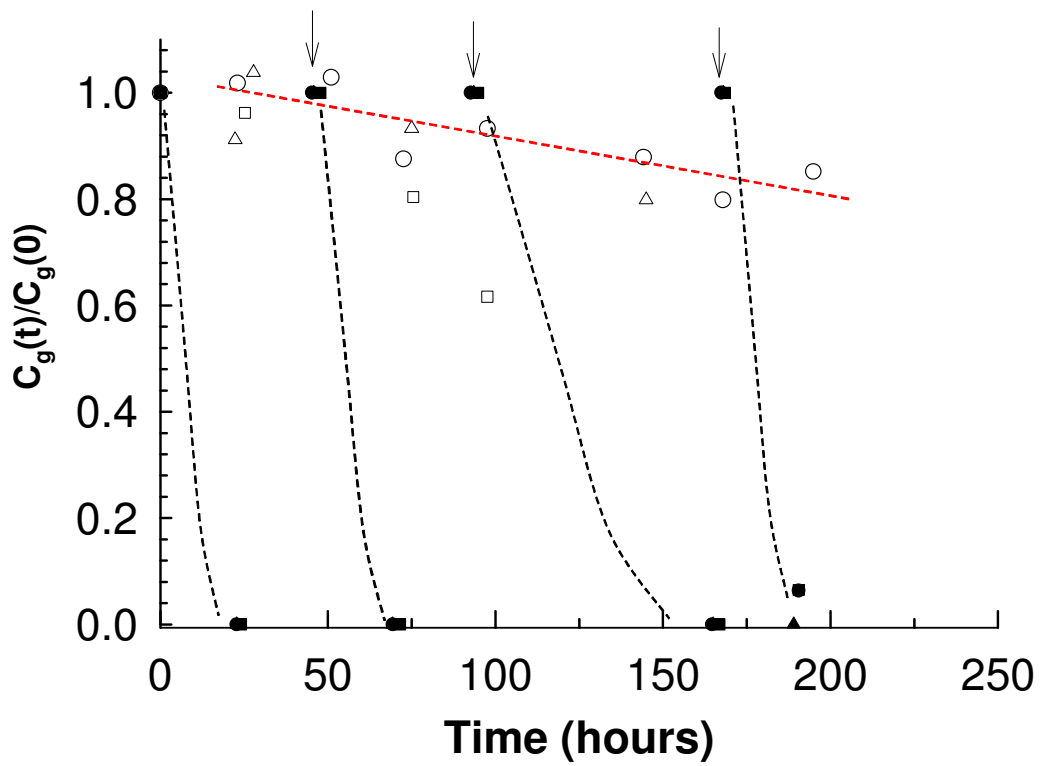


**Figure 5.1.** Oxidation of 3-methylbutanal (3-MB) in a batch reactor with repeated spikes of 3-MB. The reactor contained wood fly ash and air ( $O_2$ ) only -  $\square$ ,  $\triangle$ ,  $\circ$  is the control (w/o WFA) and  $\blacksquare$ ,  $\bullet$ ,  $\blacktriangle$ , contained WFA, and  $\downarrow$  indicates 3-MB addition.

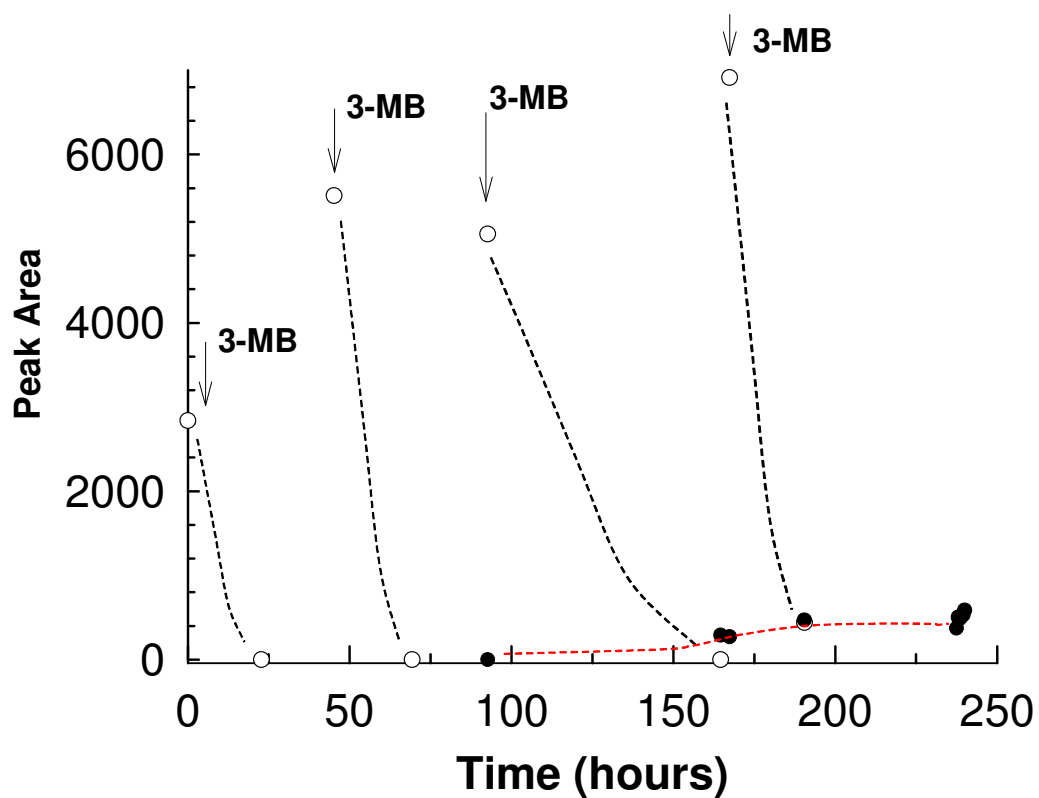


**Figure 5.2.** Plot of GC/FID peak area for 3-MB (○) contacted with a wood fly ash slurry in the presence of O<sub>2</sub> (air) and the subsequent formation of an unknown (●, ---) in the gas phase. The unknown is peak A in Figure 3 with a retention time of 4.5 minutes.

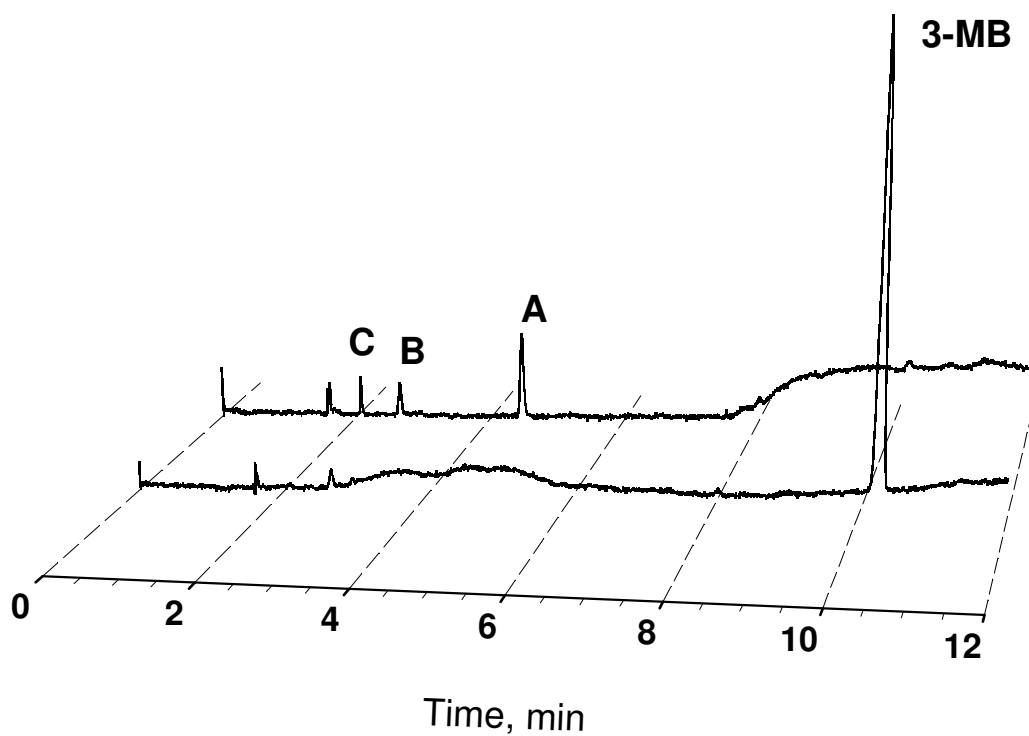


**Figure 5.3.** GC/FID chromatograms (peak signal versus time) at time zero ( $t_0$ ) and after 225 hours ( $t_1$ ). Multiple spikes of 3-MB (retention time or RT of 10.2 min) were contacted with a wood fly ash slurry in the presence of  $O_2$  after time zero and the chromatographic traces clearly show the reduction of 3-MB and formation of unknowns with shorter retention times (A, RT of 4.5 min; B, 2.7 min, and C, 2.0 min).

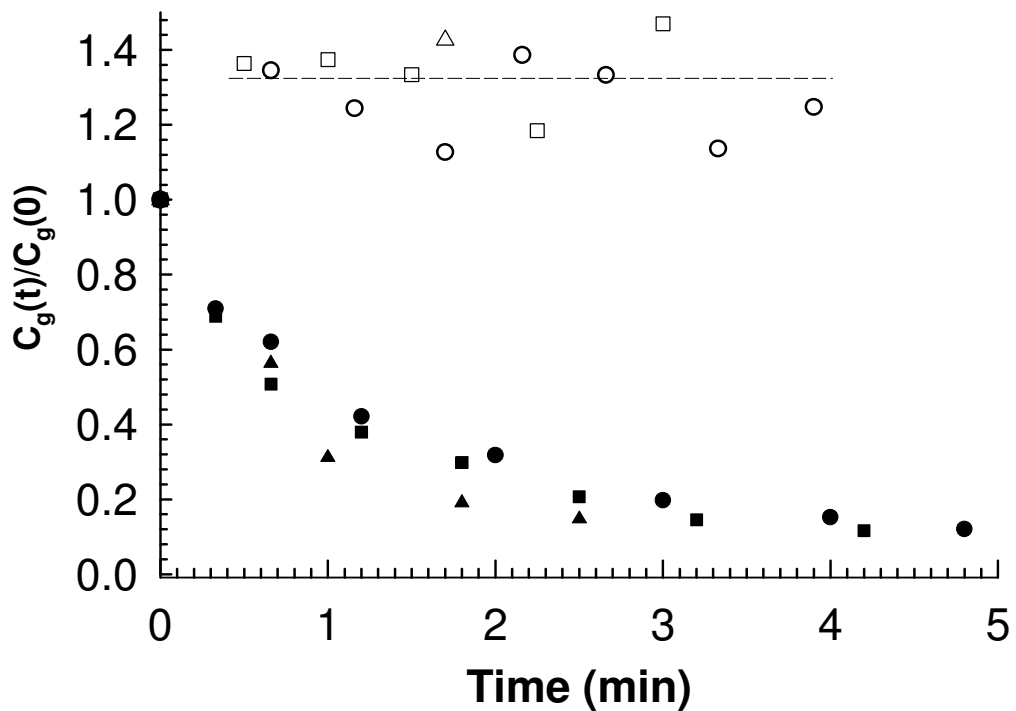


**Figure 5.4.** Oxidation of 3-methylbutanal (3-MB) in a batch reactor in the presence of just O<sub>2</sub> (■, ●, ▲) using wood fly ash as the catalyst. The reactor containing wood fly ash, ClO<sub>2</sub> and air (O<sub>2</sub>) only - □, △, ○ was a control (i.e., w/o WFA). The increase in  $C_g(t)/C_g(0)$  for the control was due to a measured increase in the 3-MB gas phase after neat liquid addition; however, the gas phase concentration in the control clearly did not change after equilibrium was established.

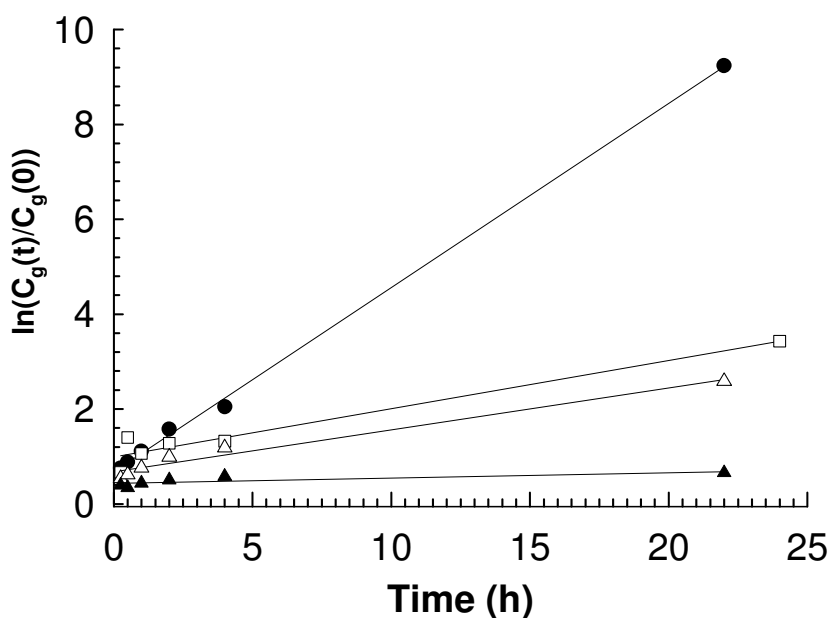
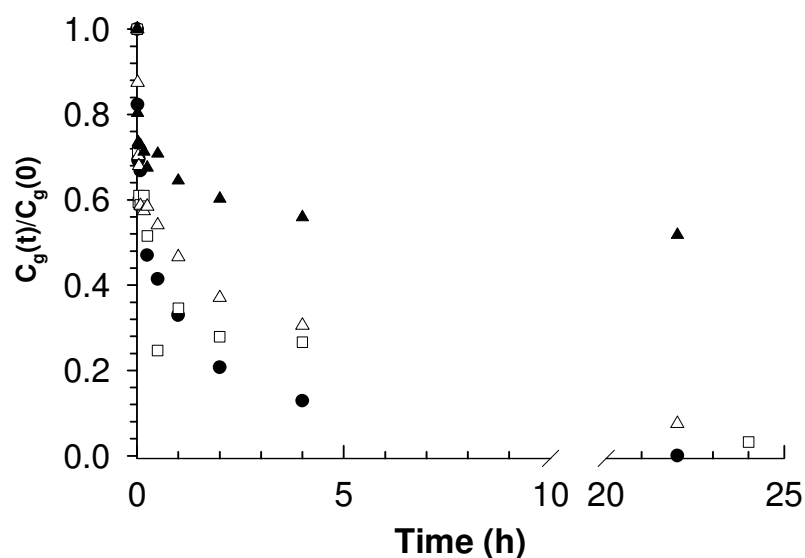


**Figure 5.5.** Change in gas phase concentration of 3-MB versus time with different amounts of wood fly ash (top), and the subsequent effect of catalyst (WFA) mass on the overall rate of 3-MB oxidation in a batch reactor in the presence  $O_2$  assuming a first order rate (bottom) – analysis was performed after the period of rapid loss (0.08 to 24 h): catalysts mass of 0.1 g (▲), 0.5 g (△), 0.75 g (□) and 1.0 g (●).

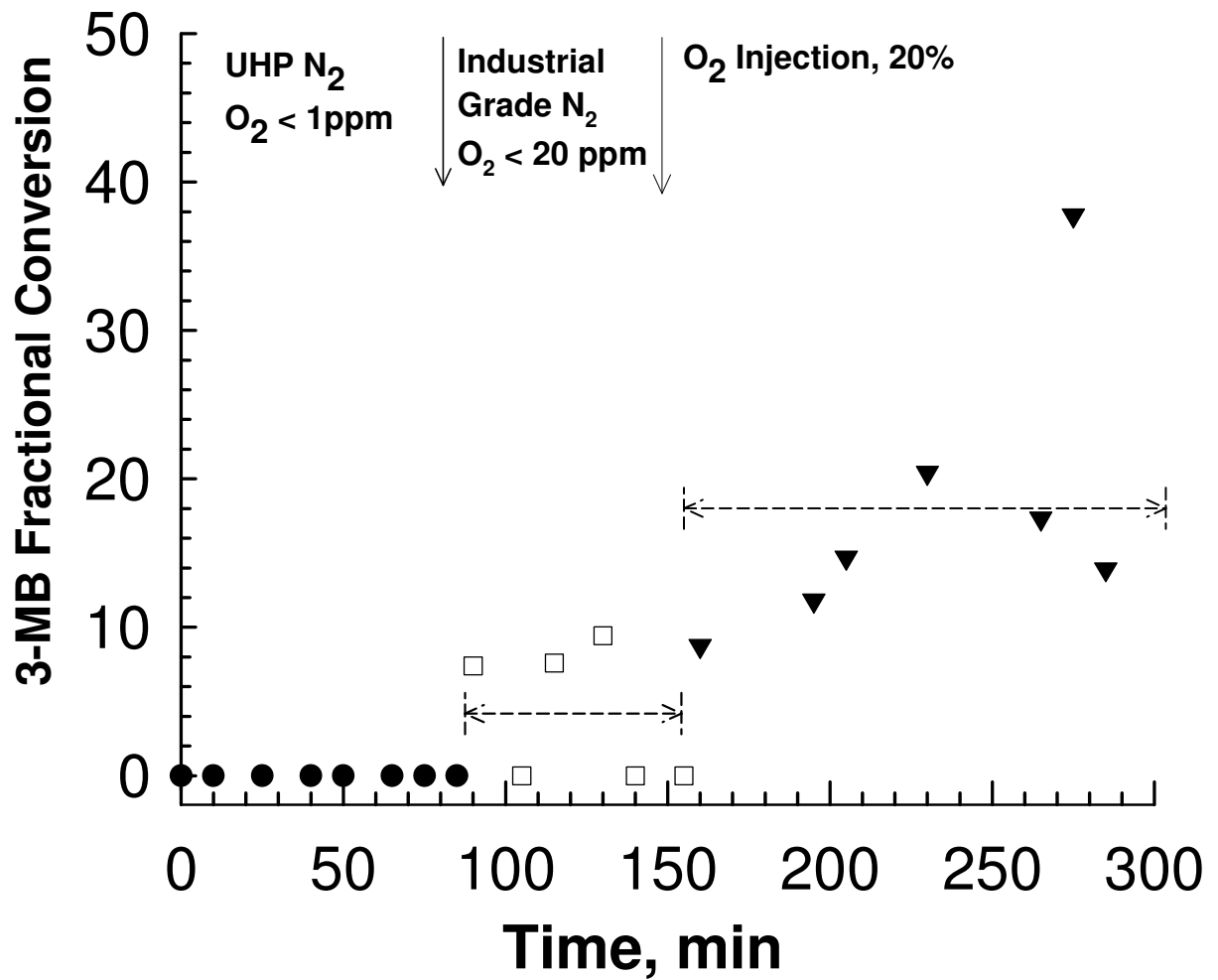


**Figure 5.6.** Effect of O<sub>2</sub> concentration on 3-MB removal in a continuous flow packed-bed reactor packed with wood fly ash - ●, no oxygen; ○, O<sub>2</sub> < 20 ppmv; ▲, O<sub>2</sub>, 20% (v/v). UHP – ultra high purity.



**Figure 5.7.** Headspace analysis (performed in triplicate) via GC/MS of the liquid phase of a wood fly ash/3-MB/O<sub>2</sub> only slurry (after 225 hours), **Top**; a wood fly ash/3-MB slurry reacting in the presence of ClO<sub>2</sub> and O<sub>2</sub> (after 200 hours).

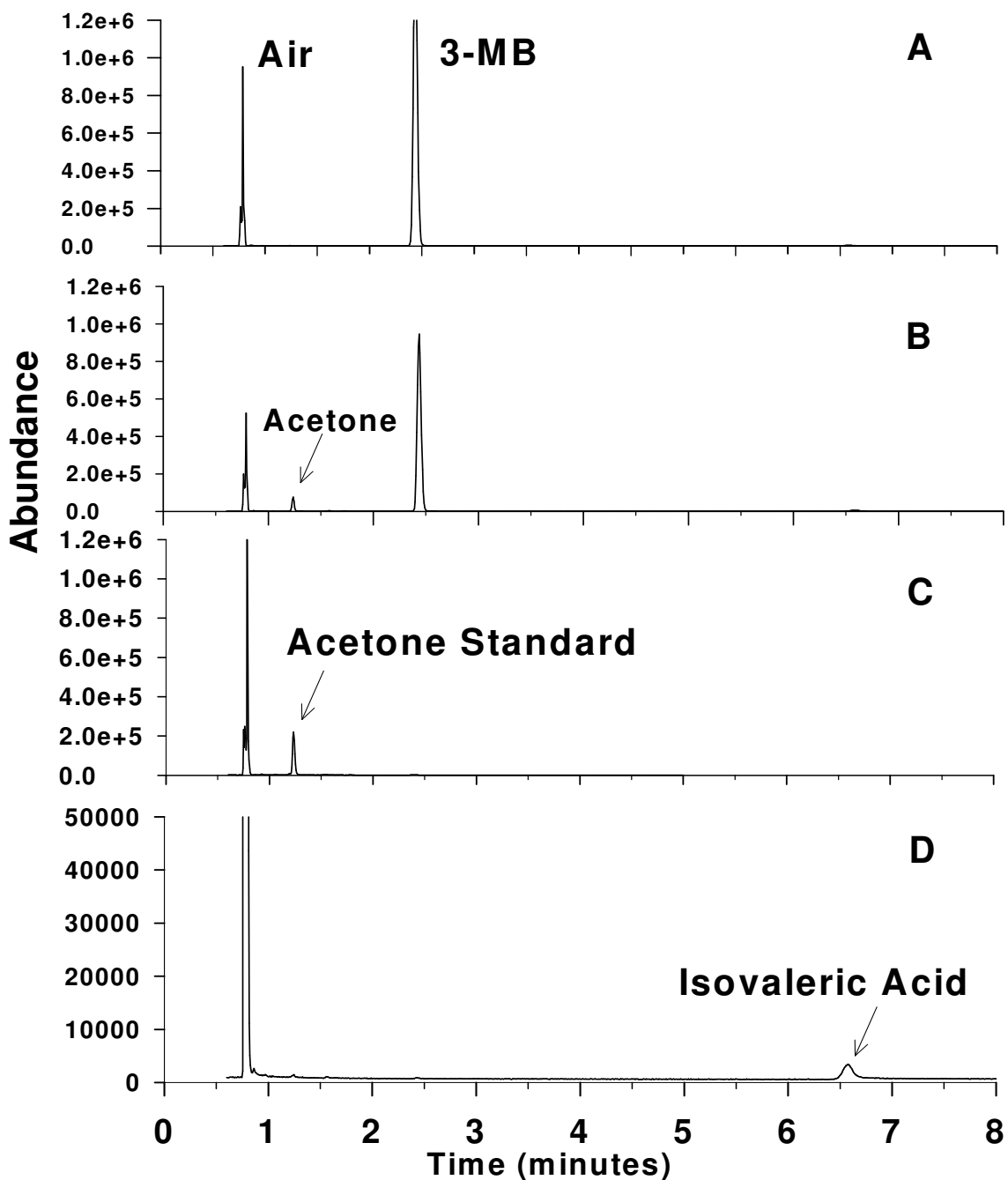


**Figure 5.8.** Typical chromatograms of the samples taken from the inlet (A) (525 ppmv, 160°C) and outlet (B) of a reactor catalytically oxidizing 3-MB using wood fly ash. Acetone was detected in the reactor outlet via mass spectral matching and compared with a neat standard (55 ppmv) for confirmation (C). Although the GC/MS was able to detect isovaleric acid (72 ppmv, D), isovaleric acid was not detected in the outlet(s).

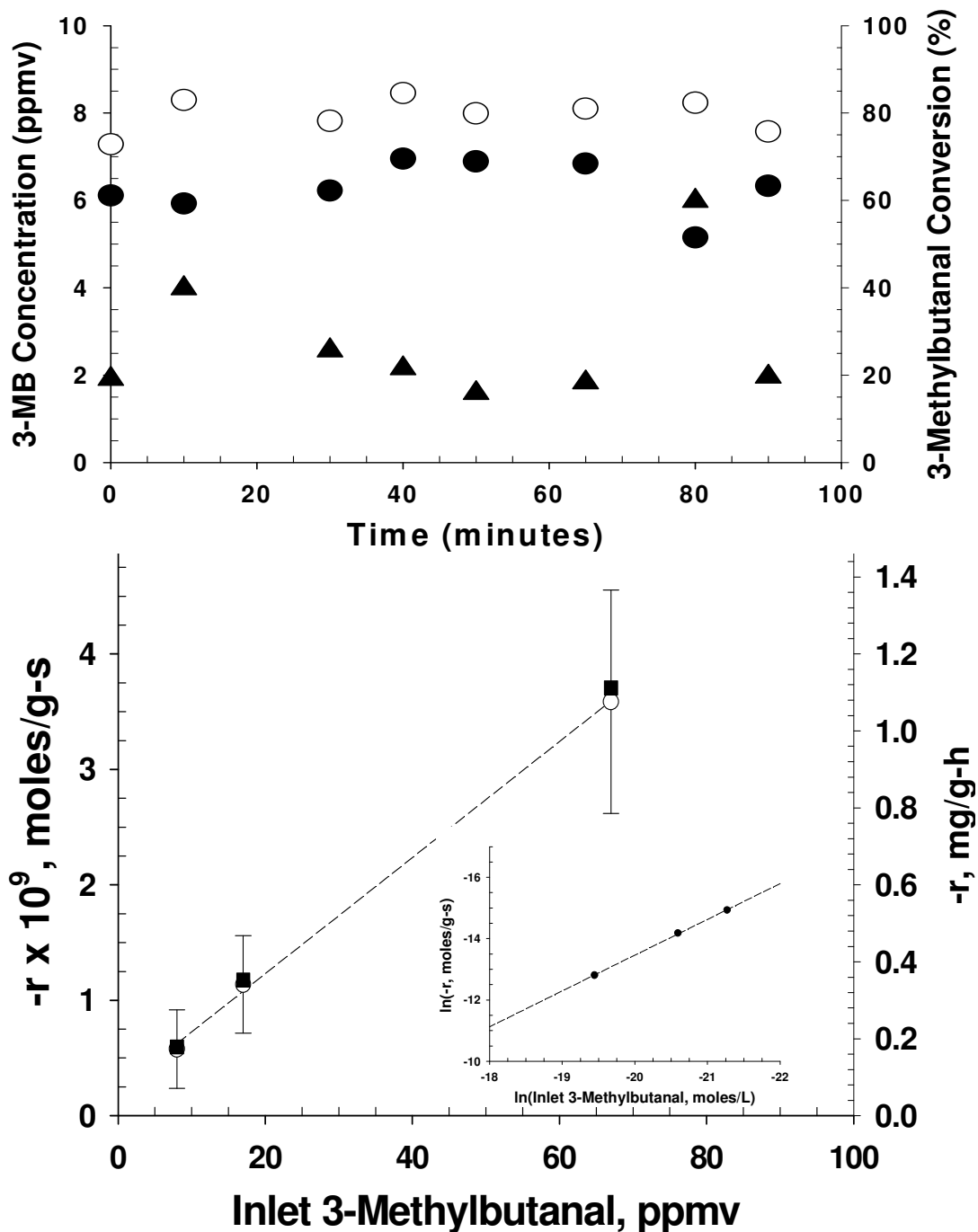


**Figure 5.9.** Continuous catalytic oxidation of 3-MB (8 ppmv inlet) in a reactor packed with wood fly ash (10 g) as determined from the measured steady-state fractional removal of 3-MB (▲) between the inlet (○) and outlet (●) of the reactor (**top**), and the effect of inlet 3-MB concentration on the measured reaction rate in different units (**bottom**): moles/g-s  $\times 10^9$ , (○) and mg/g-h, (■). The inset shows the plot of  $\ln(-r)$  versus the  $\ln(C_{3\text{-MB}})$  of the inlet concentration with the slope equal to the overall reaction order. Please note to read  $-r$  in moles/g-s the value from the graph is divided by  $10^9$ ; e.g., at 35 ppmv,  $-r \times 10^9 = 2$  and  $-r = 2 \times 10^{-9}$  moles/g-s.

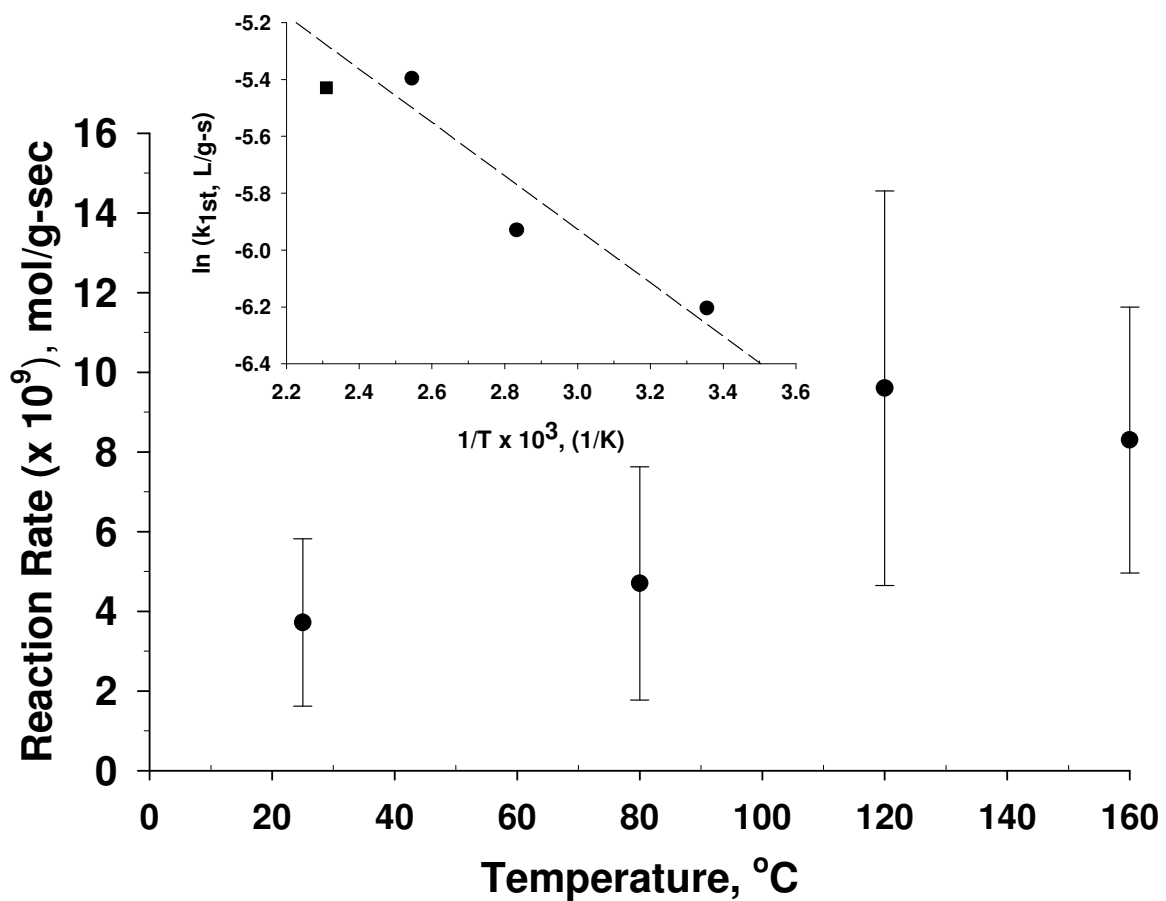


**Figure 5.10.** Effect of temperature on the rate of 3-MB oxidation and 1<sup>st</sup> order rate constant using wood fly ash (10 g, 45-68 ppmv inlet) resulting in a pre-exponential factor of 0.045 L/g-s and an activation energy of 7811 J/mol (1.87 kcal/mol), based on temperatures between 24-120°C (see inset); ■, k<sub>1st</sub> for 160°C indicating curvature in the Arrhenius plot.

**Table 5.1:** Physical and chemical characteristics of the wood fly ash used in the oxidation studies.

Properties	WFA (Mean $\pm$ SD)	
Surface Area, m <sup>2</sup> /g	44.89 $\pm$ 8.34	
pH	12.13 $\pm$ 0.17	
Bulk Density, g/cm <sup>3</sup>	0.54	
Carbon, % (dry basis)	18.75 $\pm$ 1.87	
Selected Elements (ppm or mg/kg)	Range	Mean
Co	4.5 – 5.2	4.94
Cu	32.0-39.0	34.57
Mn	500.0 – 584	542.74
Mo	2.2 – 2.7	2.43
Ni	18 – 19	18.27
V	ND	ND
Fe	6,600 – 8,300	7470.54

ND: Not Determined

<sup>1</sup> Physical properties are reported based on manufacturers data, except where noted

<sup>2</sup> Surface areas measured using BET method and pH as reported in experimental methods

## CHAPTER 6

### LOW-TEMPERATURE CATALYTIC OXIDATION OF ALDEHYDE MIXTURES USING WOOD FLY ASH: KINETICS, MECHANISM, AND EFFECT OF OZONE<sup>1</sup>

Praveen Kolar and James R. Kastner\*

Air Pollution Engineering Laboratory

Biological and Agricultural Engineering, Driftmier Engineering Center,

The University of Georgia, Athens, Georgia

\*Corresponding author contact: [jkastner@engr.uga.edu](mailto:jkastner@engr.uga.edu), 706-583-0155

---

<sup>1</sup> Kolar, P. and J. R. Kastner. To be submitted to *Applied Catalysis B: Environmental*.

## 6.1 Introduction

Many industrial operations, such as animal rendering, wastewater treatment, fuel combustion, and particle board manufacturing generate aldehydes as air pollutants (Baumann et al., 2000; Andres et al., 2004). For example, 3-methylbutanal (3-MB), 2-methylbutanal (2-MB), and hexanal are generated in poultry rendering operations when animal byproducts (meat, feathers, offal, and blood) are processed under high temperatures (150 °C) and pressures (15 MPa) to generate value added products, such as feed additives and fertilizers (Kastner and Das, 2002). The aldehydes are not only associated with negative odors (Brewer et al., 1999; Hrudey et al., 1988), but also contribute to atmospheric ozone and particulate matter formation (Wang et al., 2007). The industry routinely uses chemical wet scrubbers to treat aldehydes and other VOCs by oxidizing them with chemical oxidants, such as ClO<sub>2</sub> and/or O<sub>3</sub> (Kastner et al., 2003). However, on-site analysis of the wet scrubbers indicated low efficiencies when treating aldehydes (typically <50 % removal), due to lack of reactivity between the aldehydes and ClO<sub>2</sub> (Kastner et al., 2004).

Other potential treatment technologies such as adsorption, incineration, and biological filtration have limitations (Tsou et al., 2003). Adsorption only transfers and concentrates the VOCs from a gas phase onto a solid phase and needs further treatment for complete removal (Everaert and Baeyens, 2004). Incineration processes, which involves combustion of the VOCs at high temperatures (1000-1200 °C) using natural gas as a fuel source (Gervasini and Ragaini, 2000) are not only cost intensive, but also contribute to production of greenhouse gases (Tsou et al., 2003). Biological filtration systems on the other hand need longer residence

times (30-60 seconds) and thus require large reactors and can't handle VOC fluctuations. Hence, an effective alternative technology is needed to treat the aldehyde fraction from rendering emissions.

Catalytic oxidation is a promising alternative technology to treat VOCs emitted from various industries (Gervasini et al., 1996). The process involves reaction between VOCs and an oxidant, aided by a catalyst. The catalyst lowers the oxidation temperatures by providing alternate routes to end products, whose activation energies are less than that of non-catalytic reactions (Smith, 1981). Additionally, the catalyst increases the reaction rate; lowering the reaction temperature not only lowers the treatment costs, but also reduces the production of greenhouse gases and micro pollutants (such as dioxins, phosgene). Several types of expensive metals (e.g., gold, platinum) and metal oxides (e.g., nickel oxide, ruthenium, etc) have been tested as catalysts with a high degree of success. However, research has been limited on the development of catalyst from inexpensive materials, especially solid wastes.

Many solid waste sources contain metals or metal oxides of high surface area such that they could potentially be recycled and used as catalysts (Klose et al., 2000). Wood fly ash is one such resource that is produced in large and growing volumes in the USA (5.5 million tons/yr), with a majority land filled (Demeyer et al., 2001). Previous analysis of wood fly ash revealed crystalline phases of metal oxides (magnetite and hematite) and presence of activated carbon in its structure, wood fly ash was demonstrated to catalytically oxidize  $H_2S$  using molecular oxygen ( $O_2$ ), and

oxidized volatile organic sulfur compounds (e.g., methylmercaptan) and propanal, in the presence of ozone (Kastner et al., 2005).

Recently it was demonstrated that wood fly ash catalytically oxidized 3-methylbutanal (3-MB) at room temperature via a free radical mechanism (Kolar et al., 2007). However, a complete carbon balance on the reactions was not performed in this research and thus it was unclear if complete oxidation occurred. Additionally, this previous work focused on a single aldehyde (3-MB). In reality, rendering emissions consist of aldehyde mixtures, making it difficult to predict the catalytic performance based on a single compound. Hence, it is critical to evaluate wood fly ash as a low-cost catalyst to treat an aldehyde mixture that is normally encountered in rendering emissions. The objectives of this study were to evaluate wood fly ash as a low-cost catalyst for treating a binary aldehyde mixture at low temperatures (25-160 °C), determine the kinetics of oxidation reactions and activation parameters, identify and quantify the oxidation products, perform a complete carbon balance, and determine the effect of ozone on the oxidation processes.

## **6.2. Materials and methods**

2-methylbutanal (2-MB) and hexanal (95%, by Sigma-Aldrich) were used as representative aldehydes in this study because of their consistent occurrence in the poultry rendering emissions (Kastner et al., 2002).

### **6.2.1 Wood fly ash characterization**

The wood fly ash used in this study was obtained from a paper mill. The physical and chemical properties were determined previously (Kastner et al., 2003 and 2005). In this study we used scanning electron microscope (SEM) for imaging

the wood fly ash and energy dispersive spectroscopy (EDS) for determination of the elemental composition on the ash particles.

### **6.2.2 SEM and EDS analysis of wood fly ash**

Triplicate samples of wood fly ash were mounted on an aluminum stub covered with an adhesive carbon tab. The mounted samples were coated with ~ 120 Å of gold using a sputter coater (model SPI, SPI supplies West Chester, PA). The gold coated samples were imaged using a digital SEM (ZEISS 1450 EP, Carl Zeiss Micro Imaging, Thornwood, NY). An accelerating voltage of 5 keV was used and a back scattering detector was used for imaging the samples. The elemental composition was determined using an energy dispersive spectroscope. An accelerating voltage of 5.5 keV was used for 60-second time frame for determination of elemental composition. Subsequently, the raw data was processed using INCA software (Oxford Instruments, Oxfordshire, UK).

### **6.2.3 Continuous flow experiments**

#### **Description of experimental setup**

All experiments were performed in a continuous flow, packed-bed reactor system as shown in figure 6.1. The system consisted of a series of cylindrical glass reactors (30- cm length) for humidification (5-cm diameter), mixing (2.54-cm diameter), and catalytic oxidation (2.5-cm diameter) connected by 0.625 cm (ID) Teflon tubing. Compressed air was humidified (RH > 78%) by passing the air through a water (humidification) column. The flow of air was controlled by a mass flow controller (model: by Celerity Inc, CA). The liquid aldehyde (either 2-MB or hexanal or as a mixture) was injected into the system via using an automated

syringe pump (model 74900-30 by Cole Parmer) and a 10-cc Becton Dickinson disposable syringe at a predetermined rate to obtain the desired concentration. To minimize external mass transfer limitations, a flow of 5 L/min was chosen based on our previous experiments (data not shown). The humidified air and aldehyde vapor were allowed to mix in a glass column packed with glass beads (3-mm diameter). After mixing, the air-aldehyde mixture flowed through a packed-bed reactor containing 10 grams of wood fly ash distributed over 13-cm of glass wool. The top and bottom of the catalytic bed was also distributed with glass wool to promote plug flow conditions. The kinetics were measured at 25 °C and 1 atm pressure. The reactor was entirely covered with black felt to minimize any effects of photochemical oxidation. To attain a steady state condition, the aldehyde was injected overnight (8-10 hours) before sampling the reactor. The inlet and outlet of the reactor were simultaneously sampled using gas-tight syringes (model 1-2 mL, by VICI Precision Sampling, Inc., Baton Rouge, LA) and analyzed using gas chromatograph (GC). Typically, samples were drawn from the reactor every 20 minutes and injected into a gas chromatograph to determine the concentrations.

#### **6.2.4 Analytical methods**

The inlet and outlet gas samples were analyzed using a Hewlett-Packard 5890 GC equipped with a flame ionization detector (FID) and a SPB-1 sulfur column (0.32  $\mu\text{m}$  , 30 m) (SUPLECO, Bellefonte, PA). The samples were analyzed under isothermal conditions (column temperature: 80 °C, inlet and detector temperatures of 200 and 250 °C), and a split ratio of 30:1. A sample size of 250 $\mu\text{L}$  was used for the entire study. Standard curves of 2-MB and hexanal were prepared for a

concentration range of 0 and 200 ppmv using 1-L tedlar bags and calibrated gas syringes (model 1-2 mL, by VICI Precision Sampling, Inc., Baton Rouge, LA).

Additionally, the inlet and outlet gas samples from the continuous reactor were also analyzed using a gas chromatograph (Model 6890, Agilent) equipped with a mass selective detector (Model 5973). Ultra high pure (99.99 %) helium (3.5 ml/min) was used as a carrier gas and a SPB-1 sulfur capillary column (0.32  $\mu$ m, 30 m) (by Supelco Inc. Bellefonte, PA) was used for separation of gases. A sample size of 250 $\mu$ L (splitless) was used. All separations were performed isothermally at a column oven temperature of 80°C and detector temperatures of 250°C using a full scan mode (m/z: 40-150). Further, for carbon dioxide analysis, a separate gas chromatograph (HAPSITE by Inficon Ltd, East Syracuse, New York) attached to a mass selective detector and equipped with a Q-Plot column (SUPLECO, by Sigma Aldrich) was used. Ultra high pure nitrogen was used as a carrier gas and selective ion monitoring (SIM) based separation was adapted to selectively scan masses 22 and 44 corresponding to carbon dioxide.

### **6.2.5 Evidence of catalytic activity of wood fly ash**

Preliminary experiments were conducted to determine the effect of oxygen on catalytic oxidation of aldehydes. An experiment was conducted in the continuous flow reactor system (with wood fly ash) to determine the removal of 2-MB without oxygen. Ultra high pure helium (99.99 %) was used as the carrier gas. Inlet and outlet samples were analyzed using GC-FID. Subsequently, pure oxygen (99 %) was added to the reactor along with helium such that the oxygen

concentration was 20 %. Inlet and outlet samples were collected and analyzed using GC-FID to determine the effect of oxygen.

### 6.2.6 Kinetics of individual aldehydes

The kinetics of 2-MB and hexanal were individually determined at room temperature (25 °C) under steady state conditions. The mass of the catalyst (10 g), flow rate (5 L/min), and the oxygen concentration (21 % v/v) were maintained constant, while the concentration of aldehydes (2-MB and hexanal) was varied. The concentration ranges tested were between 20 ppmv and 100 ppmv for 2-MB and 20 ppmv and 125 ppmv for hexanal. The aldehyde was injected overnight (10-12 hours) before sampling the reactor to achieve steady state condition. After achieving a steady state, the concentration of the inlet and outlet gas samples was measured. The fractional conversion ( $X$ ) at each concentration regime was determined as

$$X = \left[ \frac{C_{in} - C_{Out}}{C_{in}} \right] \times 100 \% \quad (1)$$

The reaction rate for our assumed plug flow reactor model is expressed as

$$-r = \frac{dF_A}{dW} \quad (2)$$

Where  $F_A$  is the molar rate and  $W$  is the catalyst mass.

Assuming steady state, isothermal and isobaric conditions, and that ideal gas laws were valid, the overall rate of aldehyde oxidation was determined from equation 2 resulting in

$$-r = Q \frac{P}{RT} y \frac{X}{W} MW \quad (3)$$

where  $-r$  is the rate of oxidation of the aldehyde (mg/g-min),  $P$  is the pressure (atm),  $Q$  is the volumetric flow rate (L/min),  $R$  is the universal gas constant,  $T$  is the temperature (K),  $y$  is the inlet mole fraction,  $X$  is the fractional conversion (%) (< 30 %)  $W$  is the mass of the catalyst (g), and  $MW$  is the molecular weight of the aldehyde (g/mol).

### 6.2.7 Modeling and kinetic parameters

Two types of models have been used in this study to determine the kinetic parameters: a simple empirical power law model and a mechanistic model based on Mars van Krevelen's sequential redox steps.

### 6.2.8 Power law model

The reaction rate in terms of power-law can be expressed as

$$-r_{VOC} = \frac{d(VOC)}{dt} = k C_{VOC}^n C_{O_2}^m \quad (4)$$

where  $k$  is the reaction rate constant,  $r_{VOC}$  is the oxidation rate of the VOC in question,  $C_{VOC}$  and  $C_{O_2}$  are the concentrations of VOC and oxygen, and  $n$  and  $m$  are orders of the reaction with respect to VOC and oxygen. The above equation may be linearized and rearranged to obtain

$$\ln(-r_{VOC}) = \ln(k) + n \ln(C_{VOC}) + m \ln(C_{O_2}) \quad (5)$$

In all our experiments, oxygen was excess and constant (20.8 % v/v, 208,000 ppmv). Hence, the last term may be approximated to a constant and can be combined with the first term. The equation now assumes the following form

$$\ln(-r_{VOC}) = (k^1) + n \ln(C_{VOC}) \quad \text{where } k^1 = \ln(k) + m \ln(C_{O_2}) \quad (6)$$

From the plot of reaction rate (from equation 6) and concentration of the VOC we obtain the reaction order and the pseudo-first order rate constant.

### 6.2.9 Mars van Krevelen's redox model

This model assumes a two step mechanism consisting of: (1) oxidation of the VOCs by the lattice oxygen in the catalyst thereby reducing the catalyst (reduction step) and (2) oxidation of the catalyst by the oxygen in the gas phase (oxidation step) (see below)



Further, the oxidation rate of VOCs is proportional to the VOC concentration and the proportion of the oxidized active sites ( $\theta$ ), we obtain

$$-r_{O(\text{VOC})} = k_R C_{\text{VOC}} \theta \quad (7)$$

(2) The oxidation of the catalyst is proportional to the concentration the oxygen in the gas phase ( $C_O$ ) and the proportion of the reduced active sites ( $1 - \theta$ ), we obtain

$$-r_{O(\text{cat})} = k_O C_O (1 - \theta) \quad (8)$$

(3) Every mole of VOC needs ' $\alpha$ ' moles of oxygen for a complete reaction; we obtain for steady state equilibrium conditions the following relation

$$\alpha r_{O(\text{VOC})} = r_{O(\text{CAT})} \quad (9)$$

Combining the steps and eliminating  $\theta$ , we obtain the following equation

$$r_{\text{VOC}} = \frac{k_R k_O C_{\text{VOC}} C_O}{k_O C_O + \alpha k_R C_{\text{VOC}}} \quad (10)$$

The above equation may be linearized by inverting and rearranging as follows

$$\frac{1}{r_{VOC}} = \frac{1}{k_R C_{VOC}} + \frac{\alpha}{k_O C_O} \quad (11)$$

In all our experiments, oxygen is in excess and constant (20.8 % v/v), and hence the last term was ignored. The equation now assumes the form as shown below

$$\frac{1}{r_{VOC}} = \frac{1}{k_R C_{VOC}} \quad (12)$$

The above equation may be inverted to obtain a first order relation between the concentration and oxidation rate and the slope provides the first order rate constant.

### 6.2.10 Effect of temperature and activation parameters

Additional experiments were performed at temperatures of 80, 120, and 160 °C to determine the effect of temperature and activation parameters. The reactor was heated with a thermal heating tape controlled by a thermolyne stepless input controller (model 45515, by Barnstead International, Dubuque, IA). The inlet concentration was held constant (~ 125 ppmv) for all the temperatures tested. For a given temperature, inlet and outlet concentrations were measured to determine the fractional removal and oxidation rate (equation 3). Utilizing the oxidation kinetics obtained for each temperature regime, a linearized Arrhenius model

$(\ln(k) = \ln(A) - \frac{E}{RT})$  was used to determine the activation parameters, pre-

exponential factor (A) and activation energy (E).

### **6.2.11 Identification of reaction products and carbon balance**

Three additional experiments were conducted to identify and quantify the oxidation products and to perform a carbon balance. In one of the experiments helium was used as a carrier gas for better detection and quantification of CO<sub>2</sub>. For these experiments, the catalytic oxidation was performed at 160°C and with a high inlet concentration (400-600 ppmv) and low flow rate (2 L/min) to increase the fractional conversion. After an 12-hour equilibrium period, the inlets and outlets were analyzed simultaneously using three gas chromatographs, one equipped with a mass spectrometer for identifying the by-products, one equipped with a Q-Plot column (SUPELCO) for detecting and quantifying CO<sub>2</sub>, and one with an FID for VOC quantification.

### **6.2.12 Kinetics of aldehyde mixtures**

The oxidation kinetics of equal mass concentrations of hexanal and 2-MB were tested, for experiments with binary mixtures. Equal masses of 2-MB and hexanal were thoroughly mixed using a magnetic bar for 10 minutes before loading the mixture in the syringe. The mixture was injected into the system as described in the experimental setup section. The separation, chromatographic methods, and experimental conditions for the mixtures were similar to that were used for individual aldehydes. The inlet and outlet samples were analyzed using a GC-FID and the oxidation rates were determined as described by equation 1. In a subsequent experiment, the mass ratio of 2-MB and hexanal was changed to 1: 2 (1 part 2-MB and 2 parts hexanal, w/w) for determination of kinetics.

### **6.2.13 Effect of ozone**

In addition to oxygen, ozone was also tested as an oxidant. The reactor was maintained at 160 °C for the ozone experiments. The injection rate of the aldehydes was increased, such that the inlet concentration was 400-600 ppmv, while the residence time was increased to 4 seconds (across the catalyst packing ) by lowering the flow rate to 2 L/min. Ozone was generated via an ozone generator (Yanco Industries Inc, Canada model QL100 H) and UHP oxygen. The ozone concentration was maintained at 1500 ppmv for all experiments. Ozone was added to the reactor approximately 10 cm before the inlet allowing sufficient mixing between ozone and aldehyde ( $\tau = 0.1$  seconds) before passing through the catalytic bed. After a 12-hour equilibrium period, the inlet and the outlet of the reactor were sampled and analyzed using two gas chromatographs: one equipped with a mass spectrometer for identifying the by products and an FID for quantification.

## **6.3. Results and Discussion**

### **6.3.2 Effect of oxygen**

When ultra high pure helium (99.999 %) was used as the carrier gas (no oxygen present), fractional removal of 2-MB was limited to 2% which was probably due to sampling error. However when pure oxygen was added to the system, the fractional removal increased from less than 2 % to 10 % indicating that the removal was due to the reaction between oxygen and 2-MB (Figure 6.2). This observation was in agreement with our earlier work with 3-MB where presence of oxygen increased the fractional removal from 2 % to 20 % (Kolar et al., 2007).

### 6.3.3 Kinetics of individual aldehydes

The overall rate of 2-MB oxidation was found to increase with an increase in 2-MB concentration ( $R^2 = 0.988$ ) (Figure 6.3) and the Power Law and Mars van Krevelen models were used to determine the kinetic parameters. In both models we assumed that the oxygen concentration was in excess and thus the oxidation rates were independent of oxygen concentration (208,000 ppmv).

For the power law model, the slope and intercept of the plot between  $\ln$  (oxidation rate) and  $\ln$  (concentration) provided the order of the reaction as 1.13 and the rate constant as  $6.2 \times 10^{-4} \text{ mol}^{0.12} \text{ L}^{1.13} \text{ g}^{-1} \text{ s}^{-1}$  for 2-MB (Figure 6.4). Similarly for hexanal the reaction order and the rate constant were determined as 0.88 and  $1 \times 10^{-4} \text{ mol}^{0.12} \text{ L}^{0.82} \text{ s}^{-1}$  respectively.

When the Mars van Krevelen model was fit to the data, the slope of the plot between oxidation rate and concentration yielded a rate constant of  $1.3 \times 10^{-3} \text{ L/g-sec}$  for 2-MB and  $9 \times 10^{-4} \text{ L/g-s}$  for hexanal (Figure 6.5).

The oxidation rates of 2-MB and hexanal were similar to previously reported 3-MB oxidation rates using wood fly ash (Kolar et al., 2007). However, the rates in this work are lower than other published studies on aldehyde oxidation using metal supported catalysts (Table 6.1). For example, catalytic oxidation of acetaldehyde (360 and 510 ppmv) at 205 °C using excess oxygen (3.7 % v/v) was studied over Pt/Rh catalysts by Liakopoulos et al (2001). The oxidation rates measured ranged from  $13\text{-}14 \times 10^{-8} \text{ mol/g-sec}$ . Similarly, based on the data presented by Tang et al (2006) on formaldehyde oxidation using manganese and cerium oxide catalysts at 50-100 °C, oxidation rates were reported as  $5 \times 10^{-8} \text{ mol/g-s}$  (Kolar et al., 2007).

Our rates are also lower than other VOCs studied. For example, the reaction rates were found to range between  $1-18 \times 10^{-8}$  mol/g-sec for n-hexane (164-221 °C) and  $1-5.5 \times 10^{-8}$  mol/g-sec for benzene (140-170 °C), when deep catalytic oxidation of n-hexane (201-566 ppmv) and benzene (9-525 ppmv) using air over 0.1 % Pt, 3% Ni/ $\gamma$ - $\text{Al}_2\text{O}_3$  catalyst was studied (Gangwal et al., 1998).

The lower rates were probably due to the crude nature of our catalyst and its limited surface area ( $\sim 40 \text{ m}^2/\text{g}$  vs 200-300  $\text{m}^2/\text{g}$  for other catalysts). Additionally, the concentrations we tested were less than 125 ppmv, while the above mentioned studies were in the range of 200-570 ppmv. As will be discussed later, our presumed catalytically active phase (iron oxide and other trace minerals) constituted less than 5 % of the total mass of the wood fly ash. When analyzed using SEM, wood fly ash was found to consist of two solid phases – silica and carbon phase. The predominantly silica phase (spherical particles) consisted of carbon (20 %), silicon (19%), and trace amounts of iron, titanium, potassium and calcium (Figure 6.6). It may be noted that 18 % gold found on the wood fly ash surface was an artifact due to  $\sim 120\text{Å}$  gold coating on wood fly ash during sample preparation. Our earlier analysis of wood fly ash using X-ray diffraction technique also revealed the presence of crystalline phases of iron oxides (Kastner et al., 2007). The other phase consisted of primarily carbon (70 %) and trace amounts of calcium and potassium (data not shown). It is theorized that this carbon phase acted as an adsorbent for oxygen and the aldehyde, while the catalytic activity was associated with the silica phase that contained iron and other trace elements.

### 6.3.4 Effect of temperature and activation parameters

The effect of temperature on the reaction rate and overall rate constant was measured at an inlet concentration of 125 ppmv. For both aldehydes, the reaction rates increased linearly when the temperature was increased from 25 to 160 °C (Figure 6.7). The reaction rates for 2-MB and hexanal were same at 25 °C. However, as the temperature increased from 25 °C to 160 °C, the reaction rates of hexanal ( $r_{80} = 7$ ,  $r_{120} = 9$ , and  $r_{160} = 11.5 \times 10^{-9}$  mol/g-s) were significantly higher than 2-MB ( $r_{80} = 3.75$ ,  $r_{120} = 5.75$ , and  $r_{160} = 6.25 \times 10^{-9}$  mol/g-s). The higher oxidation rate of hexanal when compared to 2-MB was found to be in general agreement with data reported by Haisman et al (1983), where the authors reported that the oxidation rates of branched aldehydes were in general lower than branched aldehydes. We speculate that, at higher temperature, the hydrogen abstraction step (equation 13) was extremely fast and resulted in formation of relatively higher amounts of acyl peroxy radicals from 2-MB than would occur at lower temperatures. This would have inhibited the subsequent steps as 2-MB was not available for reaction. Our second proposition is that the oxidation rates of hexanal at higher temperature are higher probably due to higher desorption rates of hexanal on the wood fly ash surface which might have freed the catalytically active sites necessary for the reaction.

From these measured reaction rates, the rate constants for each temperature were calculated assuming an overall reaction order of 1.12 for 2-MB and 0.88 for hexanal (using Power Law model). A linearized Arrhenius model was used to determine the activation parameters, frequency factor (A) and activation energy (E). Arrhenius plots (not shown) for 2-MB and hexanal resulted in an activation energy of

2.6 kcal/mol and 2.8 kcal/mol. Our activation energies are in general lower than the published literature on activation energies of lower molecular weight aldehydes (acetaldehyde) and other VOCs suggesting a free radical mechanism of aldehyde oxidation. Additionally, the activation energies for higher molecular weight aldehydes are lower because they are more prone to hydrogen abstraction than lower molecular aldehydes, due to availability of several carbon-hydrogen bonds. For example, in one study on oxidation of acetaldehyde (Liakopoulos et al., 2001), on platinum/rhenium and palladium catalysts, the activation energy was determined to be 13 kcal/mol over Pt/Rh and 7.5 kcal/mol over Pd catalysts. In another study on catalytic conversion of iso-proponal over mixed  $\text{Al}_2\text{O}_3\text{-Cr}_2\text{O}_3$  catalyst between 270 and 380 °C, the apparent activation energy was determined to be 10.3 kcal/mol (Ezzo et al., 1983).

### **6.3.5 Identification of reaction products and carbon balance**

No reaction products were found when 2-MB and hexanal were studied either at room temperature (25 °C) or at higher temperature (80-160 °C). This was probably because of our inability to detect lower concentrations of VOCs. In order maintain plug flow condition and use a differential reactor model, we maintained a flow rate such that the fractional removal was less than 20-30 %. Additionally, the concentrations we tested were also less than 125 ppmv. Assuming a 20 % fractional removal, the end product concentrations formed were probably lower than our detection limit.

Hence, for identification of reaction products, additional experiments were conducted at higher inlet concentrations (400-600 ppmv), lower flow rates (2 L/min),

and higher temperatures to obtain higher fractional conversions. We used air and helium as carrier gases. Helium was used for better detection and quantification of CO<sub>2</sub>. When 2-MB was tested under these conditions, a 91 % fractional removal was obtained. Additionally, 2-butanone was detected in the outlet of the reactor (Figure 6.8). Based on the standard curves for 2-butanone, we quantified the 2-butanone formation and determined the mean yield (moles of 2-butanone produced/moles of 2-MB consumed) as 0.7. As discussed later, a free radical promoted oxidation of an aldehyde could yield a ketone as one of the end products.

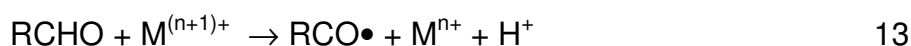
Simultaneously, we analyzed the reactor outlet for CO<sub>2</sub>. Based on the CO<sub>2</sub> formation in the outlet (Figure 6.9), a mean yield of CO<sub>2</sub> was determined to be 1.5 (moles CO<sub>2</sub>/mole 2-MB reacted) for 2- MB oxidation. Similarly, a fractional removal of 89 % was observed when hexanal (400 ppmv) was oxidized. Pentanal and butanal were identified as the end products in the outlet of the reactor (figure 11) whose yields were determined as 0.12 and 0.13 (moles of pentanal or butanal/mole of hexanal reacted) respectively. The yield of CO<sub>2</sub> was calculated as 1.18 (moles CO<sub>2</sub>/mole hexanal reacted) for hexanal oxidation. When these yields were compared with theoretical yields predicted by our proposed oxidation pathway for hexanal, the experimental yield of CO<sub>2</sub> was 40 % lower than predicted by our pathway (Table 6.3). The predicted and theoretical yields of the reaction products are tabulated in Table 6.3.

### **6.3.6 Reaction mechanism of aldehyde oxidation**

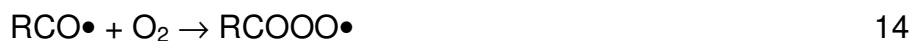
In our work with 2-MB, one of the end products was found to be 2-butanone. Formation of a ketone as one of the end products of an aldehyde oxidation has been

reported previously (Larkin et al., 1990). Additionally, this was in agreement with what we previously reported in the oxidation studies of 3-MB (at 120 °C), where acetone was formed as an end product. Based on formation of 2-butanone as one of the end products, a similar free radical mechanism is proposed in which the aldehyde, in the presence of a metal, forms a free radical via hydrogen abstraction (equation 13). The propagation reaction involves reaction of the aldehyde radical with oxygen to form acyl peroxy radicals (equation 14) and subsequent formation of peracids and regeneration of aldehyde radicals (equation 15).

**Initiation:**



**Propagation:**



The peracids can either react with aldehydes to form carboxylic acids (equation 16) or terminate to form other products.

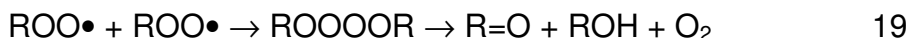
**Carboxylic Acid Production:**



However, in our work, the aldehyde concentrations tested were low and the fractional removal was fairly large (~ 90 %). Under these high temperature-high fractional removal conditions, the formation of carboxylic acids might be unlikely because of low gas phase concentration of aldehydes ( $C_{\text{VOC}} < C_{\text{O}_2}$  and  $C_{\text{CHO}} \sim 0$ ). For example, in our previous work, acetone was identified as an end product when 3-MB was oxidized at 120 °C (Kolar et al., 2007). Additionally, in the presence of metals, branched aldehydes are known to form ketones, alcohols, and hydrocarbons

(Sheldon and Kochi, 1981). One pathway could be termination of peracids to form CO<sub>2</sub>, O<sub>2</sub>, and methyl radicals (equation 17). The methyl radicals react with oxygen to form methyl peroxy radicals (equation 18) which terminate to form ketones and alcohols (equation 19).

**Termination and product formation:**

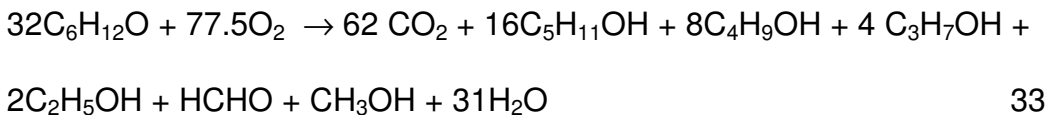


Based on the mechanisms proposed by Lehtinen and Brunow (2000), Larkin (1990), and Haisman et al (1983), oxidation mechanisms for 2-MB (Exhibit A) and hexanal (Exhibit B) are proposed and an overall reaction of 2-MB and hexanal with oxygen are presented below

**2-MB oxidation:**



**Hexanal oxidation:**



In 2-MB experiments, CO<sub>2</sub> and 2-butanone were identified as end products. However, 2-butanol, the other reaction product predicted by our proposed mechanism, was not identified by either mass spectrometer or the FID. It may be possible that the SPB-1 sulfur column that was used in all our experiments may not be equipped to separate alcohols although we did not test this hypothesis.

Similarly, in the hexanal experiments, our proposed mechanism predicted CO<sub>2</sub>, pentanol, butanol, propanol, ethanol, methanol, and formaldehyde as end products. But in all of our experiments, we consistently identified only CO<sub>2</sub>, pentanal, and butanal in the outlet (Table 6.2 and Figure 6.10 B). However, in addition to pentanal and butanal, the outlet sample also consisted of two peaks (retention time = 2.2 and 2.9 minutes) that were not conclusively identified by mass spectrometry (Figure 6.10). In our proposed reaction pathway for hexanal oxidation, we obtained methanol as one of the end products, along with other alcohols (equation 33). But methanol could not be identified, probably because the mass spectral analyses of inlet and outlet samples were performed for m/z ratios between 40 and 150 and the majority of ions (m/z) for methanol were lower than 40 (i.e., m/z's: 15, 29, 31, and 32). Further, when a neat sample of methanol was injected on the GC-FID, the retention times of the unidentified outlet peak and neat methanol matched (RT = 2.2 minutes) (data not shown) indicating that the peak could be methanol. The drawback of our proposed mechanism of hexanal oxidation is that the experimental data was found to be inconsistent with the proposed pathway. We did not identify any of the remaining alcohols or formaldehyde although the free radical reaction mechanism predicted these products. It may be speculated that hexanal was converted into pentanal and butanal in successive steps along with pentanol and butanol (Exhibit B). At this stage, as the carbon chains became shorter, further oxidation may not have been possible (under the given experimental conditions) and hence pentanal and butanal were observed in the outlet. However, our presumption that one of the unidentified peaks was methanol could not be explained with this theory.

### 6.3.8 Kinetics of binary mixture

The oxidation of binary mixtures was tested at three mass proportions. When a proportion of 1:2 (2-MB: hexanal) was tested, there appeared to be an inhibitory effect on 2-MB oxidation due to the presence of hexanal (Figure 11 A). Given our lack of extensive data, it is difficult to explain the mechanism of 2-MB inhibition due to hexanal. We speculate that this was probably due to the scavenging effect of hexanal. As 2-MB adsorbed on the catalyst, it formed free radicals (as described in earlier sections). As these free radicals propagated, they formed additional aldehyde radicals. Hexanal in this mixture probably scavenged the free radicals and inhibited the propagation reaction of 2-MB and thereby affecting the oxidation of 2-MB. This observation can be explained by looking at the hexanal oxidation rate due to presence of 2-MB (Figure 11 B). As hexanal consumed free radicals, its oxidation rate increased when compared to its individual response under similar condition. However, when the proportion of 2-MB was increased in the mixture from 33 % to 50 % (on a mass basis), the presence of 2-MB decreased the hexanal oxidation rate probably due to over production of free radicals and their subsequent termination reaction involving themselves.

### 6.3.9 Effect of temperature on oxidation of binary mixture

When tested as a binary mixture (300 ppmv each) (1:1 mass basis) at 160 °C and 2 L/min, fractional conversion of 96 % for 2-MB and 83 % for hexanal was obtained. When tested individually, the measured oxidation rates of 2-MB and hexanal at 125 ppmv, 5 L/min and 160 °C were  $5 \times 10^{-9}$  mol/g-s for 2-MB and between  $11 \times 10^{-9}$  mol/g-s for hexanal. In order to determine the effect of

temperature on oxidation of binary mixture, the data obtained for binary mixture (2 L/min) was extrapolated to 5 L/min by assuming a differential reactor model (Table 6.4). Similarly, the data obtained for individual aldehydes was also extrapolated to match the concentration that was used in mixture studies (300 ppmv). When compared, the oxidation rate of the mixture was higher than the individual aldehydes at 160°C suggesting that there was no inhibition at higher temperature. The oxidation rate of 2-MB (in presence of hexanal) was six times higher than 2-MB when tested individually. Similarly, the hexanal oxidation rate in presence of 2-MB doubled when compared to hexanal tested individually under identical conditions. It may however be noted that these calculations were performed for comparison purposes only and not to obtain kinetics.

Another interesting observation is that the by-products formed in the outlet of the reactor were similar to that for 2-MB and hexanal (Figure 6.12). The formation of by-products similar to that of individual aldehydes suggests that there was no interaction between the aldehydes at 160°C and breakdown of each aldehyde occurred independently and in parallel to each other. This observation is significant because at 25°C there was inhibition of 2-MB oxidation due to presence of hexanal and we presumed that the hexanal consumed the reactive free radicals generated by 2-MB and prevented its oxidation. However at 160°C, hexanal could also have generated free radicals along with 2-MB and in initiating its own oxidation to form butanal and pentanal and end products.

### 6.3.10 Effect of ozone

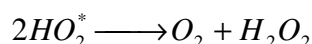
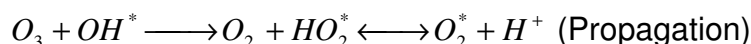
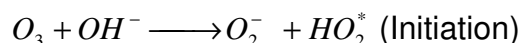
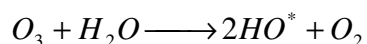
In our experiments with 2-MB and hexanal at 160 °C, although we obtained 80-96 % fractional conversion using oxygen as an oxidant, the oxidation was incomplete as indicated by the presence of 2-butanone for 2-MB and pentanal and butanal for hexanal. In order to obtain complete oxidation ( $\text{CO}_2$  and  $\text{H}_2\text{O}$  as the only end products), we tested ozone (1500 ppmv) as an oxidant under identical conditions (2 L/min flow, 10 g catalyst, and 160 °C). Initially, single aldehydes (140-180 ppmv) were tested, followed by a binary mixture of approximately equal concentrations (300 ppmv each). Removal of aldehydes due to ozone alone and ozone and wood fly ash was monitored. Samples were drawn from three ports: the inlet port, a port just after addition of ozone ( $\tau=0.1$  seconds) to monitor the effect of ozone alone, and the outlet port past the catalytic bed to monitor the effect of ozone and the wood fly ash.

Analysis of samples drawn from the reactor just after addition of ozone, but before the catalytic bed (Figures 6.13 B and 6.14 B) indicated 80 % fractional removal for 2-MB and hexanal indicating a homogeneous gas phase reaction has occurred. However, close to 100 % removal was found due to the presence of wood fly ash (Figures 6.13 C and 6.14 C, bottom) without any by-products. When compared to our experiments with oxygen (Figures 6.8 and 6.10), the presence of ozone not only increased the oxidation rate, but eliminated by-product formation. The absence of by-products in the reactor outlet suggests that a complete oxidation of the aldehydes occurred with ozone and wood fly ash (a carbon balance was not performed however).

The effect of ozone on oxidation of binary mixture was similar to individual aldehydes. Ozone reacted directly (homogeneous, no catalyst) with the binary mixture and a 70 % fractional removal was attained (Figure 6.15 B). However, when ozone and binary mixture was passed through the catalytic bed, complete oxidation was observed (Figure 6.15 C).

### 6.3.11 Potential mechanism for ozone

As an oxidant, ozone can react with VOCs in several ways in presence of a catalyst (Oyama, 2000). Ozone decomposes into  $OH^*$  radicals as described by Gunten (2003).



The above mechanism was proposed for ozone decomposition in aqueous phase and under alkaline conditions. In our work wood fly ash was used as a catalyst whose pH was close to 11. Additionally, the air was humidified (RH = 78 %) before entering the catalytic reactor. Considering the high pH and presence of water vapor, it is theorized that ozone decomposes into hydroxy radicals ( $OH^*$ ) as shown by the above mechanism (Gunten 2003).

Additionally, carbon was a major constituent of the wood fly ash and known to catalyze oxidation reactions involving ozone (Jun Ma et al., 2004). For example, in

one of our earlier studies (Kastner et al., 2007), we theorized an  $\text{OH}^*$  radical based mechanism for oxidizing propanal using activated carbon and ozone.

In the above chain reaction, while the  $\text{OH}^-$  acts as an initiator to produce a superoxide radical ion ( $\text{O}_2^-$ ), ozone acts as a promoter and reacts with hydroxyl radical ( $\text{OH}^*$ ) to regenerate superoxide radical ions ( $\text{O}_2^-$ ). The organics and other impurities (carbonate and bicarbonates) consume the hydroxyl radical ( $\text{OH}^*$ ) without producing superoxide radical ions ( $\text{O}_2^-$ ) and are appropriately termed as inhibitors.

Based on the above mechanism of  $\text{OH}^*$  formation, an overall oxidation of 2-MB and hexanal may be represented as below:



## 6.4 Conclusion

Our studies indicate that wood fly ash catalyzed the oxidation of 2-MB and hexanal- in presence of oxygen via a free radical mechanism. A pseudo-first order model was used to describe the oxidation kinetics. The oxidation rates and corresponding activation energies obtained were comparable with the published oxidation rates of other VOCs. When tested at 160°C, 90 % fractional removal was obtained and 2-butanone and  $\text{CO}_2$  from 2-MB and pentanal, butanal,  $\text{CO}_2$ , and possibly methanol from hexanal were experimentally determined as end products. As a binary mixture, the oxidation rate of 2-MB was inhibited while the oxidation rate of hexanal significantly increased. When 1500 ppmv of ozone was tested as an oxidant along with wood fly ash at 160°C, 100 % removal was achieved. Our results suggest that wood fly ash could be used as a viable catalyst along with oxygen and

ozone to treat odorous aldehydes from rendering emissions. This could potentially eliminate the need for expensive treatment options such as wet scrubbers and catalytic combustors. However, additional studies are needed to investigate the exact amount of ozone needed for complete removal and an accompanying economic analysis on ozone generation and usage to determine the feasibility of catalytic ozonation.

## References

1. D. Baumann, L.F. Lorenz, S.A. Batterman, G.Z. Zhang. *Forest Products Journal*. 50 (2000) 75-82.
2. F. Á. Anders, C. Barrachina, S. Sidhu, *Journal of Science and Food Agriculture*. 84 (2004) 2015-2021.
3. J.R. Kastner, K. C. Das, *J. Air & Waste Manage. Assoc.* 52 (2002) 459-469.
4. M. S. Brewer, J.D. Vega, E.G. Perkins, *Journal of Food Lipids*. 6 (1999) 47-61.
5. S.E. Hrudey, A. Gac, S.A. Daignault, *Water Sci. Technol.* 20 (1988) 55-61.
6. L. Wang, P. Kolar, J.R. Kastner, B. Herner, *J. Air & Waste Manage. Assoc.* 58 (2007) 412-423.
7. J.R. Kastner, K.C. Das. *Journal of Chemical Technology and Biotechnology*. 80 (2005) 1170-1179.
8. J.R. Kastner C. Hu, K.C. Das, R. McClendon. *Journal of the Air and Waste Management Association*. 53 (2003) 1218-1224.
9. J. Tsou, L. Pinard, P. Magnoux, J. L. Figueiredo, M. Guisnet. *Applied Catalysis B: Environmental*. 46 (2003): 371-379.

10. K. Everaert, J. Baeyens, *Journal of Hazardous Materials*. 109 (2004) 113-139.
11. A. G. Gervasini, V. Ragaini, *Catalysis Today*. 60 (2000) 129-138.
12. A. G. Gervasini, V. Vezzoli, V. Ragaini. *Catalysis Today*. 29 (1996) 449-455.
13. J.M. Smith, *Chemical Engineering Kinetics*. McGraw-Hill, New York, 1981.
14. F. Klose, P. Scholz, G. Kreisel, B. Ondruschka, R. Kneise, U. Knopf, *Applied Catalysis, B: Environmental*, 28(2000) 209-221.
15. J. C. Demeyer, V. Nkana, M. G. Verloo, *Bioresource Technol*. 77 (2001) 287-295.
16. J.R. Kastner, Q. Buquoi, R. Ganagavaram, K.C. Das, *Environmental Science and Technology*, 39 (2005) 1835-1842.
17. P. Kolar, J.R. Kastner, J. Miller, *Applied Catalysis B: Environmental*. 76 (2007) 203-217.
18. J.R. Kastner, K.C. Das, J.Q. Buquoi, N.D. Melear, *Environmental Science and Technology*. 37 (2003) 2568-2574.
19. Liakopoulous, S. Pouloupoulos, C. Philippopoulos, *Industrial & engineering chemistry research*. 40 (2001) 1476-1481.
20. X. Tang, Y. Li, X Huang., Y Xu., H Zhu., J Wang., W. Shen, *Applied Catalysis B: Environmental*. 62 (2006) 265-273.
21. S.K. Gangwal, M.E. Mullins, J.J. Spivey, P.R. Caffery, B.A. Tichenor, *Applied Catalysis*. 36 (1998) 231-247.
22. J.R. Kastner, R. Ganagavaram, P. Kolar, A. Teja, C. Xu, *Environmental Science and Technology*. 42 (2008) 556-562.

23. V. Haisman, P. Stampachova, J. Vcelak, V. Chvalovsky. *Oxidation Communications*, 4 (1983) 229-236.
24. E.M. Ezzo, N.A. Yousef, H.S. Mazhar, *Surface Technology*. 19 (1983) 373-378.
25. D. Larkin, *J. Org. Chem.* 55 (1990) 1563-1568.
26. R.A. Sheldon, J.K. Kochi. *Metal-Catalyzed Oxidations of Organic Compounds*. Academic Press. New York. 1981.
27. C. Lehtinen and G. Brunow, *Organic Process Research & Development*. 4 (2000) 544-549.
28. S. T. Oyama, *Catal. Rev-Sci. Eng* 42:3 (2000) 279-322.
29. U.V Gunten, *Water Research*. 37 (2003) 1443-1467.
30. J. Ma, M. H. Sui, Z. L. Chen, L. N. Wang, *Ozone: Science and Engineering*. 26 (2004) 3-10.
31. I. N, Martyanov, S. Uma., S. Rodrigues., K.J. Klabundle. *Langmuir*. (21 (2005) 2273-2280.
32. J. R Kastner, R. Ganagavaram, P. Kolar, A. Teja, and C. Xu. *Environmental Science and Technology*. 42:2 (2008) 556–562.

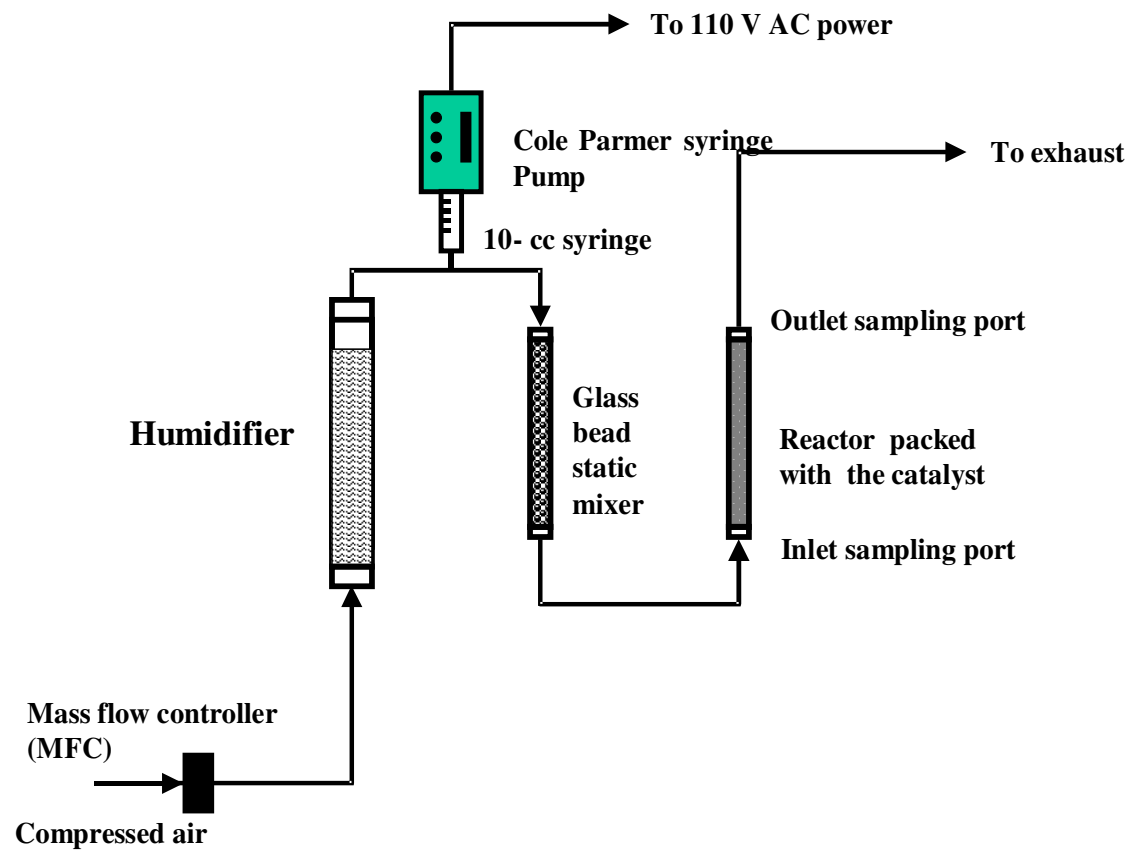


**Figure 6.1.** Schematic of the continuous fixed bed reactor system that was used in this study.

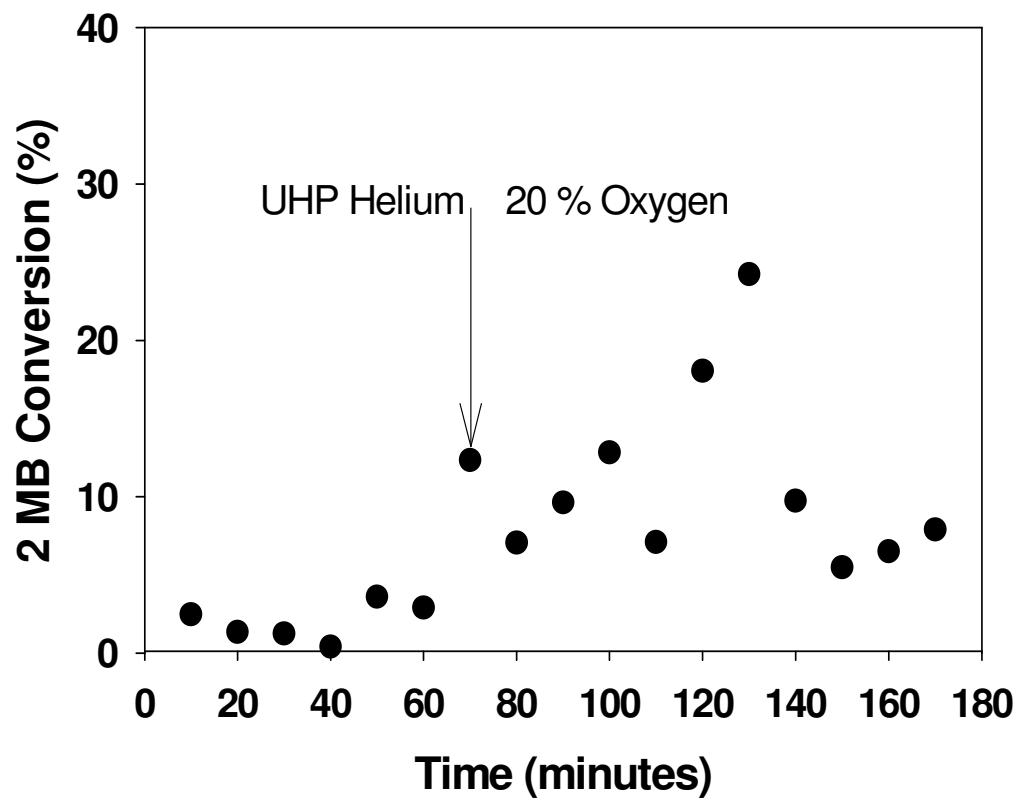


**Figure 6.2.** Effect of oxygen on oxidation of 310 ppmv 2-MB using 10 g of wood fly ash at 2 L/min and 25 °C.

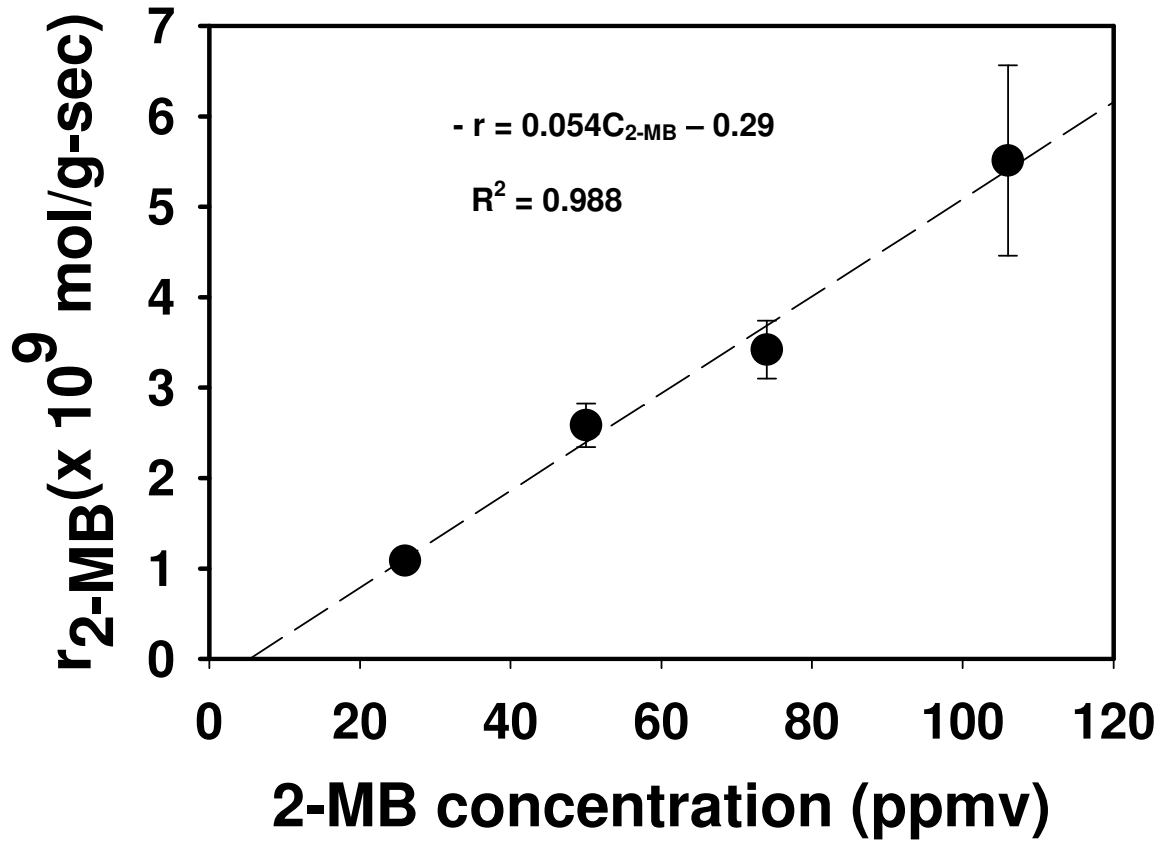


**Figure 6.3.** Effect of concentration on oxidation rate of 2-MB. The oxidation rates of 2-MB (5 L/min, 25°C, and 10 g wood fly ash) increased linearly with an increase in concentration

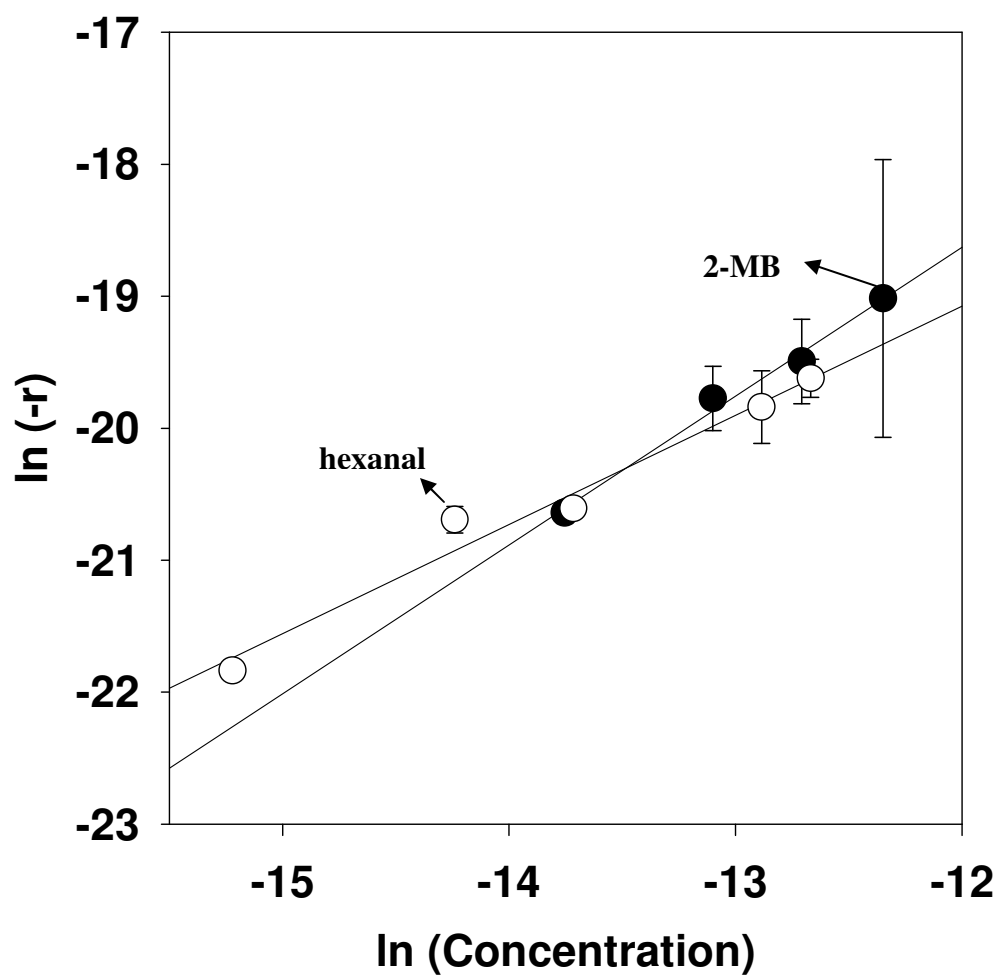


**Figure 6.4.** The kinetic parameters of 2-MB (●) and hexanal (○) oxidation were determined using a pseudo-first order power law model ( $k_{2\text{-MB}} = 0.0062 \text{ mol}^{0.12} \text{ L}^{1.13} \text{ g}^{-1} \text{ s}^{-1}$ ) and ( $k_{\text{hexanal}} = 0.0001 \text{ mol}^{0.12} \text{ L}^{0.82} \text{ s}^{-1}$ ).

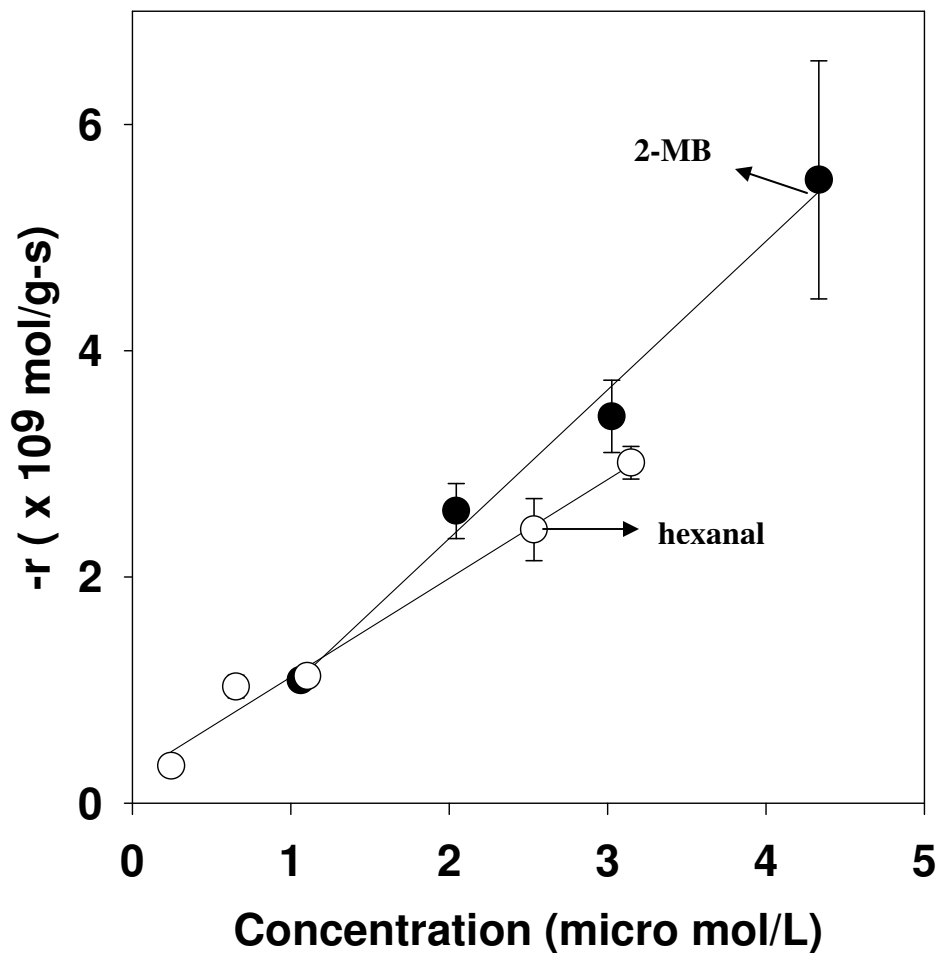
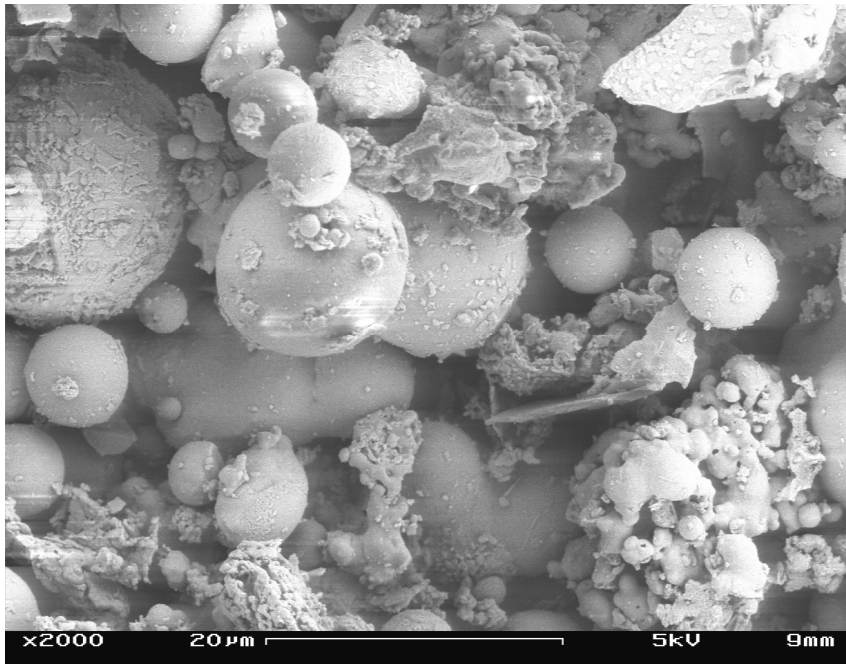


**Figure 6.5.** The kinetic parameters of 2-MB (●) and hexanal (○) oxidation were determined using Mars van Krevelen model. ( $k_{2\text{-MB}} = 0.0009$  L/g-sec and  $k_{\text{hexanal}} = 0.0013$  L/g-sec).



### Quantitative results

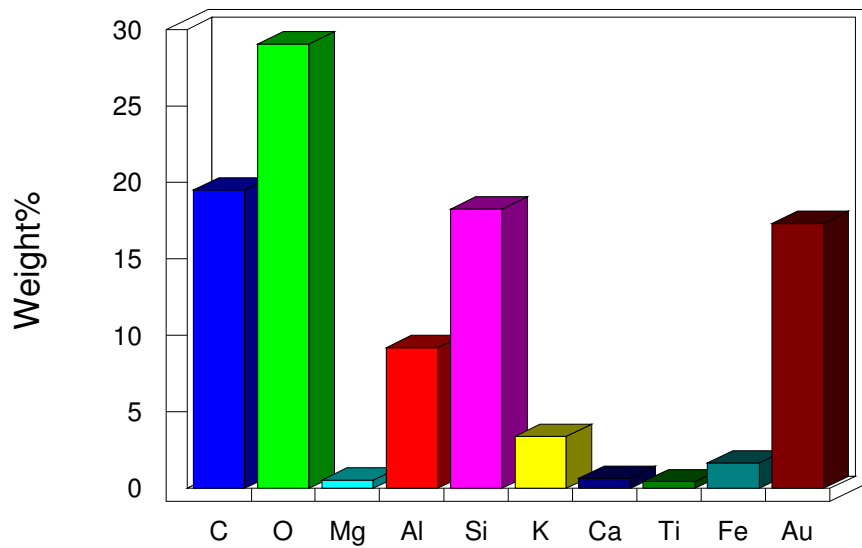


**Figure 6.6.** Micrograph of wood fly ash using scanning electron microscope (SEM) (Top) and energy dispersive spectroscopy (EDS) (bottom).

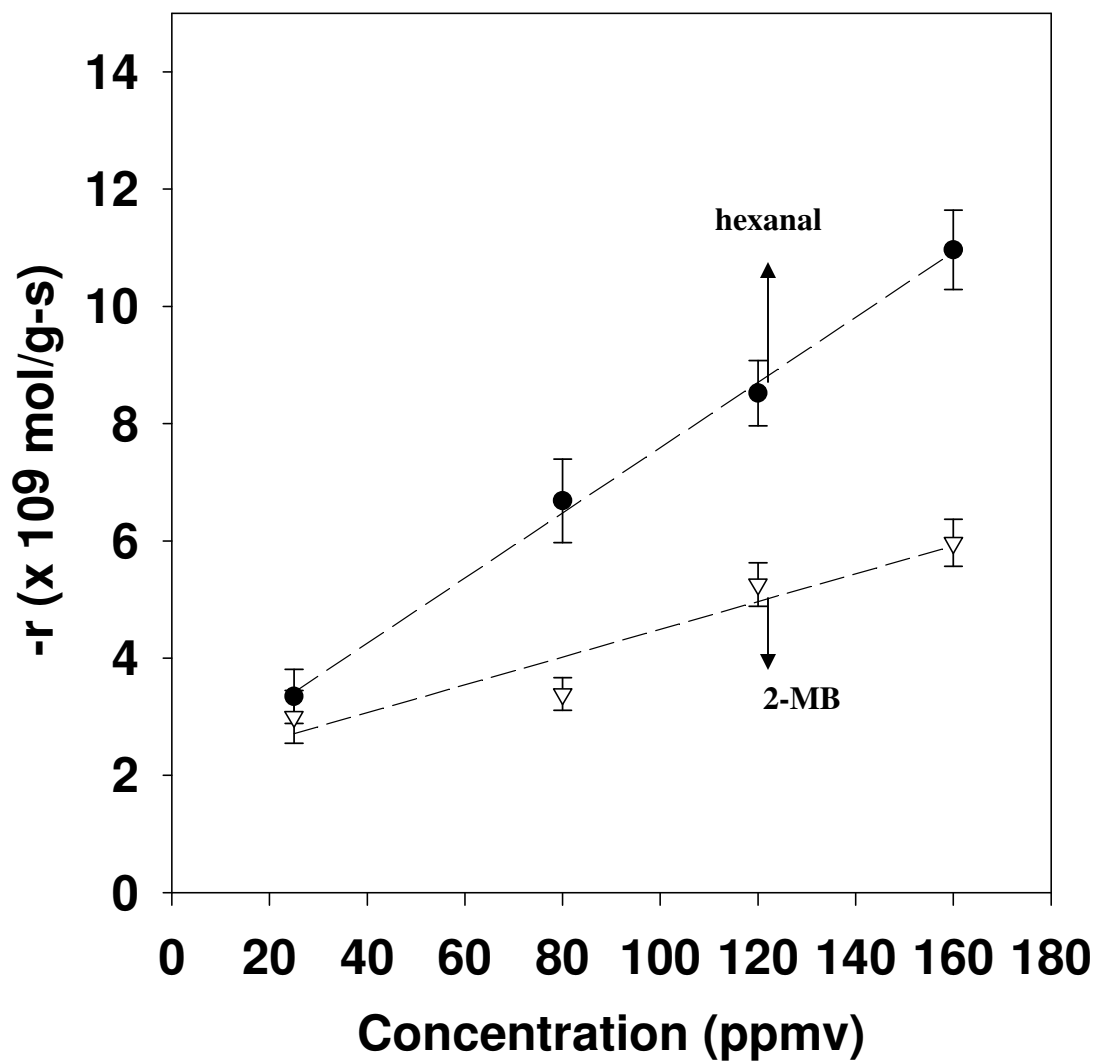


**Figure 6.7.** Effect of temperature on oxidation of 2-MB ( $\blacktriangledown$ ) and hexanal ( $\bullet$ ) when tested at 125 ppmv and 5 L/min.

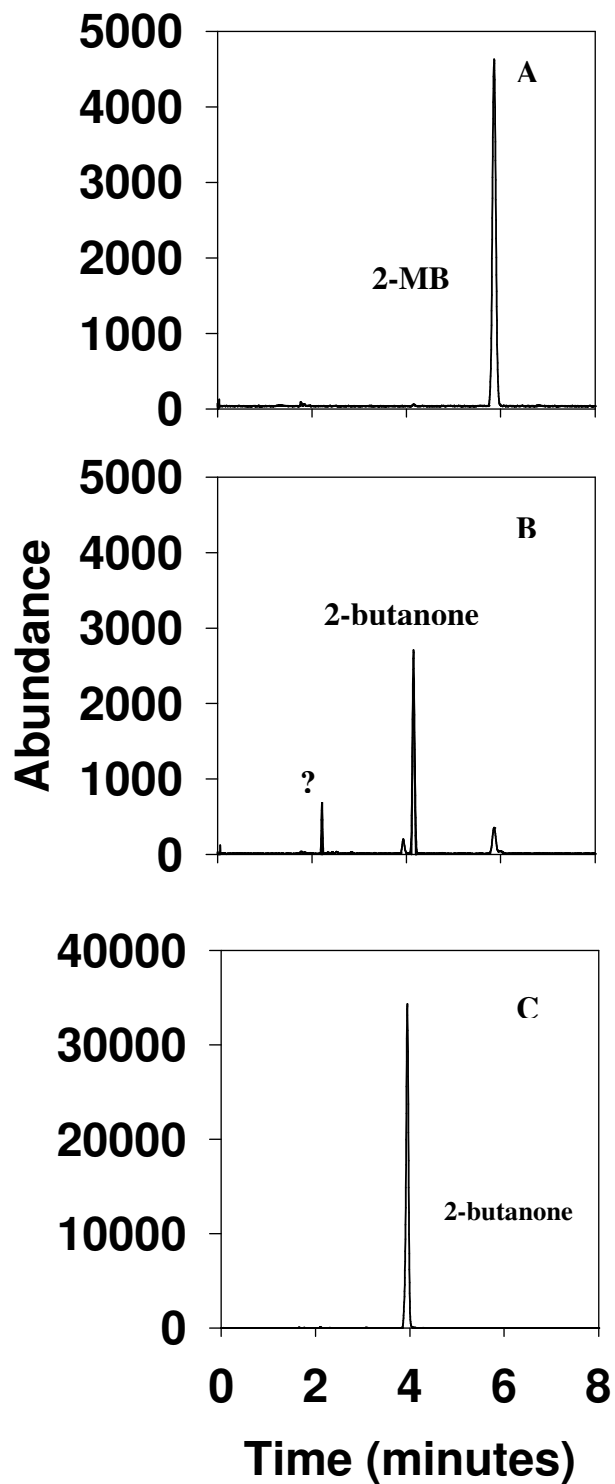


**Figure 6.8.** Typical chromatograms of inlet (A) (510 ppmv, 160°C) and outlet (B) taken from the reactor that oxidized 2-MB using 10g wood fly ash. 2-butanone was detected in the outlet and compared with a neat standard of 2-butanone (C).

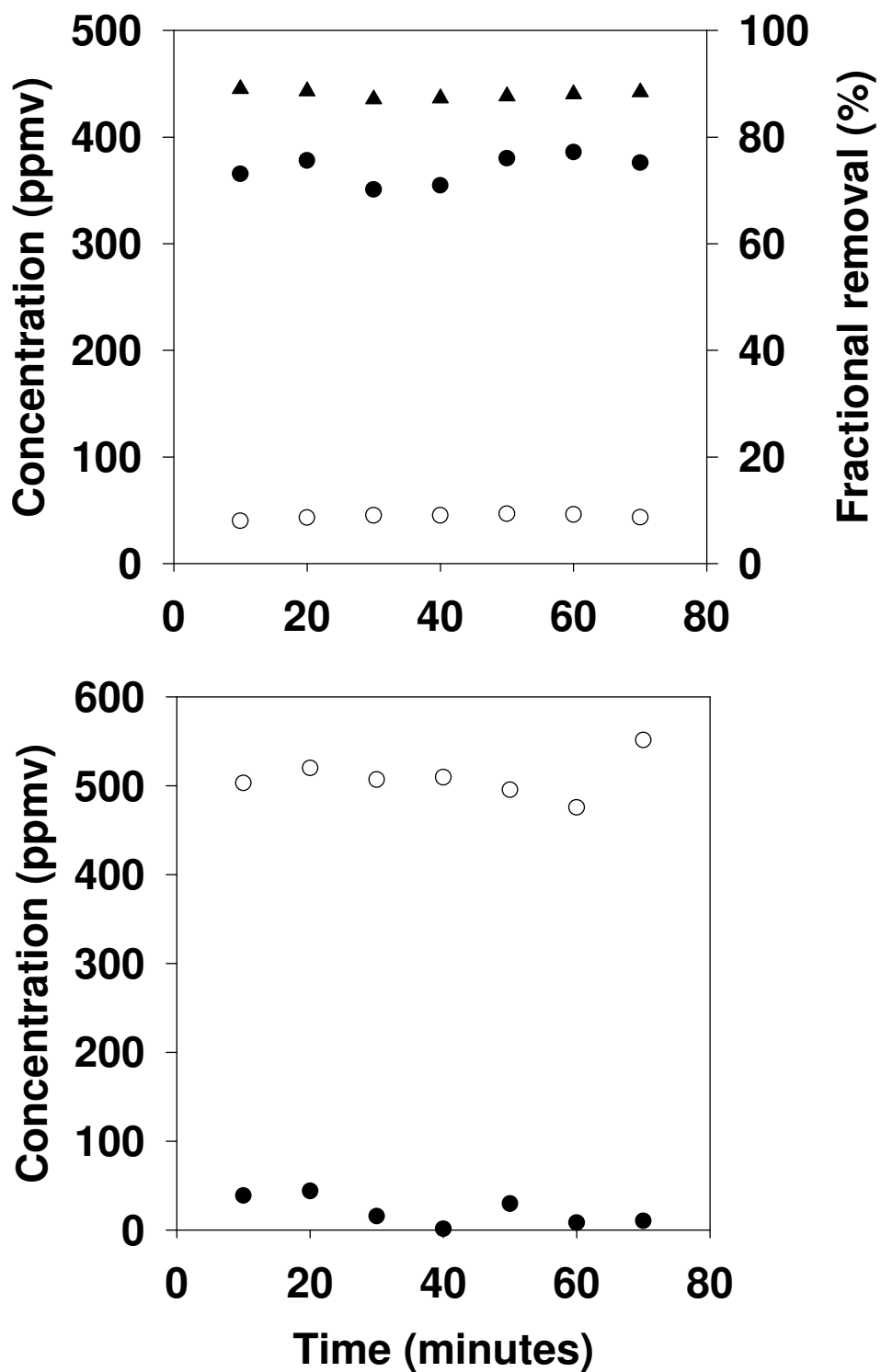


**Figure 6.9.** Disappearance of 2-MB (A, top) and production of CO<sub>2</sub> (B, bottom) at 160°C using 10 g wood fly ash and 2 L/min helium (● is the inlet, ○ is the outlet, and ▲ is the fractional removal).

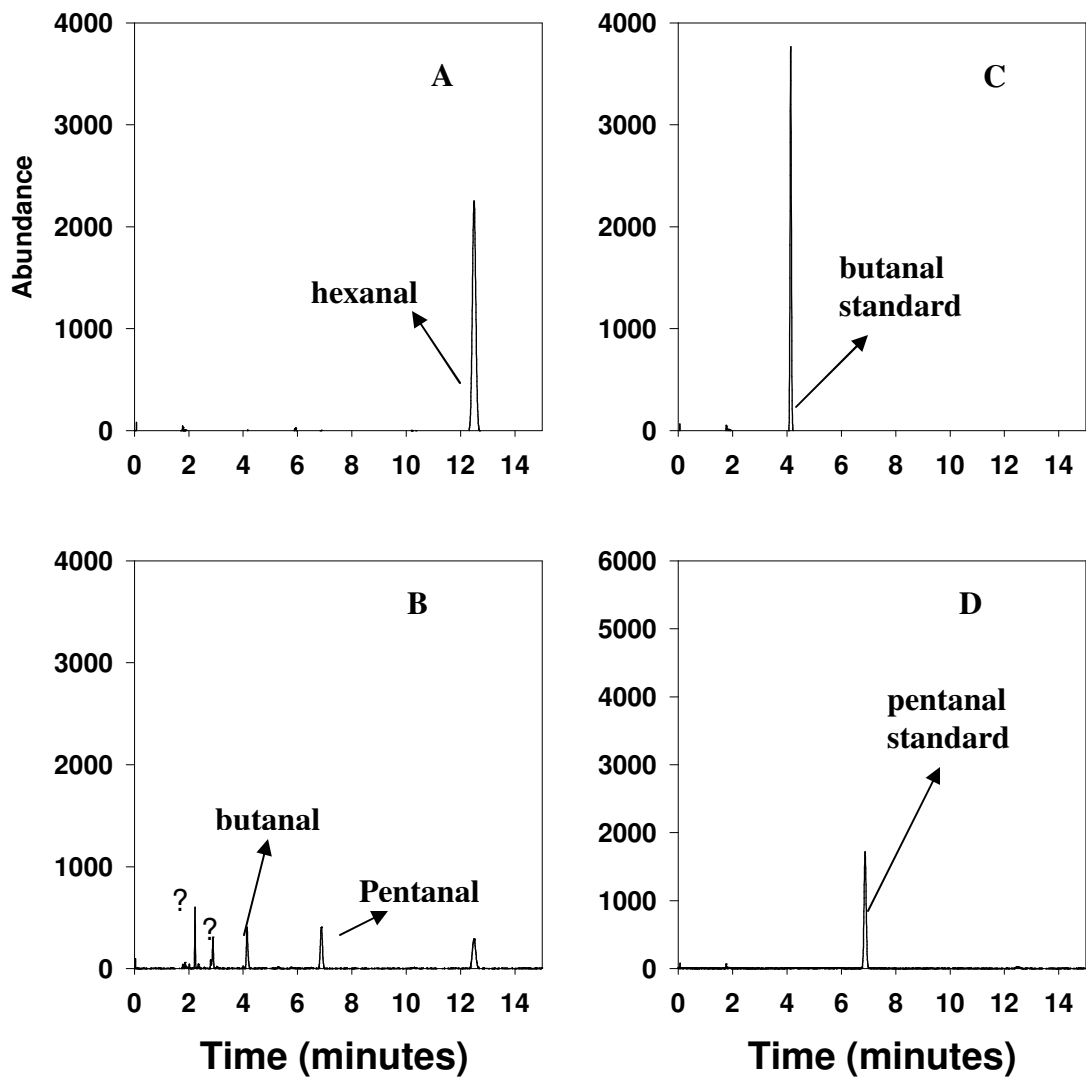


**Figure 6.10.** Typical chromatograms of inlet (A) (350 ppmv, 160°C) and outlet (B) taken from the reactor that oxidized hexanal using 10g wood fly ash. Pentanal and butanal were detected in the outlet and compared with neat standards of butanal (380 ppmv, C) and pentanal (225 ppmv, D).

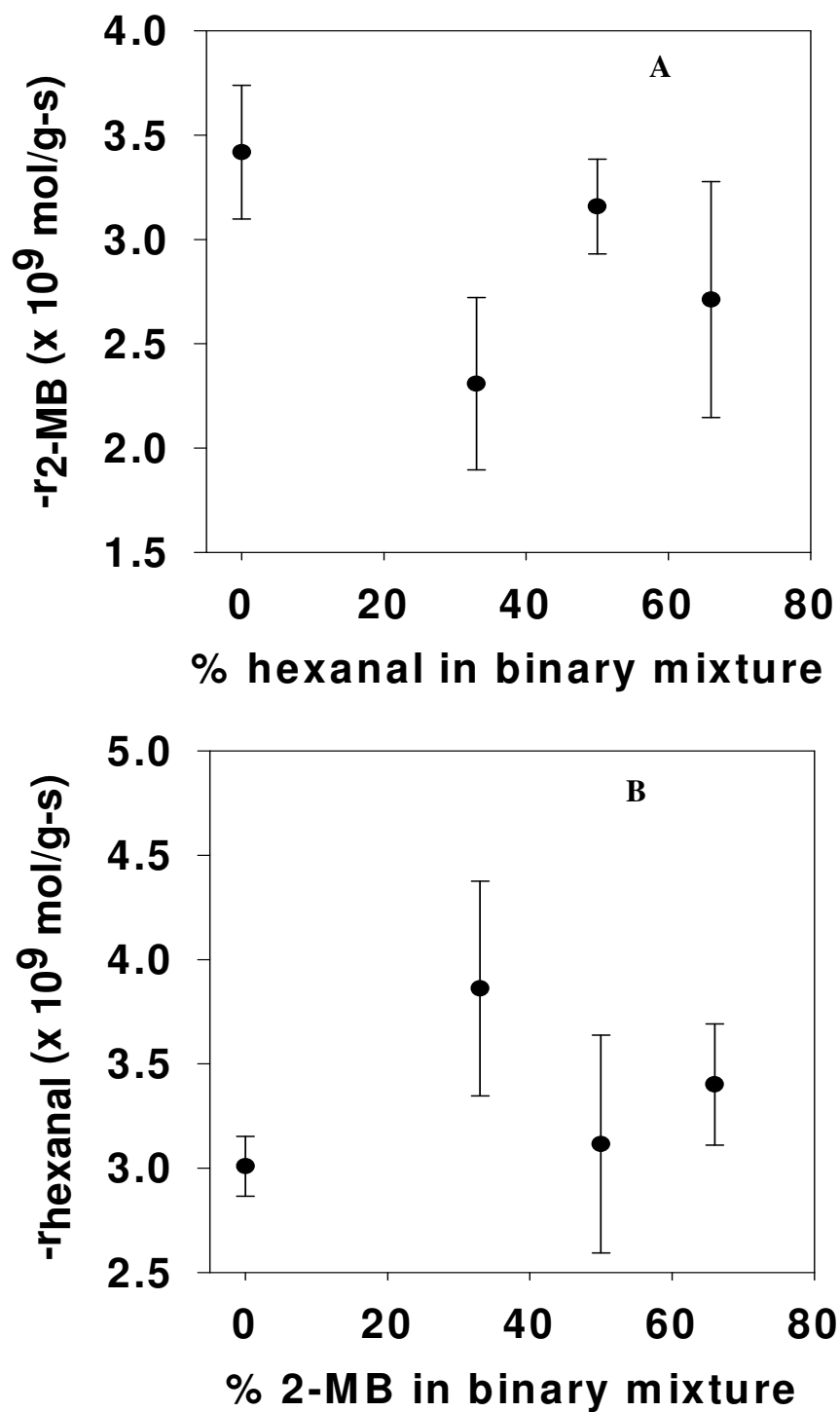


**Figure 6.11.** Effect of 2-MB and hexanal on oxidation of binary mixture at 70 ppmv inlet concentration, 25°C, 5 L/min, and 10 g wood fly ash. Effect of hexanal on the oxidation of 2-MB (A) and effect of 2-MB on the oxidation of hexanal (B).

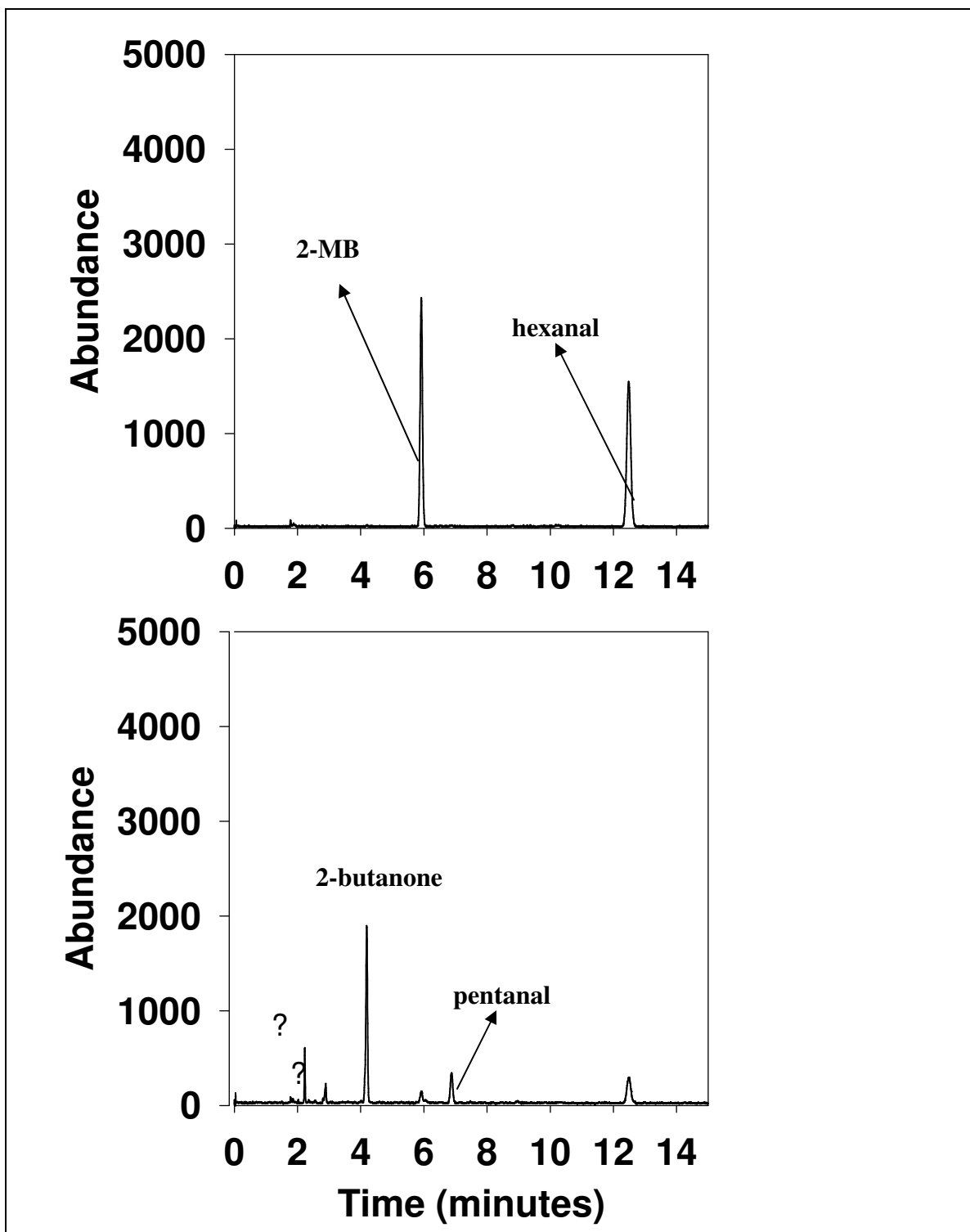


**Figure 6.12.** Typical chromatograms of inlet (A, top) and outlet (B, bottom) taken from the reactor that oxidized 2-MB (300 ppmv) and hexanal (300 ppmv) using 10 g wood fly ash at 160°C. 2-butanone and pentanal were detected as end products.

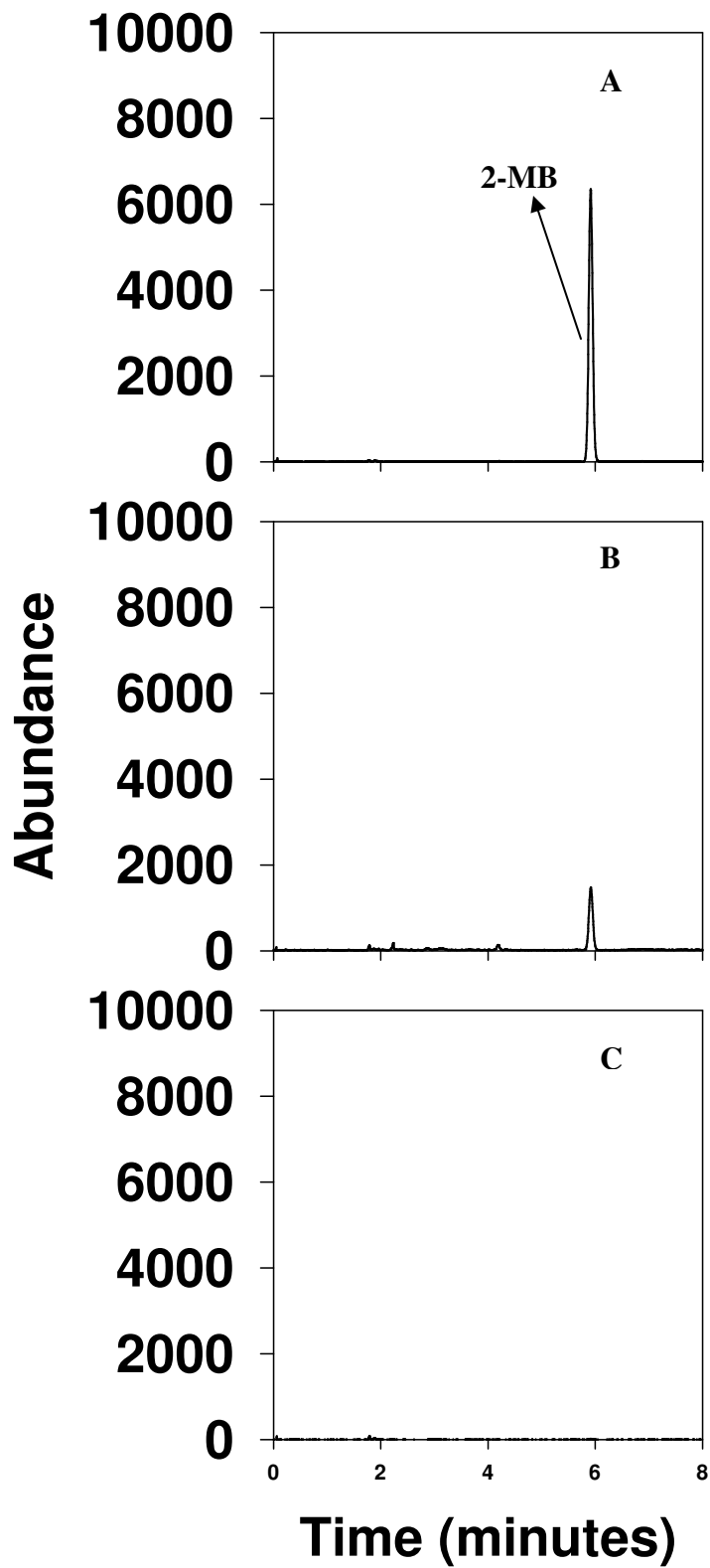


**Figure 6.13.** Effect of 1500 ppmv ozone on oxidation of 140 ppmv 2-MB using 10 g wood fly ash at 160 °C. Typical chromatograms showing inlet (A), reaction with ozone alone (B), and reactor outlet (C).

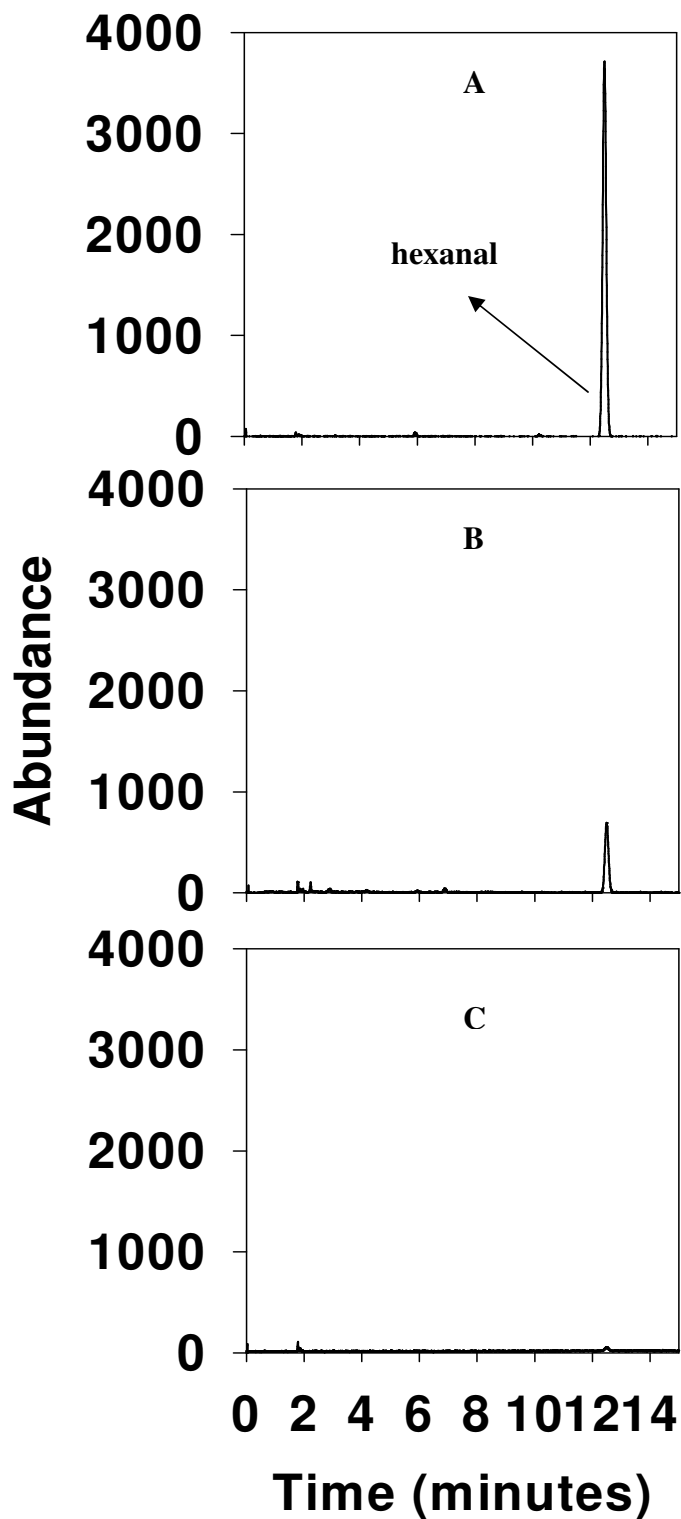


**Figure 6.14.** Effect of 1500 ppmv ozone on oxidation of 180 ppmv hexanal using 10 g wood fly ash at 160 °C. Typical chromatograms showing inlet (A), reaction with ozone alone (B), and reactor outlet (C).

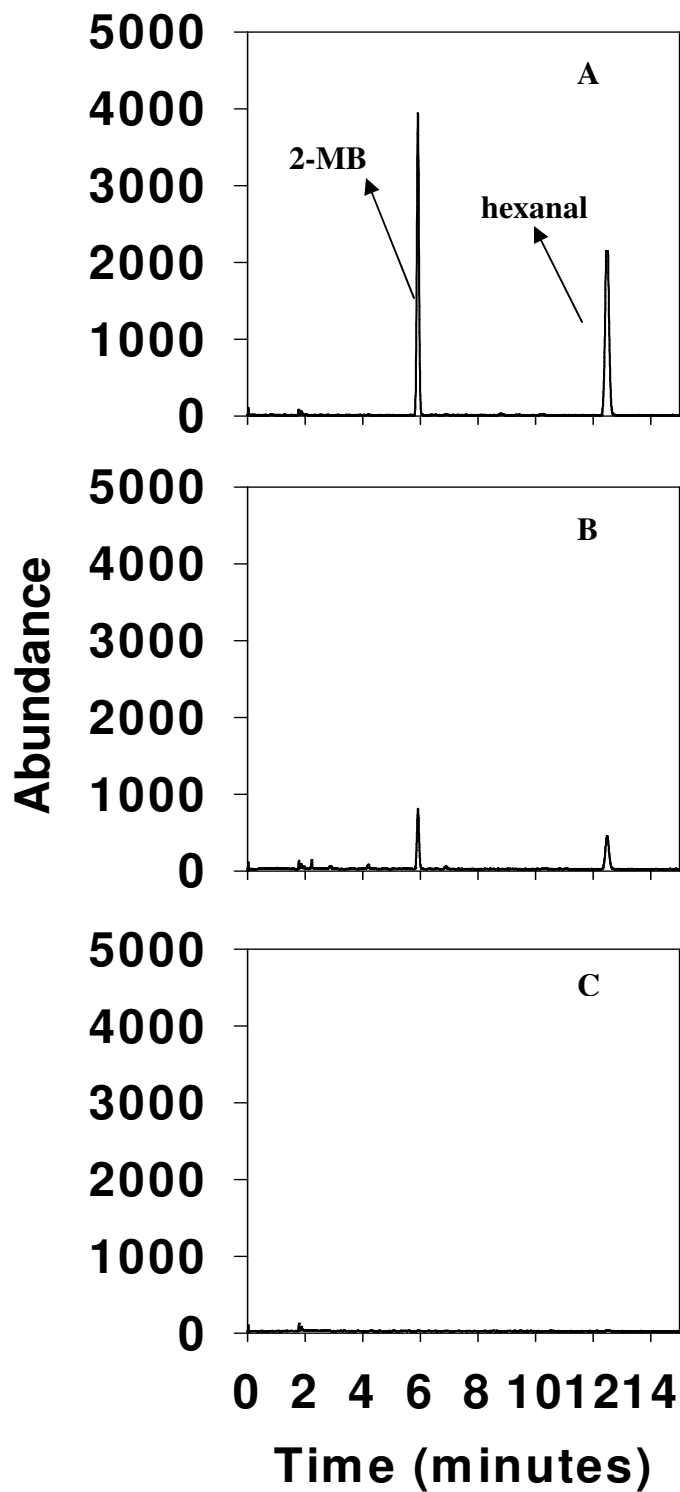


**Figure 6.15.** Effect of 1500 ppmv ozone on oxidation of binary mixture of 2-MB and hexanal (450 ppmv each) using 10 g wood fly ash at 160 °C. Typical chromatograms showing inlet (A), reaction with ozone alone (B), and reactor outlet (C).

**Table 6.1.** Comparison of oxidation rates of aldehydes with various catalysts including wood fly ash that was used in this research.

VOC	Concentration (ppmv)	Catalyst	Temp (K)	End products	Reaction rate (mol/g-s)	References
Propanal	20,000	Mn <sub>3</sub> O <sub>4</sub>	400-560	Acetaldehyde CO <sub>2</sub>	11 x 10 <sup>-10</sup>	Linders et al., 2001
Formaldehyde	580	Oxides of Mn- Ce	333-373	ND	50 x 10 <sup>-9</sup>	Martyanov et al., 2005
3-MB	45-68	Wood fly ash	298-433	acetone	4-10 x 10 <sup>-9</sup>	Kolar et al., 2007
2-MB	20-120	Wood fly ash	298-433	2-butanone	3-5 x 10 <sup>-9</sup>	This work
Hexanal	20-120	Wood fly ash	298-433	pentanal butanal,	3-11 x 10 <sup>-9</sup>	This work
Acetaldehyde	360-510	Pt/Rh	498	CO <sub>2</sub>	110-140 x 10 <sup>-9</sup>	Liakopoulos et al., 2001

**Table 6.2.** Mass spectral analysis of the outlet samples based on experimental and neat standards when 2-MB and hexanal were oxidized at 160 °C using wood fly ash and molecular oxygen.

<b>Substrate</b>	<b>Proposed end products</b>	<b>m/z experimental</b>	<b>m/z NIST standard</b>	<b>Match factor<sup>2</sup></b>
2-MB	2-butanone	48, 57, 67, 72	48, 57, 72	53
2-MB	2-butanol	ND <sup>1</sup>	45, 59	ND <sup>1</sup>
hexanal	pentanal	41, 44, 58, 67	41, 44, 58	72
hexanal	butanal	43, 57, 72	27, 44, 57, 72	59
hexanal	methanol	ND <sup>1</sup>	15, 29, 31	ND <sup>1</sup>

<sup>1</sup>ND: Not detected in the outlet of the reactor

<sup>2</sup>Maximum match factor: 100

**Table 6.3.** Comparison of measured and theoretical yields of the byproducts when 2-MB and hexanal were oxidized using 10 g wood fly ash at 160°C and 2 L/min flow rate.

VOC	Moles reacted	By-products	Moles formed	Yield=moles formed/moles reacted	Yield (proposed reaction pathway-partial oxidation)	Yield (complete oxidation)
2-MB	$7.64 \times 10^{-7}$	CO <sub>2</sub>	$1.14 \times 10^{-6}$	1.50	1	5
		2-butanone	$5.32 \times 10^{-9}$	0.7	0.5	0
		2-butanol	0	0	0.5	0
hexanal	$8.58 \times 10^{-7}$	CO <sub>2</sub>	$1.01 \times 10^{-6}$	1.180	2	6
		pentanol	0	0	0.5	0
		butanol	0	0	0.25	0
		propanol	0	0	0.125	0
		ethanol	0	0	0.0625	0
		methanol	0	0	0.03125	0
		formaldehyde	0	0	0.03125	0

**Table 6.4.** Comparison of oxidation rates of 2-MB and hexanal in a mixture with individual 2-MB and hexanal oxidation rates at 160 °C.

VOC	Temp (°C)	Flow rate L/min	Concentration ppmv	X (%)	-r (x 10 <sup>-9</sup> mol/g-s)
2-MB	160	5	125	15	5
hexanal	160	5	125	15	11
2-MB	160	5	300		12 <sup>1</sup>
hexanal	160	5	300		26 <sup>1</sup>
2-MB	160	2	300-400	96	
hexanal	160	2	300-400	83	
2-MB	160	5	300-400		73 <sup>2</sup>
hexanal	160	5	300-400		52 <sup>2</sup>

<sup>1</sup>Extrapolated from data obtained at 160 °C, 5 L/min, and 125 ppmv inlet.

<sup>2</sup>Extrapolated from the data obtained at 160 °C, 2 L/min, and 300 ppmv inlet.

## Exhibit A

### Proposed 2-MB oxidation pathway

#### Summary

2-MB to 2-butanone and 2-butanol

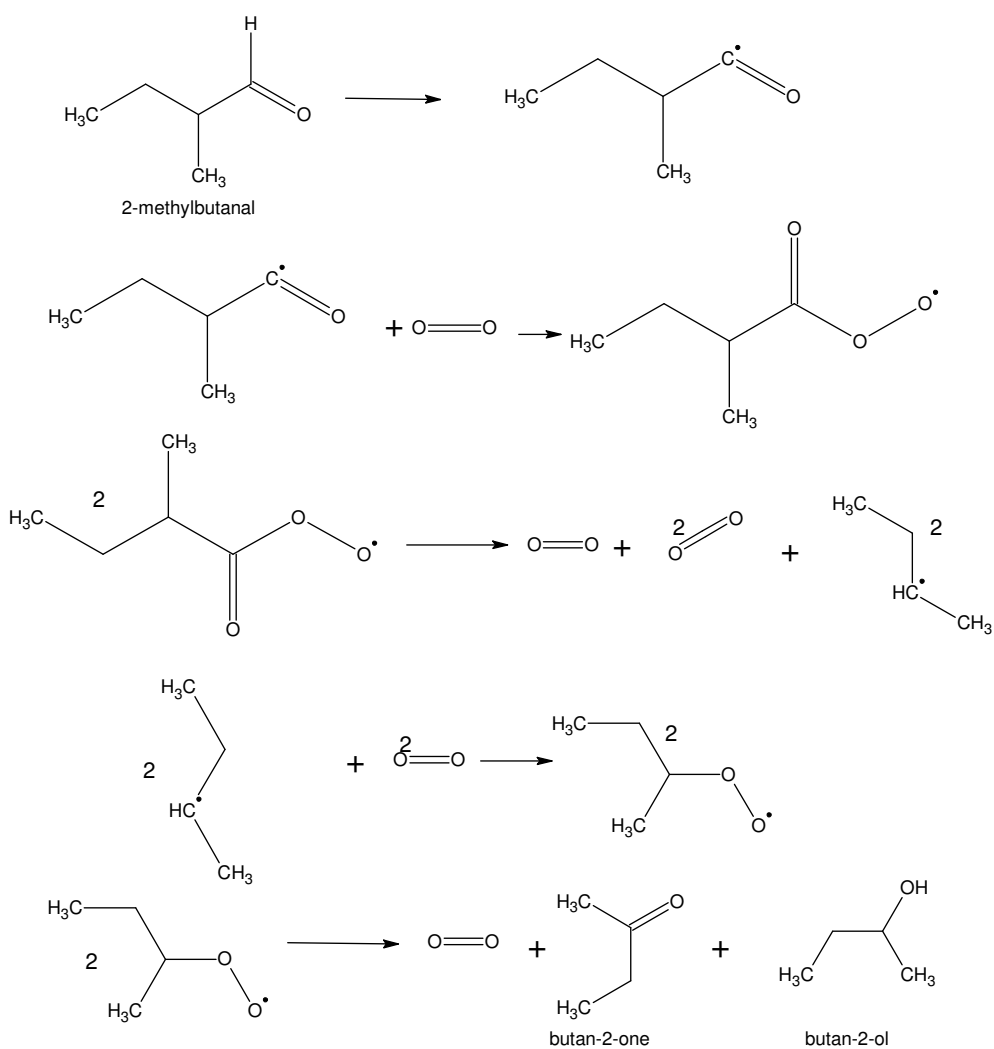


## **Exhibit B**

### **Proposed pathway of hexanal oxidation**

#### **Summary:**

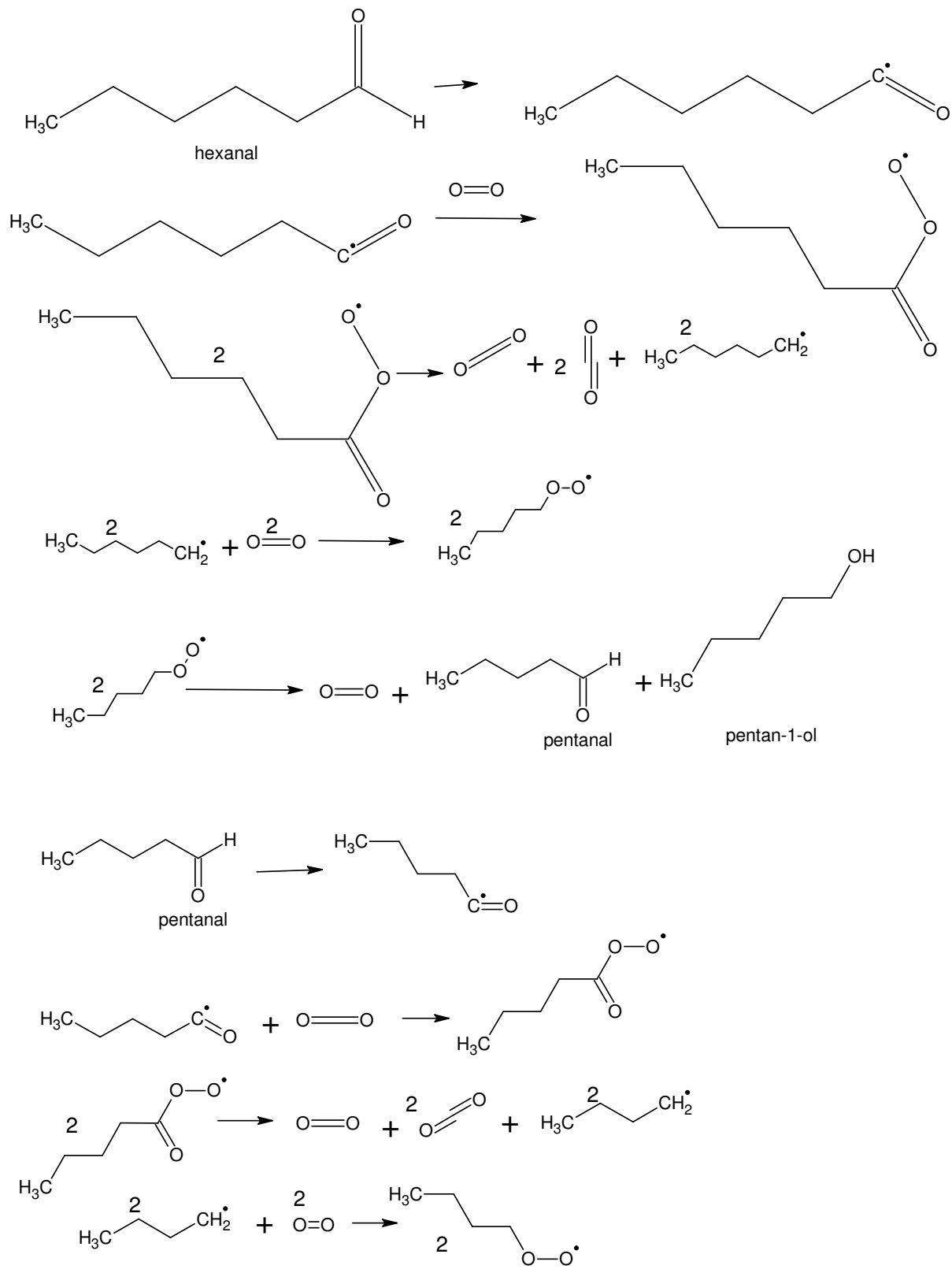
step 1: hexanal to pentanal and pentanol

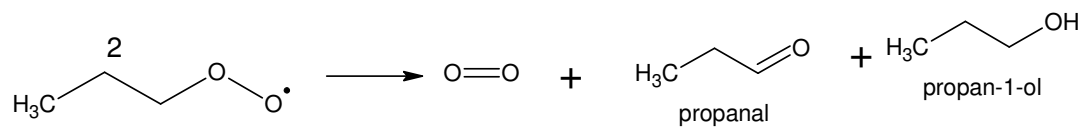
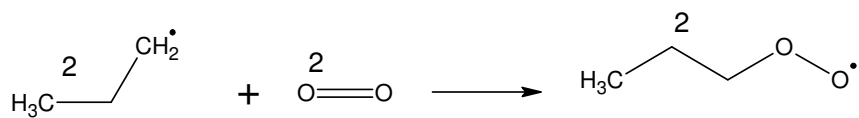
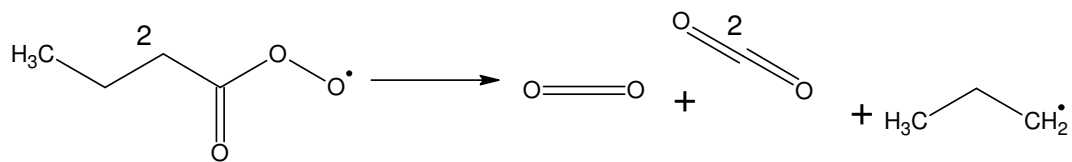
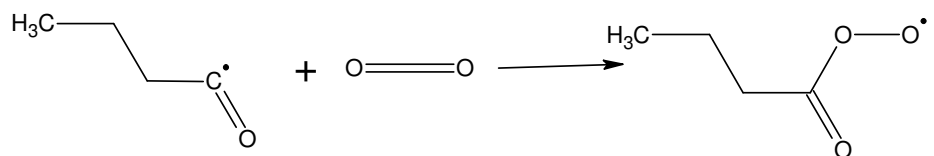
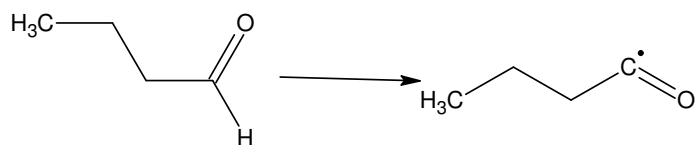
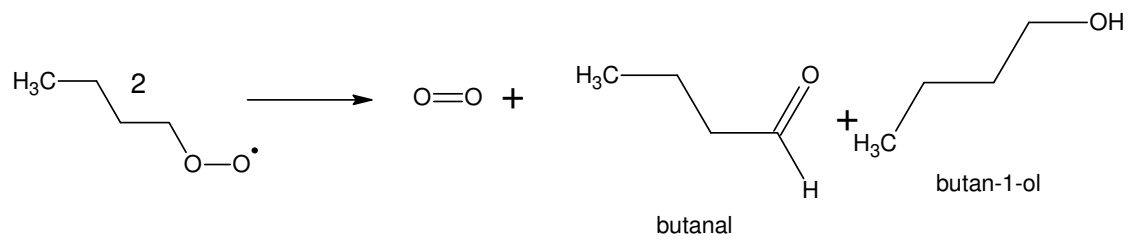
step 2: pentanal to butanal and butanol

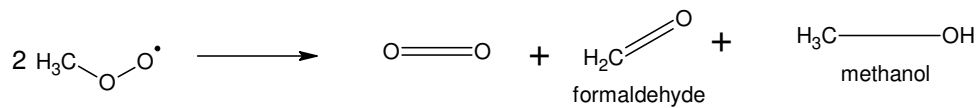
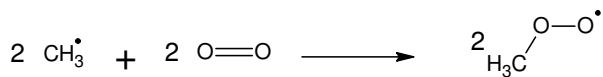
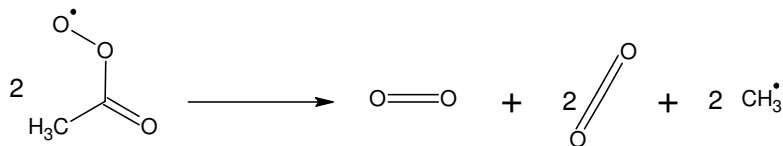
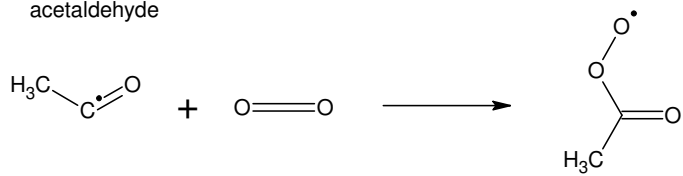
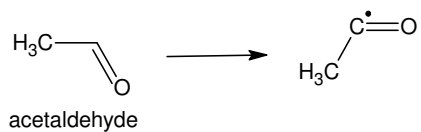
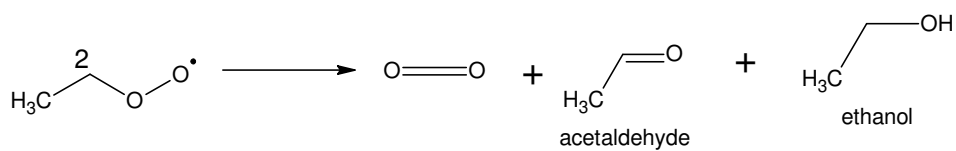
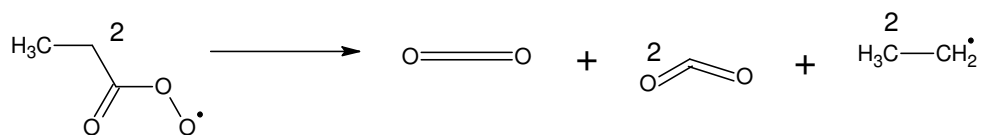
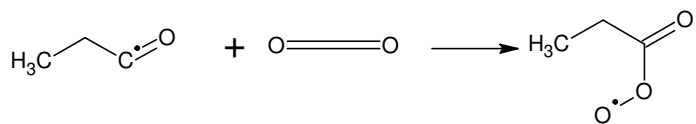
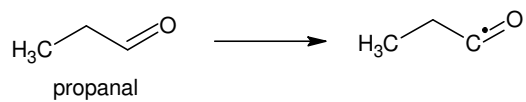
step 3: butanal to propanal and propanol

step 4: propanal to acetaldehyde and ethanol

step 5: acetaldehyde to formaldehyde and methanol







## CHAPTER 7

### ROOM-TEMPERATURE OXIDATION OF ALDEHYDES USING CATALYSTS SYNTHESIZED BY ELECTROCHEMICAL DEPOSITION

#### 7. 1 Introduction

Poultry rendering operations generate mixtures of volatile organic compounds (VOCs), such as aldehydes and organic sulfur compounds (Kastner et al., 2000). Our past work revealed that present treatment techniques, such as chemical wet-scrubbers, were ineffective against removing aldehydes (Kastner et al., 2002). Aldehydes are regulated VOCs and are associated with odor and health problems, formation of particulate matter, and atmospheric ozone (Leikauf, 2002). Hence an effective treatment technology is needed to treat aldehyde fractions in rendering emissions.

Catalytic oxidation is emerging as a promising alternate technology to treat VOCs emitted from various industries (Gervasini et al., 1996). The process involves reaction between VOCs and an oxidant, aided by presence of a catalyst. The use of the catalyst lowers the oxidation temperatures by providing alternate routes to end products whose activation energies are less than that of non-catalytic reactions (Smith, 1981). Additionally, presence of a catalyst increases the reaction rate. Lowering the reaction temperature not only lowers the treatment costs, but also reduces the production of green house gases and micro-pollutants (such as dioxins, phosgene).

Because the reaction between VOCs and the oxidant occurs on the metal surface, efforts have been made to increase the available metal surface area. In these processes, the catalysts were added as either fine particles or powders (Hu et al., 1999). But when added as powders or fine particles, the catalysts were prone to sintering thereby inactivating the catalyst. One method for improving the performance of the catalyst is by dispersing the catalyst particles on a support that has a high surface area. This would not only prevent sintering, but also allow for recovering the catalyst after the reaction. Traditionally inorganic materials such as silica and alumina are used as supports for dispersing catalysts. However, under humid and low pH conditions, these supports tend to become unstable and become deactivated (Gaur et al., 2005). Recently, activated carbon has been used as a catalyst support because of its stability, availability, and extremely high surface area (500-1500 m<sup>2</sup>/g). If the same metallic powders are dispersed on activated carbon, the activity of the catalyst could increase several fold due to increased availability of exposed catalytic sites.

Efforts have been made in the recent past focusing towards development of highly active catalysts. Researchers such as Gomez et al (1999) synthesized high surface area catalysts by dispersing metal on high-surface area supports, thereby increasing the effective surface area and catalytic activity. However, with the advances in nanotechnology and textural characterization techniques efforts are focused towards development of nano-catalysts.

Recent developments in nanotechnology have allowed for synthesis of nano-particles of defined size. The physical, chemical and electronic properties of

materials change as the size approaches the nano-level (Daniel and Astruc, 2004; Li et al., 2006). These properties are being utilized in many medical (Xu and Zhu, 2006), electronic (Matsui, 2005), and catalytic (Narayan and Sayed, 2005) applications. Some of the properties that could be used for applications in heterogeneous catalysis are based on surface and catalytic activity and size.

Typical techniques for synthesizing nano-catalysts include dispersion of metal phase by impregnation, precipitation, and chemical vapor deposition. Impregnation and precipitation techniques are well studied, but the control of the particle size is difficult. Chemical vapor deposition is expensive and mainly used in electronics and semi-conductor industries. Electrochemical deposition (ED) on the other hand, is promising and can potentially be used to synthesize particles of various sizes. ED would allow for control of the chemical and catalytic properties of the materials that are deposited (Natter and Hempelmann, 2003). For example, electrochemical techniques have been used to synthesize magnetic nanoparticles on carbon nanowall templates (Yang, 2002). Similarly, binary manganese-cobalt oxides were deposited on graphite substrates (Chuang and Hu, 2005). Recently, activated carbon was used as a substrate to deposit precious metals. Kumar et al (2004) described synthesis of micro-crystals on activated carbon via electrochemical deposition. Additionally, platinum nano crystals were generated on activated carbon surface by Adora's group (2001). However, electrochemical deposition techniques have not been used to synthesize catalysts for VOC abatement. Hence, the goal of this research was to develop highly active metal oxide catalysts by impregnation and electrochemical deposition techniques for treating aldehydes emitted from poultry

rendering emissions. For this project, propanal was chosen as a representative aldehyde because of its low propensity for oxidation and offensive odor. Similarly, iron, nickel, and cobalt were used as model catalysts because of their documented catalytic activities in oxidizing VOCs. Specific objectives were to (1) synthesize iron oxide on activated carbon supports using traditional impregnation, (2) deposit nickel and cobalt oxide on activated carbon supports using electrochemical deposition, and (3) test the catalysts for treating propanal vapors.

## **7.2 Experimental methods**

### **7.2.1 Synthesis of catalysts**

#### **7.2.2 Pelleted activated carbon (PAC)**

Commercially available pelleted activated carbon (PAC) (NORIT) was used as a catalyst and a catalyst support to deposit iron, nickel and cobalt oxides. Prior to use, the PAC was cleaned with deionized water (DIW) three times to remove finely suspended carbon particles. The washed PAC was then soaked for 24 hours in 5 % HCl as described by Hu et al (1999). Subsequently the PAC was washed with DIW three times and dried at 105 °C for eight hours and stored in air-tight containers.

#### **7.2.3 Traditional impregnation of iron oxide on PAC**

Iron oxide was deposited on PAC via three different methods. In all the methods described below, the final metal loading on PAC was maintained at 10 % (w/w).

In the first method, the precursor salt, 8 grams of iron nitrate ( $\text{Fe}(\text{NO}_3)_3 \cdot 9\text{H}_2\text{O}$ ) was dissolved in 10 mL DIW. 10 grams of cleaned and 5 % HCl washed PAC was soaked in the above prepared solution for 30 minutes. The

sample was dried at 105 °C in an air convection oven for 8 hours. The dried sample was calcined at 300 °C for one hour in a furnace with an air flow of 10 L/min.

As mentioned above, DIW was used as a solvent to dissolve the precursor salt. However, activated carbons are known to be hydrophobic and hence in the above described method of catalyst synthesis, DIW might not have completely wetted the surface and iron might not have adsorbed on the PAC surface. In order to improve the wetting of PAC surface and deposition of iron on PAC surface, acetone was used as a solvent in the second method while the precursor loading, drying, and calcination conditions were identical as previous method.

In the third method, the effect of ozone was tested. Ozone was recently used to enhance the activity and add carboxylic and oxygen functional groups to activated carbon surfaces. We theorized that exposing PAC to ozone might add (1) oxygen groups and hence water could wet more readily and (2) other functional groups which might increase the interaction between precursor and PAC surface. In this method, the PAC was exposed to 1500 ppmv of ozone for 8 hours. Subsequently, the PAC was deposited with iron oxide as described in the first method.

#### **7.2.4 Electrochemical deposition of nickel and cobalt oxides on PAC**

The PAC was used as a support for depositing nickel and cobalt. The synthesis was carried out in a 200-mL glass beaker that contained a reference electrode, working electrode, and a platinum counter electrode. The electroplating bath for cobalt consisted of a solution of 5 mM CoSO<sub>4</sub>, 0.1 M Na<sub>2</sub>SO<sub>4</sub> and 0.1 M boric acid adjusted to a pH of 5.0. The PAC pellets were mounted on a two-sided copper tape which acted as a cathode (working electrode). A potential of 1.6 V was

applied across the electrodes and deposition was carried out for 4 minutes at room temperature (25 °C) while the bath was constantly stirred at 6 rpm.

For nickel plating, a bath consisted of NiSO<sub>4</sub> · 6 H<sub>2</sub>O (300 g/L), NiCl<sub>2</sub> · 6 H<sub>2</sub>O (45 g/L), and boric acid (40 g/L) adjusted to a pH of 4.8 was used. Deposition was carried out for 10 minutes at 60 °C with constant stirring @ 6 rpm with a constant current density of 3 amps/dm<sup>2</sup>.

After deposition, the pellets were removed from the copper tape, washed with DI water, and dried at 105 °C for eight hours. Subsequently, the catalysts were calcined at 300 °C for 1 hour in a furnace with an air flow of 10 L/min.

### **7.2.5 Catalyst characterization**

The physical and chemical properties of PAC which included pH, density, and specific surface area (nitrogen-based BET method,) were determined (Table 1). The specific surface area was determined by the standard nitrogen-based 6-point BET method (model: Nova 3000, by Quantochrome). The samples were degassed @ 100 °C for eight hours prior to surface area analysis.

For surface characterization, the samples were analyzed using scanning electron microscope. Triplicate samples of catalysts were mounted on an aluminum stub covered with an adhesive carbon tab. The mounted samples were coated with ~ 120 Å of gold using a sputter coater (model SPI, SPI supplies West Chester, PA). The gold coated samples were imaged using a digital SEM (ZEISS 1450 EP, Carl Zeiss Micro Imaging, Thornwood, NY). An accelerating voltage of 5 keV was used and a back scattering detector was used for imaging the samples.

The elemental composition was determined using an energy dispersive analyzer. An accelerating voltage of 5.5 keV was used for 60-second time for determination of elemental composition. Subsequently the raw data was processed using INCA software.

### **7.2.6 Experimental setup for measurement of catalytic activity**

All experiments were performed in a continuous flow, packed-bed reactor system as shown in figure 7.1. The system consisted of a series of cylindrical glass reactors for humidification (5-cm diameter), mixing (2.54-cm diameter), and catalytic oxidation (2.5-cm diameter) connected by 0.625 cm (ID) Teflon tubing. Compressed air was humidified ( $RH > 78\%$ ) by passing the air through a water (humidification) column. The flow of air was controlled by a mass flow controller (model: by Celerity Inc, CA). Propanal was used as a model compound due to its recalcitrance to oxidation at room temperatures (oxidation using  $O_2$  and using  $O_3$  without a catalyst). Liquid propanal was injected into the system via using an automated syringe pump (model 74900-30 by Cole Parmer) and a 10-cc Becton Dickinson disposable syringe at a predetermined rate to obtain the desired concentration. The injection rates varied between  $0.3 \mu\text{L}/\text{min}$  and  $2.3 \mu\text{L}/\text{min}$  to obtain a concentration of 20 – 250 ppmv for an overall flow rate of 6L/min. The humidified air and propanal vapor were allowed to mix in glass column packed with glass beads (3-mm diameter). Ozone was added to the air-propanal mixture approximately 10 cm before the reactor inlet. After mixing, the air-aldehyde-ozone mixture flowed through a packed-bed reactor that contained catalyst. The top and bottom of the catalytic bed was also distributed with glass wool to promote plug flow conditions. The fractional removal was

measured at 25 °C and 1 atm pressure. To attain a steady state condition, propanal was injected overnight (8-10 hours) before sampling the reactor. The inlet and outlet of the reactor were simultaneously sampled using gas-tight syringes (model 1-2 mL, by VICI Precision Sampling, Inc., Baton Rouge, LA) and analyzed using gas chromatograph (GC). Typically, samples were drawn from the reactor every 20 minutes and injected into a gas chromatograph to determine the concentrations. From the measured inlet and outlet concentrations, the fractional conversion (X) at each concentration regime was determined as

$$X = \left[ \frac{C_{in} - C_{out}}{C_{in}} \right] \times 100 \% \quad (7.1)$$

The reaction rate for our assumed plug flow reactor model is expressed as

$$-r = \frac{dF_A}{dW} \quad (7.2)$$

Assuming that steady state, isothermal and isobaric conditions and ideal gas laws were valid, the overall rate of aldehyde oxidation was determined by modifying and simplifying equation 7.2

$$-r = Q \frac{P}{RT} y \frac{X}{W} MW \quad (7.3)$$

where  $-r$  is the rate of oxidation of the aldehyde (mg/g-min), P is the pressure (atm), Q is the volumetric flow rate (L/min), R is the universal gas constant, T is the temperature (°K), y is the inlet mole fraction, X is the fractional conversion (%) (< 30 %), W is the mass of the catalyst (g), and W is the molecular weight of the aldehyde (g/mol).

### **7.2.7 Analytical methods**

The inlet and outlet gas samples were analyzed using a Hewlett-Packard 5890 GC equipped with a flame ionization detector (FID) and a SPB-1 sulfur column (0.32  $\mu\text{m}$  , 30 m) (SUPLECO, Bellefonte, PA). The samples were analyzed under isothermal conditions (column temperature: 80 °C, inlet and detector temperatures of 200 and 250 °C), and a split ratio of 30:1. A sample size of 250 $\mu\text{L}$  was used for the entire study. Standard curves of propanal were prepared for a concentration range of 0 and 200 ppmv using 1-L tedlar bags and calibrated gas syringes (model 1-2 mL, by VICI Precision Sampling, Inc., Baton Rouge, LA).

### **7.3 Results and discussion**

Activated carbons generally possess high surface area and are associated with high adsorption capacities. When used as a catalyst or as a catalyst support for VOC abatement, it is critical to determine whether the removal is due to adsorption or due to a catalytic reaction. Therefore, we conducted a simple experiment to determine the time required for the propanal to saturate and breakthrough the activated carbon bed. For this experiment, a constant propanal inlet concentration of approximately 130 ppmv was injected into the reactor system. Immediately upon injection, inlet and outlet samples were drawn periodically using gas tight syringes, and injected in a gas chromatograph as described in the methods section. For the first 20 minutes, the outlet concentrations were close to zero indicating adsorption of propanal on activated carbon surface (Figure 7.2). Subsequently, the outlet concentration gradually increased and finally reached about 130 ppmv around 300 minutes. This indicated that the effect of adsorption is negligible beyond 300

minutes. In all our subsequent experiments, an equilibration time of 8 hours was used so that the measured difference in the inlet and outlet concentration truly represented the effect of catalytic reaction.

### **7.3.1 Measurement of catalytic activity**

### **7.3.2 Pelleted activated carbon (PAC)**

Initially PAC was tested as a catalyst for treating 50-200 ppmv propanal vapors. Two grams of PAC was packed in the reactor and 1500 ppmv of ozone was used as an oxidant. A fractional removal of 70 % was obtained with PAC alone at 25 °C (Figure 7.3). The reaction rates thus calculated were between 90 and 300 x 10<sup>-9</sup> mol/g-s (Figure 7.4). The rates we obtained were significantly higher than similar aldehydes previously tested. For example, when 600 ppmv of formaldehyde was oxidized to CO<sub>2</sub> using oxygen at 100 °C (what type of catalyst), the reaction rates were in the order of 50 x 10<sup>-9</sup> mol/g-s (Martyanov et al., 2005). But in our work, ozone was used as an oxidant and we used 25 °C as our oxidation temperature. In our earlier work with propanal (Kastner et al., 2007), we tested granular activated carbon for oxidizing propanal at 25 °C and the rates obtained were ten times less than our current rates. The higher oxidation rates obtained for PAC may be due to a variety of reasons. The higher activity of the PAC may have been due to the fact that in our earlier work, the granular activated carbon had a surface area of about 425 m<sup>2</sup>/g where as the PAC used in the current work had a surface area of about 784 m<sup>2</sup>/g. Moreover, the average particle size of the PAC was less than the granular activated carbon tested in our earlier work, which could have increased the oxidation rate of PAC when compared to granular activated carbon. The higher activity of the

PAC may be due to higher ozone concentrations that were used (1500 ppmv for PAC vs 100 ppmv for granular activated carbon). Finally, the higher activity of PAC may be attributed to the source of carbon and the activation conditions.

It may however be noted that the reaction rates calculated for PAC may not be accurate because the measured fractional removal ( $X$ ) was greater than 30 %, which was inconsistent with the differential reactor model assumption (equation 7.3).

### **7.3.3 Mechanism of ozonation on PAC**

Activated carbons are known to catalyze oxidation reactions especially in presence of ozone. For example, in an earlier work, we demonstrated oxidation of propanal at room temperature using granular activated carbon (Kastner et al, 2007). Ozone, as an oxidant could have reacted with propanal in several ways. The reaction could have been between adsorbed ozone and adsorbed propanal. Another possibility could be via an advanced oxidation process involving  $\text{OH}^*$  radicals due to decomposition of ozone. Considering the high pH of the activated carbon and the presence of moisture in the air that carried propanal, reaction between  $\text{OH}^*$  radicals and propanal seems to be a likely possibility.

### **7.3.4 PAC deposited with iron oxide particles**

The iron oxide deposited PAC catalysts were tested under identical conditions as control PAC. When tested, the activities of all three iron oxide catalysts were significantly lower than PAC (Figure 7.5). The rates of all iron oxide catalysts were between  $7 \times 10^{-9}$  mol/g-s and  $60 \times 10^{-9}$  mol/g-s which are an order less than PAC (Table 7.2). In our previous study on propanal oxidation using iron oxide catalysts, we clearly demonstrated significantly higher oxidation rates when compared to a

control (granular activated carbon). However, in this case the opposite is true. This may have been due to our deposition procedure where we speculate that the PAC pores were plugged by iron particles which may have reduced the surface area. It may also be possible that the form of iron that was deposited on PAC may not be an oxide or catalytically active. Since we do not have an X-ray diffraction analysis data for the prepared catalysts, it is not known what crystalline structure of iron actually formed during the calcinations.

### **7.3.5 Electrochemically synthesized nickel and cobalt oxides**

When tested as catalysts, as expected, nickel and cobalt oxides generated higher reaction rates than PAC. At low concentrations ( $\sim 100$  ppmv) (Figure 7.6), the differences in rates were small. However, as the concentration increased, the rate of propanal oxidation for nickel and cobalt catalysts increased significantly when compared to PAC. Interestingly, the reaction rates of cobalt and nickel were similar under similar experimental conditions (Table 7.2). Metal oxides especially nickel and cobalt are catalytically active due to their variable oxidation states. Additionally, electrochemical deposition allowed for coating the entire surface of PAC with a thin layer of metal (Figure 7.7 and 7.8). The thin film so formed would have acted in two ways: by increasing the effective surface area available for the reaction and increasing the inherent catalytic activity by increasing the surface atomic density.

## **7.4 Conclusion**

Our results indicated that pelleted activated carbon is catalytically active in treating propanal vapors using ozone at room temperature. It is theorized that ozone decomposed to form  $\text{OH}^*$  radicals that oxidized propanal. When PAC was deposited

with iron oxides the oxidation rates of propanal were an order less than original PAC. However, when PAC was electrochemically deposited with nickel and cobalt oxides, the overall oxidation rate of propanal was increased by 25-50 %.

## References

1. Adora, S, Y S. Oliver, R. Faure, R. Durand. 2001. Electrochemical preparation of platinum nanocrystallites on activated carbon studied by X-ray absorption spectroscopy. *J. Phys. Chem. B.* (105): 10489-10495.
2. Chuang, P. Y. C. C. Hu. 2005. The electrochemical characteristics of binary manganese-cobalt oxides prepared by anodic deposition. *Materials Chemistry and Physics.* (92): 138-145.
3. Daniel, M. C. and D. Astruc. 2004. Gold nanoparticles: assembly, supramolecular chemistry, quantum-size-related properties, and applications toward biology, catalysis, and nanotechnology. *Chem. Rev.* (104): 293-346.
4. Gaur, V, A. Sharma, and N. Verma. 2005. Catalytic oxidation of toluene and *m*-xylene by activated carbon fiber impregnated with transition metals. *Carbon.* 43 (15): 3041-3053.
5. Gervasini, A, G. C. Vezzoli, V. Ragaini. 1996. VOC removal by synergic effect of combustion catalyst and ozone. *Catalysis Today.* (29): 449-455.
6. Gomez, M. J. I, E. Raymundo-Piñero, A. García-García, A. Linares-Solano, and C. Salinas-Martínez de Lecea. 1999. Catalytic NO<sub>x</sub> reduction by carbon supporting metals. *Applied Catalysis B: Environmental.* 20 (4): 267-275.

7. Hu, X, L. Lei, H. P. Chu, P. L. Yue. 1999. Copper/activated carbon as a catalyst for organic waste water treatment. *Carbon*. 37(4): 631-637.
8. Kastner, J.R, K. C Das. 2002. Wet Scrubber Analysis of Volatile Organic Compound Removal in the Rendering Industry. *J. Air & Waste Manage. Assoc.* (52): 459-469.
9. Kastner, J. R, C. Hu, K. C. Das, R. McClendon. 2003. Effect of pH and Temperature on the Kinetics of Odor Oxidation Using Chlorine Dioxide. *Journal of the Air and Waste Management Association.* (53): 1218-1224.
10. Kastner, J. R, R. Ganagavaram, P. Kolar, A. Teja, and C. Xu. 2008. Catalytic Ozonation of Propanal Using Wood Fly Ash and Metal Oxide Nanoparticle Impregnated Carbon. *Environmental Science and Technology.* 42 (2), 556–562.
11. Kumar V. S, B. M. Nagaraja, V. Shashikala, A. H. Padmasri, S. S. Madhavendra, B. D. raju, and K. S. Rama Rao. 2004. Highly efficient Ag/C catalyst prepared by electro-chemical deposition method in controlling microorganisms in water. *Journal of Molecular Catalysis A: Chemical.* (223): 313-319.
12. Leikauf, G. D. 2002. Hazardous air pollutants and Asthma. *Environ. Health Perspect.* (110): 505-526.
13. Li, L., M. Fan, R. C. Brown, J. V. Leeuwen, J. Wang, W. Wang, Y. Song, and P. Zhang. 2006. Synthesis, properties, and environmental applications of nanoscale iron-based materials: A review. *Critical Reviews in Environmental Science and Technology.* (36): 405-431.

14. Martyanov, I. N, S. Uma., S. Rodrigues., K.J. Klabundle. 2005.  
Decontamination of Gaseous Acetaldehyde over CoOx-Loaded SiO<sub>2</sub>  
Xerogels under Ambient, Dark Conditions. *Langmuir*. (21): 2273-2280.
15. Matsui, I. 2005. Nanoparticles for electronic device applications: a brief  
review. *Journal of Chemical Engineering of Japan*. 38(8): 535-546.
16. Narayan, R and M. A. E. Sayed. 2005. Carbon-supported spherical  
palladium nanoparticles as potential recyclable catalysts for the Suzuki  
reaction. *Journal of Catalysis*. (234): 348-355.
17. Natter, H and R. Hempelmann. 2003. Tailor-made nanomaterials designed  
by electrochemical methods. *Electrochimia Acta*. 49: 51-61.
18. Smith. J. M. 1981. Chemical Engineering Kinetics. Mc.Graw-Hill Book  
Company, New York, USA.
19. Xu, Q., Y. Zhao, J. Z. Xu, and J. J. Zhu. 2006. Preparation of functionalized  
copper nanoparticles and fabrication of glucose sensor. *Sensors and  
Actuators B*. (114): 379-386.
20. Yang, B, Y. Wu, B. Zong, and Z. Shen. 2002. electrochemical synthesis and  
characterization of magnetic nanoparticles on carbon nanowall templates.  
*Nanoletters*. 2 (7): 751-754.

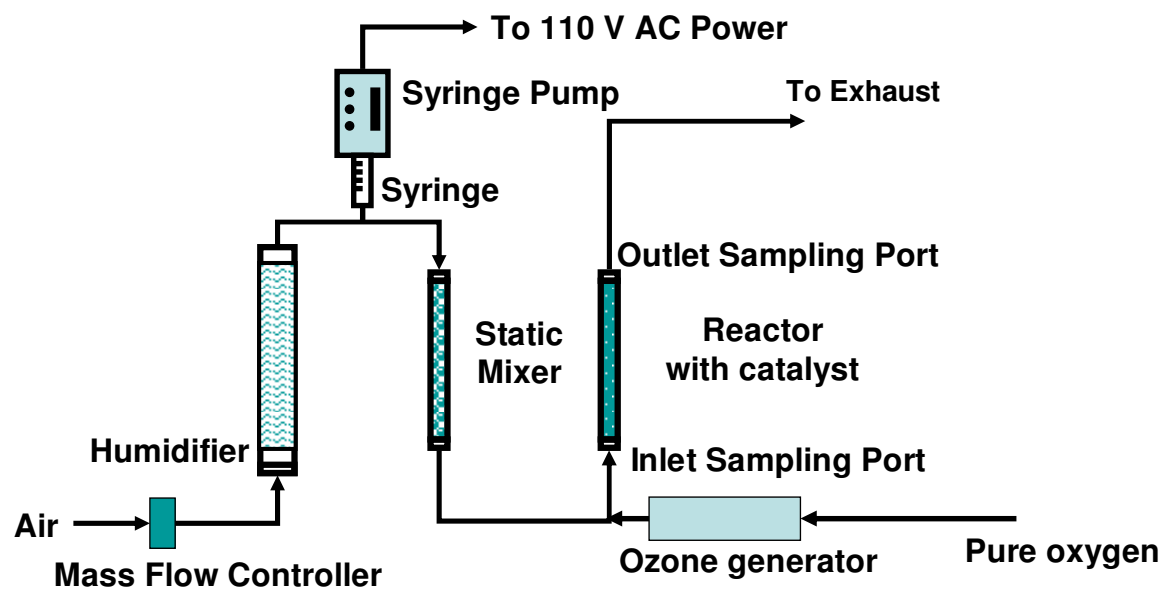


**Figure 7.1.** Schematic of the continuous flow system used in this study.

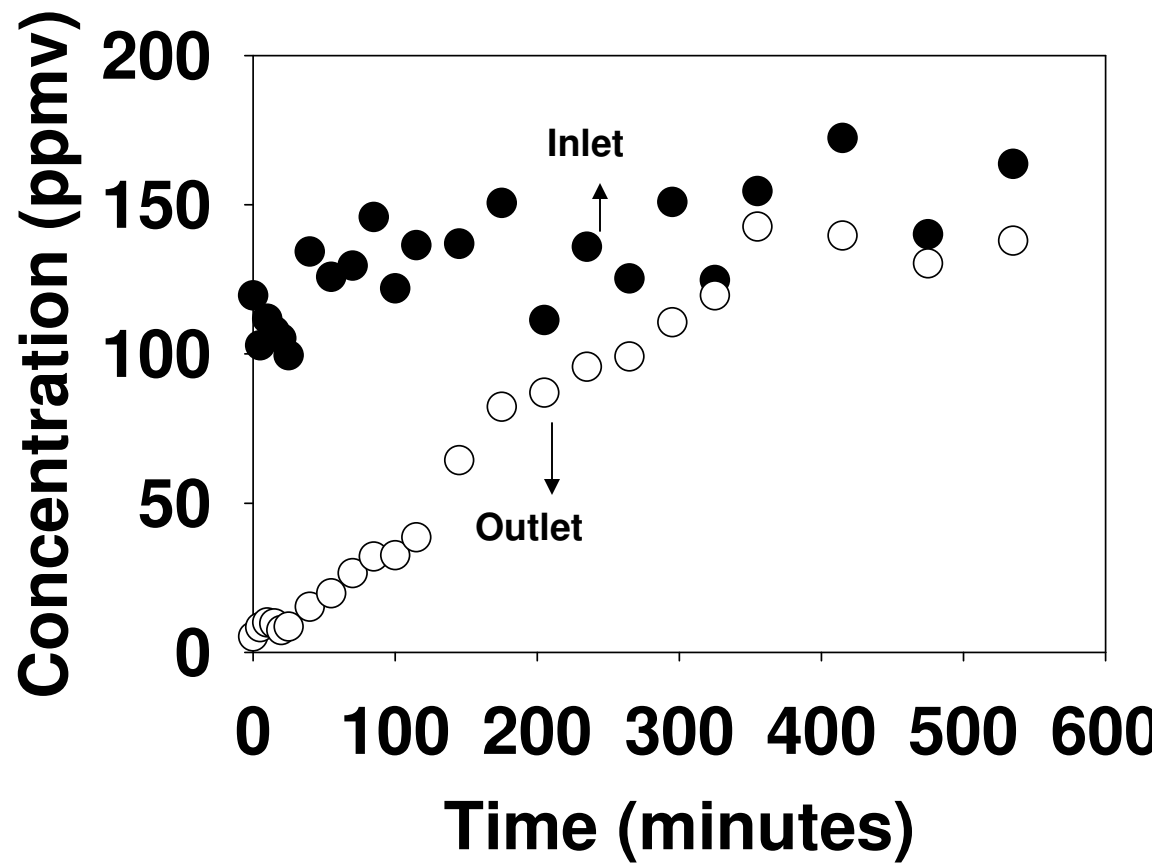


**Figure 7.2.** Adsorption breakthrough curve for 130 ppmv propanal on pelleted activated carbon at 25°C.

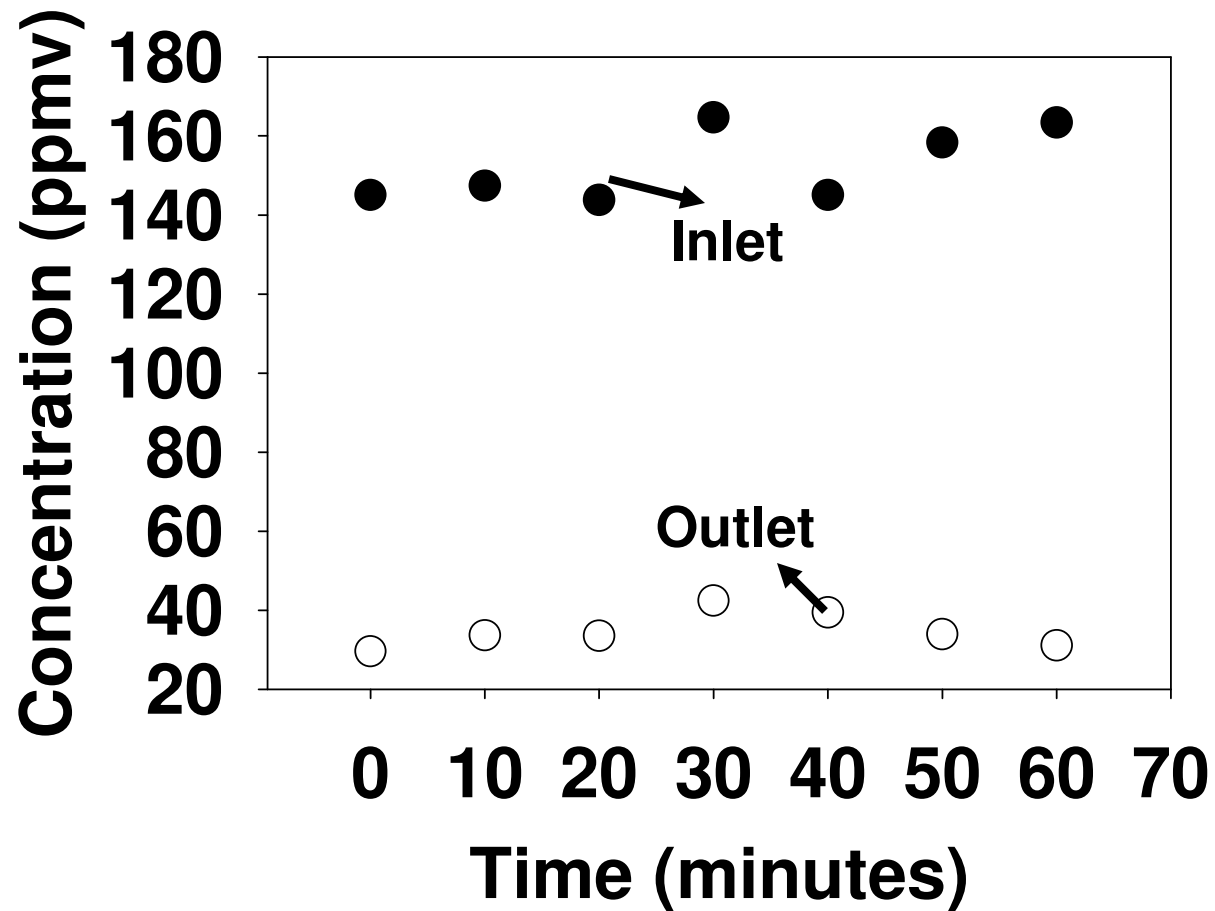


**Figure 7.3.** Typical fractional removal (70 %) obtained when PAC was tested at 25°C for removal of 150 ppmv of propanal with 1500 ppmv of ozone.

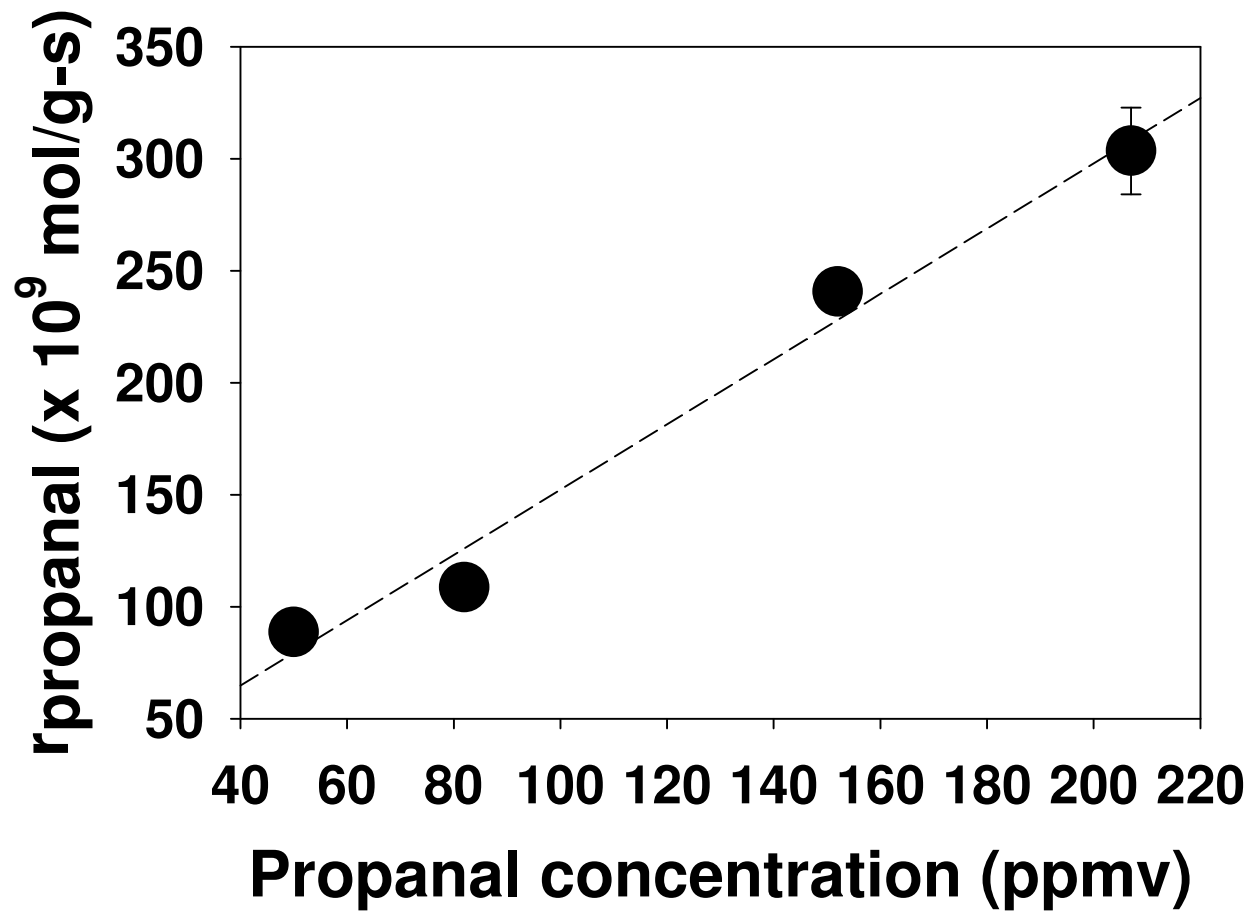


**Figure 7.4.** Effect of propanal concentration on overall oxidation rate when tested with 2 g of PAC at 25°C using 1500 ppmv of ozone as an oxidant.

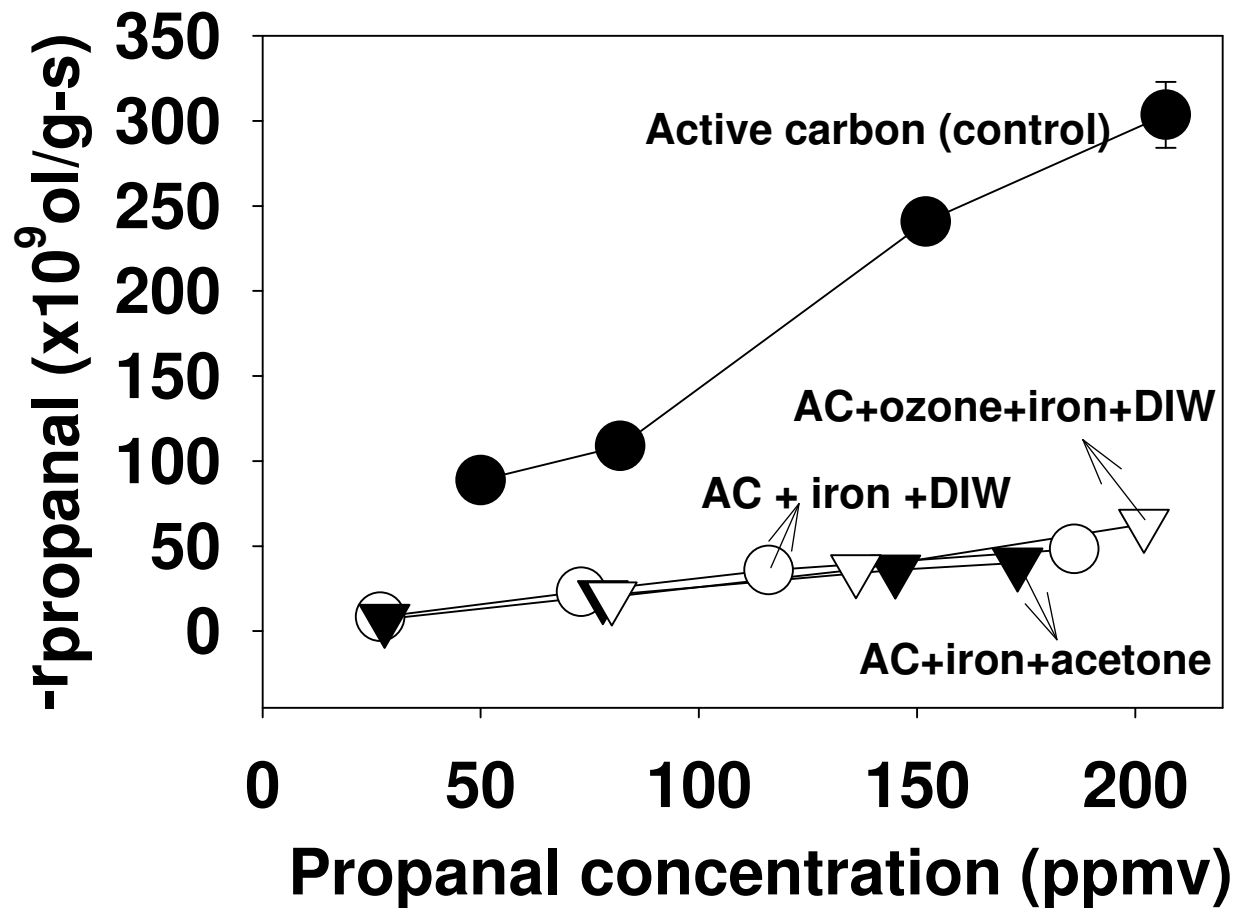


**Figure 7.5.** Comparison of PAC deposited with iron oxide with PAC (control, ●). The oxidation rates of propanal when tested with PAC deposited with iron in DIW (○), acetone (▼), and iron oxide deposited on ozone treated PAC using DIW (downward facing open triangles) , were significantly less than PAC.

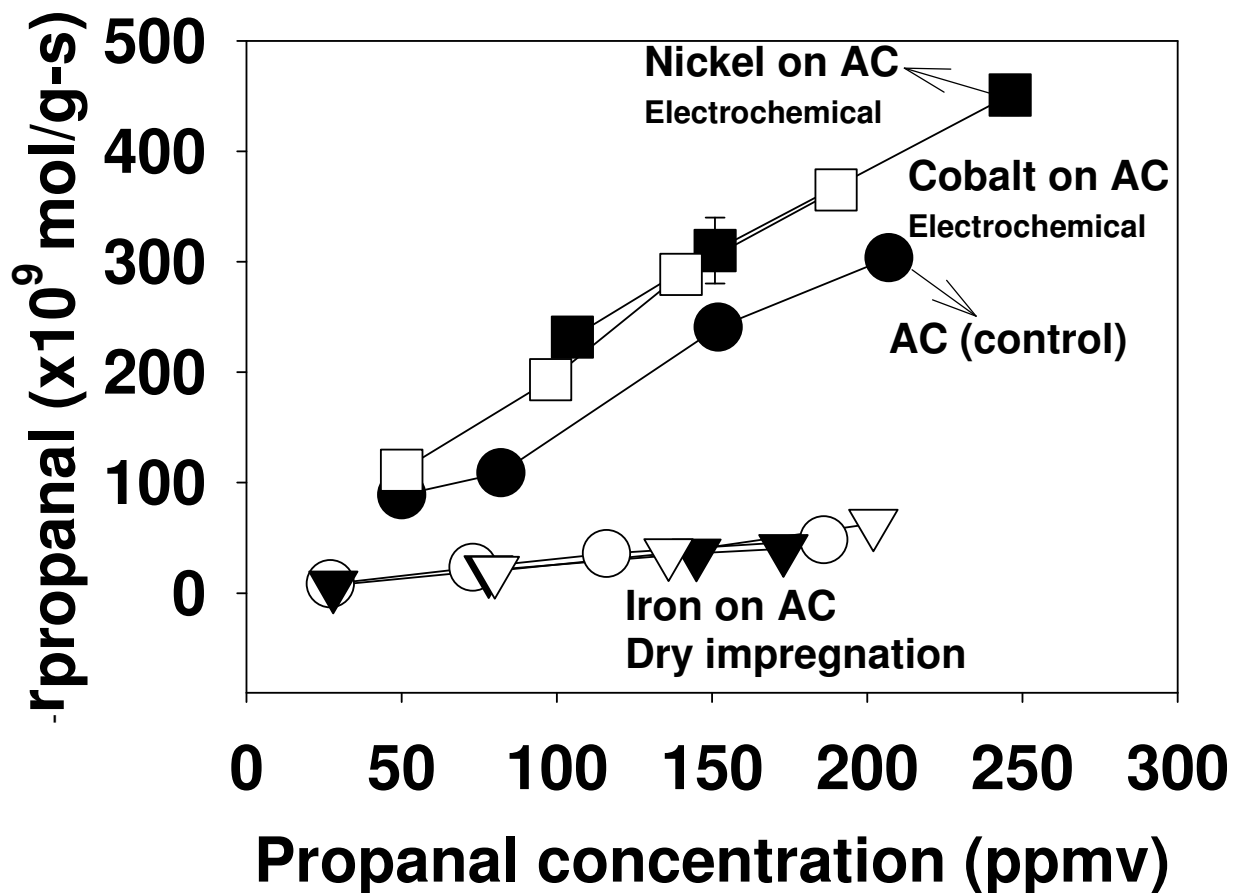


**Figure 7.6.** Comparison of PAC electrochemically deposited with nickel and cobalt oxides with PAC (control, ●). The oxidation rates of propanal when tested with PAC deposited with nickel (■) and cobalt (□) were significantly higher than PAC.

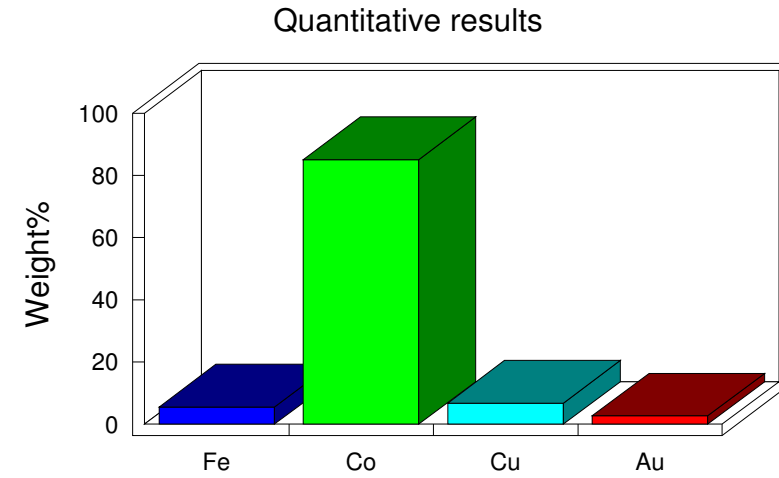
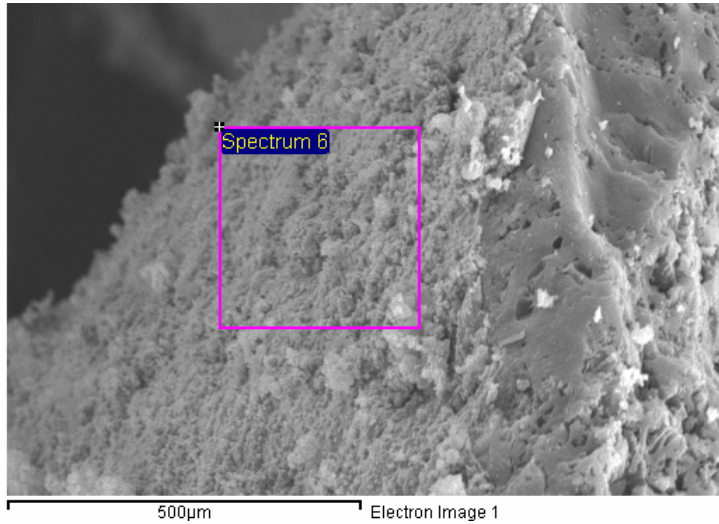


**Figure 7.7.** Sample micrograph and energy dispersive spectroscopy (EDS) of pelleted activated carbon deposited with cobalt oxide.

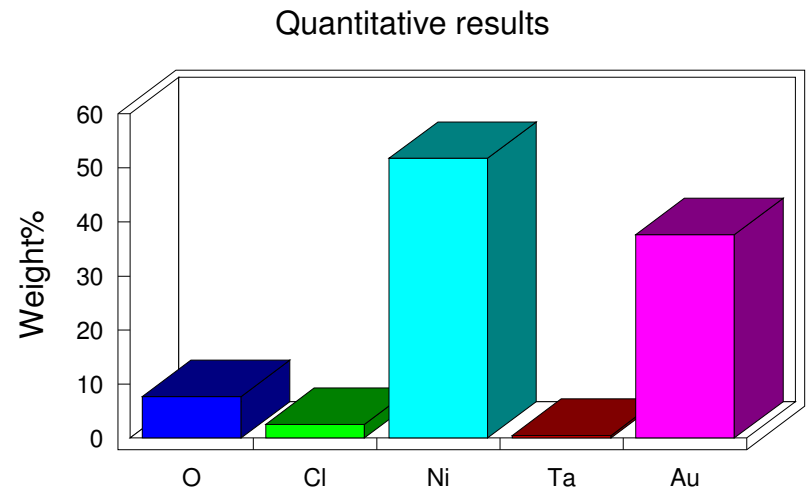
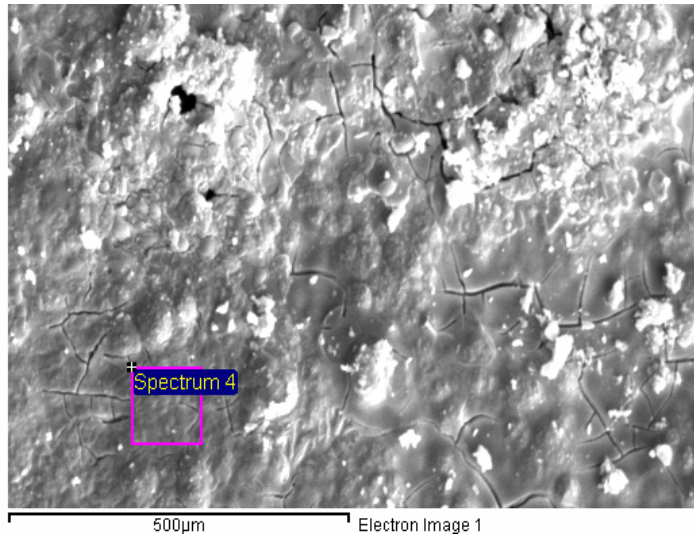


**Figure 7.8.** Sample micrograph and energy dispersive spectroscopy (EDS) of pelleted activated carbon deposited with nickel oxide.

**Table 7.1.** Physical properties of pelleted activated carbon used in this study.

<b>Property</b>	<b>Value</b>
Size	3-6 mm
pH	9.7
Density (g/cc)	1.01
Original surface area (m <sup>2</sup> /g)	784
Surface area after nickel deposition	656
Surface area after cobalt deposition	671

**Table 7.2.** Propanal reaction rates at 25 °C using the following catalysts and 1500 ppmv of ozone.

<b>Catalyst</b>	<b>Concentration (ppmv)</b>	<b>Reaction rate (x 10<sup>-9</sup> mol/g-s)</b>
Pelleted activated carbon (PAC)	50-207	88-303
Cobalt on PAC	50-190	111-365
Nickel on PAC	105-246	232-450
Iron oxide on PAC with DIW	27-186	8-48
Iron oxide on PAC with acetone	28-173	7-40
Iron oxide on PAC with DIW (ozone treated)	80-202	20-62

## **CHAPTER 8**

### **SCALEUP, DESIGN, AND ECONOMICS OF CATALYTIC OXIDATION APPLIED TO THE POULTRY RENDERING INDUSTRY**

#### **8.1 Introduction**

The overall goal of this research has been to develop a low-temperature catalytic oxidation process for treatment of aldehydes from poultry rendering emissions. As a part of that goal, wood fly ash was used a potential catalyst and kinetic data was obtained for 2-methylbutanal, 3-methylbutanal, and hexanal at 25 °C, which were detailed in chapters five and six. Chapter five evaluated the catalytic activity of wood fly ash and chapter six focused on removal of aldehyde mixture using oxygen and ozone as oxidants. The next logical step in this project would be to utilize the data obtained to size the catalytic oxidation systems, propose designs, and study the economics of such proposed designs, which are the primary objectives of this chapter. To simplify the scale up calculations, several assumptions have been made which are listed as under

- 1) The overall removal rate is governed by the aldehyde that has the lowest reaction rate, i.e. hexanal or 3-methylbutanal,
- 2) Wood fly ash used in this research had a surface area of 40 m<sup>2</sup>/g. It is assumed that entire surface area of the wood fly ash is catalytically active and was available for oxidation of 3-methylbutanal or hexanal,
- 3) No heat and mass transfer limitations exist in the reactor system,

- 4) The catalytic activity of wood fly ash does not decline with time,
- 5) Isothermal and isobaric conditions are always maintained in the proposed reactor, and
- 6) Oxygen or ozone concentration is always in excess.

## 8.2 Scale up calculations

The design equation for a plug flow reactor is derived by performing a mole balance on a steady state catalytic plug flow reactor as shown below:

Molar flow in – Molar flow out + Molar rate of generation = Molar rate of accumulation

$$F_W - F_{W+\Delta W} + r \Delta W = 0$$

Dividing by  $\Delta W$  and rearranging we obtain

when  $\lim \Delta W \rightarrow 0$

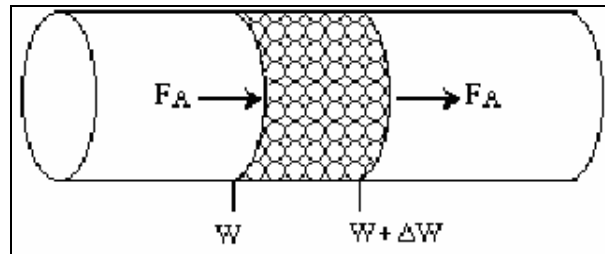


Figure 8.1 A differential mole balance on any species in plug flow reactor model yields a design equation for plug flow (adapted from Fogler, 2005).

$$-r = \frac{dF_A}{dW} \quad (8.1)$$

where  $F$  is the molar flow rate (mol/s) and  $W$  is the catalyst mass (g).

Rearranging equation 8.1, we obtain

$$dW = \frac{dF}{-r} \quad (8.2)$$

Also, the flow rate  $F = C * Q_0$ , where C is the concentration of VOC and  $Q_0$  is the inlet flow rate (L/min) of the gas, which is assumed to be constant (note, Q is assumed to remain constant).

Now equation 8.2 may be written as

$$dW = \frac{Q_0 dC}{-r} = Q_0 \left( \frac{dC}{-r} \right) \quad (8.3)$$

Or

$$W = Q_0 \int_{C_{in,et}}^{C_{Outlet}} \frac{dC}{-r} \quad (8.4)$$

where  $C_{in}$  is the inlet concentration and  $C_{Out}$  is the outlet concentration of any given species in the reactor.

Throughout our study, we assumed a pseudo-first order oxidation model in which oxygen or ozone was assumed to be present in excess and was expressed as

$$-r = k' C^n \quad (8.5)$$

where  $k'$  the pseudo is rate constant and  $n$  is the order of the oxidation reaction.

Combining equations 8.4 and 8.5 we obtain

$$W = -Q_0 \int_{C_{in,et}}^{C_{Outlet}} \frac{dC}{k' C^n} = -\frac{Q_0}{k'} \int_{C_{in,et}}^{C_{Outlet}} \frac{dC}{C^n} \quad (8.6)$$

Integrating and simplifying equation 8.6

$$W = -\frac{Q_0}{k'} \left[ \frac{C_{Outlet}^{(1-n)} - C_{Inlet}^{(1-n)}}{1-n} \right] = \frac{Q_0}{k'} \left[ \frac{C_{Inlet}^{(1-n)} - C_{Outlet}^{(1-n)}}{1-n} \right] \quad (8.7)$$

Equations 8.4 and 8.7 may be used to determine the mass of the catalyst required for any required fractional removal if the oxidation rate and the flow of the pollutant stream are known. In our project, the oxidation rate,  $-r$ , was determined experimentally (as shown in chapters five and six) and a rate law was developed by fitting a power law model to the oxidation rate data obtained for several inlet concentrations of 2-methylbutanal, 3methylbutanal, and hexanal at 25°C. For example, the oxidation rates for 2-methylbutanal, 3methylbutanal, and hexanal at 25°C were determined as  $3 \times 10^{-9}$  mol/g-s,  $3.5 \times 10^{-9}$  mol/g-s, and  $3 \times 10^{-9}$  mol/g-s for an approximate inlet concentration of 70 ppmv.

Assuming a pollutant stream of 10,000 ft<sup>3</sup>/min (or cfm), and an inlet aldehyde concentration of 70 ppmv, we can estimate the amount of wood fly ash required for a fractional removal of say 99 % at 25°C

$$Q = 10,000 \text{ cfm} = 20,000 \times 28 \text{ LPM} \quad (1 \text{ cfm} = 28 \text{ LPM})$$

$$C_{inlet} = 70 \text{ ppmv} = \frac{70 \times 10^{-6}}{0.08206 \times 298} \frac{\text{mol}}{\text{L}}$$

$$C_{outlet} = 0.01 \times 70 \text{ ppmv} = \frac{0.01 \times 70 \times 10^{-6}}{0.08206 \times 298} \frac{\text{mol}}{\text{L}}$$

$$-r_{Hexanal} = 3 \times 10^{-9} \frac{\text{mol}}{\text{g-s}}$$

Using the above data and equation 8.4, we have

$$W = 4410 \text{ Kg}$$

However, the aldehydes are generated in the cooker whose temperatures are typically around 150°C. It may be possible to use these temperatures to our advantage by treating the VOC vapors immediately as they exit from the cookers.

Foreseeing this opportunity, we obtained the oxidation rates of the aldehydes at several temperatures including 160 °C. Using the following rate data at 160 °C,

$$Q = 10,000 \text{ cfm} = 20,000 \times 28 \text{ LPM} \quad \text{as } 1 \text{ cfm} = 28 \text{ LPM (cfm} = \text{ft}^3/\text{min)}$$

$$C_{Inlet} = 125 \text{ ppmv} = \frac{70 \times 10^{-6}}{0.08206 \times 433} \frac{\text{mol}}{\text{L}}$$

$$C_{Outlet} = 0.01 \times 125 \text{ ppmv} = \frac{0.01 \times 70 \times 10^{-6}}{0.08206 \times 433} \frac{\text{mol}}{\text{L}}$$

$$-r_{Hexanal} = 12 \times 10^{-9} \frac{\text{mol}}{\text{g} \cdot \text{s}}$$

We obtain the amount of wood fly ash as

$$W = 1360 \text{ Kg}$$

As shown above, catalyst requirement is reduced by 70 % when the gases from the cooker are immediately treated.

However, it is to be noted that in all our experiments with oxygen as an oxidant, the oxidation of the aldehydes was only partial or incomplete. For example, pentanal and butanal were formed as end products when hexanal was oxidized using oxygen and wood fly ash. It naturally follows that our proposed reactor, if used, would also yield these end products. Hence, additional treatment (such as biological filtration) is required to completely oxidize the by products. However, our research suggested that ozone could completely oxidize aldehydes with wood fly ash. Hence an attempt is made to use catalytic ozonation for complete oxidation of aldehydes by assuming that

- 1) 1500 ppmv of ozone is needed for complete oxidation,
- 2) Total flow of aldehydes to be treated is 10,000 ft<sup>3</sup>/m,

- 3) The concentrations of aldehydes are less than 500 ppmv,
- 4) The source of ozone is pure oxygen @ 500 L/min, and

Based on the above assumptions, calculations performed to estimate the total ozone requirement yielded 0.166 g/L. With an oxygen inflow of 500 L/min, the required ozone mass production rate is around 120 kg/day of ozone. To generate such high ozone concentrations, industrial scale ozone generators are needed. For example, ozone generators manufactured by Ozonia have an ozone output of greater than 500 kg ozone/day and cost about \$5,000,000 (rough estimate). Additionally, based on the manufacturer's specifications, the cost of operating the equipment is \$350/day including the electricity and oxygen (rough estimate). However, assuming 4 % depreciation each year, the total money invested on ozone generated would be recovered in 25 years and the cost of ozone generation would be approximately \$330,000/yr.

### **References**

1. Fogler, H. S. 1999. Elements of chemical reaction engineering. 4 th Ed. Prentice Hall International Series.

## CHAPTER 9

### SUMMARY, CONCLUSION, AND FUTURE DIRECTIONS

The goal of this dissertation was to develop a low-temperature-catalytic oxidation technology for treating volatile organic compounds emitted from rendering operations. A two-part approach was used to achieve the goal.

In the first part (chapters 5 and 6), wood fly ash was evaluated as a low-cost catalyst for oxidizing VOCs at low temperature (25-160 °C). In chapter 5, 3-methylbutanal (3-MB) was used a model contaminant for oxidation using wood fly ash as a low-cost catalyst and air (O<sub>2</sub>) as an oxidant. The experiments were conducted in batch and continuous mode at 25 °C. In the batch experiments, 3-MB was found to react only in presence of wood fly ash confirming catalytic properties of wood fly ash. Additionally, acetone was measured as an end product indicating that the removal was not due to adsorption. Further, in the continuous flow experiments, 3-MB was removed only in presence of wood fly ash, confirming the catalytic properties of wood fly ash. Additionally, in the continuous experiments, the removal of 3-MB was limited to less than 3% without presence of oxygen, which indicated that oxygen acted as an oxidant in 3-MB oxidation. Subsequently, kinetic data was obtained at 25 °C using a pseudo-first order power law model, assuming that oxygen concentration (20.8 %) was in excess. Further, the effect of temperature on 3-MB oxidation was evaluated at 25, 80, 120, and 160 °C. For experiments at higher temperatures, the reactor was heated with a heating tape and an automated heater.

Data obtained from these experiments were used to determine the activation energy of 3-MB which was found to be about 1.87 kcal/mol. Experiments on 3-MB oxidation also provided an opportunity to predict the oxidation mechanism. In one of the experiments at 120 °C, acetone was observed as a byproduct. Based on the acetone production and the nature of 3-MB molecule, a free radical mechanism was proposed to describe the oxidation process. This proposed free radical reaction yielded acetone as one of the end products, which was also confirmed experimentally. Experiments with wood fly ash confirmed the catalytic properties of wood fly ash and opened opportunities for additional research with VOC mixtures.

In chapter 6, a mixture of 2-methylbutanal (2-MB) and hexanal was tested using a continuous flow differential reactor system with wood fly ash as a catalyst at low temperatures (25-160 °C). Initially, the kinetic and activation parameters were determined for individual aldehydes (2-MB and hexanal). The oxidation rates for 2-MB and hexanal were similar to 3-MB oxidation rates that were obtained earlier (chapter 5), under similar conditions ( $T = 25\text{ °C}$ , 20.8 %  $\text{O}_2$ , and 10 g WFA). Additionally, a carbon balance was performed on 2-MB and hexanal oxidation by measuring by-products ( $\text{CO}_2$  and other partial oxidation products) in the outlet. For these experiments, the flow was reduced to 2 L/min, while temperature and the concentration were increased to 160 °C and 400-600 ppmv. When 2-MB was tested, the outlet sample yielded  $\text{CO}_2$  and 2-butanone as major by products. Similarly, hexanal was oxidized into pentanal, butanal, and  $\text{CO}_2$ . A gas chromatograph equipped with a Q-Plot column was used to measure  $\text{CO}_2$  and a mass spectrometer was used to identify the other end products. Again, when a free radical mechanism

was proposed, many of the theoretical end products were identical to the identified by-products from the experiments. Based on the results from this chapter and chapter 5 we theorize that the metallic phase in wood fly ash catalyzed the oxidation of 2-MB, 3-MB, and hexanal via a free radical mechanism.

In addition to oxygen, 1500 ppmv ozone was also tested as an oxidant in the oxidation of 2-MB and hexanal. For these experiments, the flow was reduced to 2 L/min, while temperature and the concentration were increased to 160 °C and 400-600 ppmv. The sampling and chromatographic conditions were similar to experiments with individual compounds. It was observed that 80-90 % removal of 2-MB and hexanal was obtained just with ozone alone (residence time ~ 0.1 seconds). However, when wood fly ash was used as a catalyst (total residence time ~ 4 seconds), close to 100 % removal was obtained.

Based on our experimental data, catalytic oxidation could be applied as an effective technology to treat aldehydes emitted from rendering emissions. Although our data suggested that the oxidation rates of aldehydes using wood fly ash were comparable with other catalysts, improvements and modifications to the process are possible to increase effectiveness of the process, obtain higher reaction rates and complete oxidation.

Future research on catalytic oxidation using wood fly ash may be undertaken using a three-pronged approach:

- 1) Studies may be focused on catalytic oxidation of aldehydes and volatile organic sulfur compound (VOSC) mixtures. The present research focused only on aldehydes removal using wood fly ash. Since rendering emissions

consist of a mixture of aldehydes and organic sulfur compounds (e.g., methanethiol), it will be worthwhile to investigate how wood fly ash responds to a mixture of dissimilar compounds. It would be interesting to know how 2-MB interacts with methanethiol and whether free radicals generated during 2-MB oxidation can co-oxidize methanethiol. Kinetic data so obtained may be used to design and size of the reactor. If wood fly ash can simultaneously catalytically oxidize methanethiol and aldehydes, then the proposed reactor system could potentially eliminate chemical wet scrubbers resulting in considerable savings in terms of money and water usage.

- 2) Research to clearly identify the catalytically active phase in wood fly ash and modification of wood fly ash to reduce pressure drop in a packed bed reactor is required. Based on our scanning electron microscopic analysis of wood fly ash in the current form, it consists of particles of activated carbon (1-3 mm) and spherical clusters of silica, iron and other trace metals (2-10  $\mu\text{m}$ ). It is theorized that activated carbon particles adsorb and concentrate the reactants on the surface followed by oxidation reactions catalyzed by iron and other trace elements. Further research is required to validate this hypothesis. For example, the silica spheres containing metals could be separated and tested for catalytic activity to determine if iron is actually the active phase. Moreover, due the small size of wood fly ash particles, it may not be practical to use as a catalyst in pilot scale or field scale applications even if wood fly was found to effectively oxidize mixtures of aldehydes and organic sulfur compounds. Hence, additional research may be focused on modifying the

wood fly ash (pelletizing for example) to increase the overall porosity of the catalyst. This may not only reduce the pressure drop but also render the wood fly ash easier to handle.

- 3) Determine the optimum ozone concentration for complete oxidation of VOC mixtures and the rate law as a function of ozone concentration. In the current work, ozone was tested as an oxidant and was found to completely remove aldehyde mixtures at 160 °C. However, the ozone concentration was set at 1500 ppmv based on earlier experience with ozone and other VOCs. As this is rather high and in excess of what is required for complete oxidation, kinetic studies as a function of ozone concentration could be undertaken to determine the optimum ozone concentration of ozone that can completely remove the aldehyde mixture, but not high enough for ozone to remain in the outlet. Developing a model for the rate law in terms of ozone concentration would also provide a more rigorous method to size the reactor.

The second part of this research focused on developing novel catalysts to treat VOCs. For this project, commercially available pelleted activated carbon (PAC) was used as a support material to disperse metals that potentially acted as catalysts. The goal was to synthesize nano-scale metal oxides on the support, which we theorized would increase the aldehyde oxidation rates. Oxides of nickel and cobalt were dispersed as catalysts on GAC using electrochemical deposition. Further, these catalysts were calcined @ 300 °C in a furnace with a 10 L/min flow of air. Subsequently, the catalysts were tested for their activities in oxidizing propanal using 1500 ppmv of ozone as an oxidant. All experiments were conducted at 25 °C and 6

L/min flow rate. Initially 2 grams of PAC, which acted as a control, was tested as catalyst. The oxidation rates for PAC obtained ranged from  $90\text{-}300 \times 10^{-9}$  mol/g-s for propanal concentrations from 50-250 ppmv. When tested under similar conditions, nickel and cobalt oxides exhibited higher catalytic activities ( $230\text{-}450 \times 10^{-9}$  mol/g-s for nickel and  $100\text{-}350 \times 10^{-9}$  mol/g-s for cobalt). Although, these catalysts had higher activity than PAC and wood fly ash at room temperature, opportunities for future research are possible, which are summarized as the following:

- 1) A differential reactor was assumed for all the experiments in this study.

However, in some cases the measured fractional removal was greater than 50 %. Hence the obtained kinetic data may not truly represent a differential reactor. Studies are therefore recommended to obtain kinetic data either by conducting the experiments using a smaller amount of catalyst to limit the fractional removal to less than 30 % or increase the flow rate to obtain the same effect. Alternatively, an integral reactor model may be used and different flow rates may be tested to obtain the kinetics. This approach would allow for determination of correct kinetic parameters and allow for proper scale up and design.

- 2) The synthesis of catalysts (nickel and cobalt) was carried out at a fixed temperature, pH, voltage, current, mixing speed, electrolyte concentration, and the time of deposition. However, each of these parameters is known to affect the deposition process. For example, an increase in temperature could allow for greater transport and might allow for increased deposition. Hence,

additional research is required to vary each of these parameters for optimal deposition of the metal on the GAC surface.